Benthic subtidal assemblages and ecological processes in urbanized seascapes of Puget Sound, Washington, USA

Eliza C. Heery

A dissertation

submitted in partial fulfillment of the

requirements for the degree of

Doctor of Philosophy

University of Washington

2017

Reading Committee:

Kenneth P. Sebens, Chair

Megan N. Dethier

Jennifer L. Ruesink

Program Authorized to Offer Degree:

Biology

University of Washington

Abstract

Benthic subtidal assemblages and ecological processes in urbanized seascapes of Puget Sound, Washington, USA

Eliza C. Heery

Chair of Supervisory Committee:
Professor Kenneth P. Sebens
Department of Biology

Urbanization is a major process altering nearshore habitats in many parts of the world. One important aspect of urbanization in marine settings is the proliferation of artificial structures, such as seawalls, breakwaters, and jetties. Urban artificial structures can fundamentally shift marine communities and alter ecological processes at multiple spatial scales. Though they are common in both intertidal and subtidal habitats, their effect on subtidal ecosystems is particularly understudied. I examined the communities that form in association with subtidal artificial structures and their effects on surrounding sedimentary habitats in an urbanized estuary.

In the first chapter, I evaluated detrital influx from artificial structures to surrounding sediments. Photoquadrat and sediment surveys indicated that red macroalgae and epilithic invertebrates were the major producers of detrital material on artificial structures in the Seattle area and that detritus from artificial structures was moving into adjacent sediments. Through a

series of experiments, I then assessed the potential effects of these detrital inputs on macrofaunal assemblages. Sediments receiving one-time additions of red macroalgae and shell material were relatively resilient to detrital influx and exhibited little to no change in macrofaunal composition. However, rapid reductions in sediment chlorophyll and phaeopigment following detrital additions suggested that delivery of red macroalgae into sediments surrounding artificial structures may be frequent. In a follow up experiment, sediments were enriched with red macroalgae on a weekly basis to reflect more frequent delivery rates. Though I hypothesized that red macroalgae would serve as a subsidy for macrofaunal assemblages, I observed no positive opportunistic responses among macrofauna to weekly additions. Rather, frequent inputs of red macroalgal detritus led to decreases in abundance for the majority of macrofaunal taxa. Red macroalgae may therefore have negative impacts on macrofaunal assemblages, though this effect is likely minor compared with hydrodynamic alterations and other changes to sedimentary habitats that are associated with artificial structures.

In the second chapter, I examined urban-related spatial distribution patterns and habitat-use the giant Pacific octopus (*Enteroctopus dofleini*). Urbanization is known to facilitate certain terrestrial mesopredators and I sought to evaluate whether similar patterns relative to urbanization were evident for this marine mesopredator. Modeling of citizen-contributed octopus presence/absence data suggested that urbanization impacts differed with depth. Octopus occurrence probability was positively correlated with urbanization intensity in deeper habitats only (> 24 m). In shallower environments (< 18 m), occurrence probability was higher in rural areas than in urban areas. In separate field surveys, I found that octopus diets were unrelated to urbanization, and that octopus abundance was positively correlated with the number of artificial structures on the seafloor. Though trophic mechanisms for urban-related distribution patterns of

giant Pacific octopus are therefore unlikely, provisioning of shelter and denning habitat from artificial structures may be an important factor for octopus populations in urban areas.

In the final chapter, I examined benthic composition on rocky artificial structures and natural reefs across an urban gradient. Photoquadrats were collected at 36 sites across Puget Sound. Consistent with studies in other regions, I found that artificial structures supported distinct and more variable benthic assemblages than natural reefs. In addition, rocky subtidal habitats in heavily urban areas had fewer kelps and more filamentous algal turf than those in less urban areas. Importantly, analyses from this study highlighted an important challenge in evaluating benthic composition relative to urbanization. Coastal cities tend to be located in protected bays and at the mouths of rivers, where benthic communities are subject to strong salinity gradients and low water flow. Strong collinearity in these naturally occurring environmental variables and urbanization intensity will be an important consideration for future studies that aim to characterize effects of urbanization on marine ecosystems.

TABLE OF CONTENTS

LIST OF TABLES

LIST OF FIGURES

Dedicated to my grandmothers,

Maude Elizabeth Wood Heery and Ella Lee Freed Lowrey,

For their inspiring inquisitiveness, scholarship, and wit

ACKNOWLEDGEMENTS

I wish to thank my PhD advisor, Ken Sebens, for his enthusiasm and faith in my abilities, and for allowing me to build my research with a freedom and autonomy that facilitated my development as a scientist. Members of my committee also provided invaluable guidance and support. I am indebted to Megan Dethier for the countless hours she spent discussing research ideas, reviewing written drafts, providing training in infaunal identification, and guiding my professional and personal development. Jen Ruesink was also a source of tremendous inspiration, and provided helpful guidance on experimental design, field and laboratory techniques, and data analysis, as well as access to essential laboratory equipment. I am also grateful for the quantitative guidance and insights provided by Tim Essington, and for the invaluable support, opportunities, and professional network facilitated by Terrie Klinger, both in her role as a committee member, and as director of the IGERT Program on Ocean Change.

This work would not have been possible without the help of many people who graciously volunteered their time in the field and in lab. Rhoda Green, Ed Gullekson, and Dave Thoreson were particularly instrumental in field operations and diving. I am also grateful to Amy Green, Dave Rintoul, E.J. Rauschl, Miguel Stutz, Sam Fletcher, and Whitney Grover for their support in the field. Jessica Blanchette, Amy Green, Avida Knebel, Shelley Johnson, Michelle Louie, Michael Pantalos, Rianne Peterson, Monisha Ray, and Dara Yiu made invaluable contributions through the many hours they contributed to laboratory analyses. Lab work was further supported by Nadia Ahmed, Bryson Albrecht, Jeremy Aspée, Anna Bakker, Jack Berrigan, Angeline Blattenbauer, Alia Hidayat, Tiffany Huang, Maria Huynh, Kim Jones, Juliette Kirkner, Ian McQuillen, Christopher Mowers, Jessica Nordstrom, Ashley Pierson, Rachel Podell-Eberhardt,

Maya Rosenfield, Gina Rudisill, Deja Sanchez, Mia Tien Sebek, Alexandra van Inwegen, Marisa Yonemitsu, and Danielle Z'Berg.

I am also grateful for the many people who provided data, laboratory access, and analytical support. I wish to thank Aaron Morello and Jan Newton for their assistance with fluorometric analyses, and Parker MacCready for providing estimates of flow, temperature, and salinity. Christy Pattengill-Semmens and divers in the REEF program kindly provided data on octopus sightings that formed a central part of my analysis. I also wish to thank Tom Mumford, Kathy Ann Miller, Aaron Galloway, and Charlie O'Kelly for their help in identifying a vast array of mystery rhodophytes. Thanks also to Rus Highley of Highline College for providing access to experimental tanks at the Marine Science and Technology Center in Des Moines, WA, and to Oscar Beijbom for his guidance and support in using CoralNet.

I would like to thank Laura Airoldi, Melanie Bishop, Bob Paine, David Scheel, and Sally Woodin for the time they took to consider my work and provide feedback and guidance. Questions from and discussion with Stefanie Broszeit, Ana Bugnot, Katherine Dafforn, Emma Johnston, and Mariana Mayer-Pinto were also extremely helpful. I received valuable feedback from past and present member of the Sebens Lab (Tim Dwyer, Robin Elahi, Will King, Derek Smith, Kevin Turner, and Chris Wells), and am also grateful for many others who supported and encouraged me over the years, especially Hilary Hayford, Jaquan Horton, Alex Lowe, Ned Schaumberg, Laura Vary, and Oscar Vary-Horton. Emily Grason provided essential insights and feedback both as a friend and colleague, and her commitment to scientific inquiry, rational thought, and humility continue to be a great source of inspiration. I am indebted to the universe for delivering one Ms. Megsie Siple, who has been a life teacher and partner-in-crime as I learn to follow my heart as a scientist while cultivating wit, joie de vivre, and a fashionable wardrobe.

I am deeply grateful to Loretta Lowrey, Laura Heery, Anna Heery, Lenne Klingaman, Meegan Corcoran, my Seattle Book Club sisters, and many others who make up a congress of wise women and spiritual guides that has been instrumental in my completion of this degree. Finally, thank you to all of my parents and siblings for your unwavering encouragement and support. Mom, Dad, Liz, Hukki, Charles, Anna, Mark – it truly takes a village, and you are the best village a girl could ask for.

This research was funded by the National Science Foundation (NSF) Integrative Graduate Education and Research Traineeship (IGERT) Program on Ocean Change (DGE 1068839), the NSF GK-12 Program (DGE 0742559), the Robert T. Paine Experimental and Field Ecology Endowed Fund (UW Biology, 2013 and 2014), and the Friday Harbor Award (UW Biology, 2012).

CHAPTER 1: Material fluxes from artificial structures to soft sediment environments in an urban estuary

Abstract

Artificial structures are proliferating rapidly in marine habitats as coastal zones become increasingly populated. These structures are particularly common in sedimentary seascapes, where they alter a variety of biotic and abiotic processes and facilitate changes in macrofaunal assemblages. An improved mechanistic understanding of the impact of artificial structures on sedimentary ecosystems is needed to support current and future coastal zone management. This study evaluated the effect of biogenic material fluxes from artificial structures to sediments in urban subtidal waterways of Puget Sound, Washington, USA. We identified biogenic materials in sediment core samples collected 1, 7, and 15 m from artificial structures, and evaluated their origin through a combination of photoquadrat surveys and microscopy. Red macroalgae and epilithic invertebrates that grew on artificial structures were the primary contributors of macroscopic biogenic material in sediments surrounding artificial structures. Macrofaunal assemblages differed significantly with increasing distance from artificial structures, and were correlated with the amount of red macroalgal detritus and epilithic shell material in sediment cores. We then performed a series of experiments to test whether there were causal linkages between the presence of these materials and macrofaunal community structure. We found that one-time additions of shell and algal material were of limited consequence for macrofauna when evaluated after 8 and 16 weeks. However, repeated measurements of sediment chlorophyll and phaeopigment levels following algal additions indicated that weekly macroalgal additions would be a more appropriate representation of the ambient rate of influx. In a final experiment, weekly additions of red macroalgae led to decreases in invertebrate abundance across multiple taxa after 3 and 7 weeks. No positive opportunistic responses to weekly additions were observed. Delivery of macroalgal detritus to sedimentary ecosystems had weak or negative effects on infaunal

communities in these experiments and should be examined in future work. However, gradients in macrofaunal assemblages surrounding artificial structures are likely influenced more heavily by other drivers. Studies such as these help to prioritize the potential mechanisms through which artificial structures alter sedimentary habitats, which could ultimately inform design criteria that prevent loss of ecosystem function as ocean sprawl proliferates.

Introduction

Coastal zones are becoming increasingly developed and modified by human activities as global population increases and shifts towards the coasts (Crossland et al., 2005; Small and Nicholls, 2003). In a process known as "ocean sprawl" (Duarte et al., 2012), large amounts of artificial structures, such as seawalls, breakwaters, pipelines, mooring blocks, and cables, are being added to the marine environment (Bulleri and Chapman, 2010; Dafforn et al., 2015; Dugan et al., 2011). Artificial structures are particularly extensive in marine sedimentary habitats (Bugnot et al. in preparation), where they have considerable impacts on soft-bottom communities (Dethier et al., 2016; Dugan et al., 2008; Nordstrom, 2014). Numerous studies have documented changes in macrofaunal assemblages associated with artificial structures (Ambrose and Anderson, 1990; Barros et al., 2001a; Bertasi et al., 2007; Martin et al., 2005). However, there have been few efforts to experimentally determine the mechanisms that drive these changes (Heery et al., 2017). Understanding these mechanisms is important for mitigating effects of further ocean sprawl, and could inform the design of artificial structures that protect growing coastal populations from sea level rise (Gittman et al., 2016a, 2016b; Neumann et al., 2015). Since sedimentary ecosystems are essential components of biogeochemical cycling, pollutant filtration, and other processes (Snelgrove, 1999), ocean sprawl mitigation and ecological engineering that is informed by a strong mechanistic understanding is essential both for conservation and for maintaining the ecosystem goods and services upon which humans rely.

Gradients in macrofaunal composition and diversity are a common feature of sediments surrounding artificial structures (reviewed by Heery et al. 2017). Past studies have highlighted several potential drivers of these gradients. Artificial structures modify hydrodynamic conditions, leading to changes in sediment transport, residence times, sedimentation rates,

benthic profile, granularity, and organic content (Bertasi et al., 2007; Danovaro et al., 2002; Dethier et al., 2016; Zanuttigh et al., 2005). Artificial structures can also introduce or trap contaminants (Neira et al., 2014; Sim et al., 2015), increase predation rates and disturbance from reef-associated mobile consumers (Davis et al., 1982), and alter ecological connectivity (reviewed by Bishop et al. 2017). Though each of these processes likely impacts macrofaunal communities to some degree, it is unclear whether they represent the complete suite of potential mechanisms by which artificial structures alter sedimentary ecosystems.

One alternative driver that has received little attention in the literature and may be important in shaping macrofaunal assemblages surrounding artificial structures is the influx of novel detritus and biogenic debris. Artificial structures are inhabited by epilithic organisms that often form novel assemblages compared with natural hard substrates in the same region (Bulleri and Chapman, 2010; Connell and Glasby, 1999; Glasby, 2000). Many epilithic flora and fauna generate considerable amounts of biological material, such as macroalgal detritus and shell fragments (Britton-Simmons et al., 2009; Lastra et al., 2008). This material can move into adjacent areas and become mixed into sediments as a result of physical processes or burying activity by deposit-feeders and bioturbators, such as polychaetes, thalassinids, and other decapods (Botto et al., 2006; Emmerson, 2000; Hughes et al., 2000; Kristensen and Mikkelsen, 2003; Nordström et al., 2006; Papaspyrou et al., 2004; Raffaelli, 2000; Reise, 1985; Vonk et al., 2008). In doing so, it may alter physical, chemical, and biotic conditions for sedimentary organisms (Airoldi et al., 2010; Ambrose and Anderson, 1990; Barros et al., 2001b; Machado et al., 2013). Recent work has demonstrated the importance of material fluxes in shaping the structure and function of marine communities in recipient habitats (Marczak et al., 2007; Polis et al., 1997), and macrofaunal assemblages are known to shift in response to detrital influx

(Gladstone-Gallagher et al., 2014; Norkko et al., 2004). Despite this, the extent to which material fluxes drive effects from artificial structures on surrounding macrofaunal communities has yet to be empirically tested (though see Airoldi et al. 2010).

In this study, we employed a combination of quantitative descriptive and experimental techniques to evaluate the effect of biogenic materials from artificial structures on a subtidal macrofaunal community in Puget Sound, WA, USA. Puget Sound is a large, fjordal system with estuarine circulation and extensive sedimentary habitat. Shoreline development and urbanization have resulted in numerous subtidal artificial structures within certain areas of Puget Sound. Our study addressed the following questions: (1) What are the major producers of biogenic materials on subtidal artificial structures in the study area? (2) Which biogenic materials enter surrounding sedimentary habitats? (3) How do infaunal assemblages respond to infrequent vs. regular biogenic material additions? (4) How do infaunal responses differ over short and intermediate temporal scales? We used quantitative surveys to characterize biogenic materials from artificial structures in surrounding sediments. Biogenic matter in this study included any material that was produced by benthic flora or fauna. A series of field experiments was then performed in a sedimentary habitat where artificial structures were absent to test the effect of biogenic materials from surveys on infaunal assemblages. Field studies were conducted over four consecutive summers, from 2012 to 2015. This study is among the first to systematically evaluate the effect of subtidal artificial structures on sedimentary communities from a mechanistic standpoint using field experiments, and contributes to our understanding of the effects of ocean sprawl on marine ecosystems.

Methods

Study area

This study was conducted at six locations in the Seattle Metropolitan Area containing rocky artificial structures in the subtidal zone (Figure 1): Alki Pipeline (AP), Centennial Park (CP), Don Armeni Boat Ramp (DA), Elliott Bay Marina Breakwater (EBMB), Jack Block Park (JBP), and Shilshole Marina Breakwater (SMB). AP is a decommissioned sewer outfall covered in boulders that forms a small artificial reef (~ 600 m^2) at 5-8 m depth. CP and DA are sloped shorelines protected by seawalls that extend 4-6 m into the subtidal zone. Rocky subtidal habitat from breakwaters at EBMB and SMB extends to approximately 8m and 6m depth, respectively. JBP is a submerged breakwater that runs parallel to shore at a depth of 4-7 m. Epilithic communities were evaluated at five of the six sites (SMB, CP, DA, AP, and JBP), infaunal communities and sediment characteristics were evaluated at two sites (EBMB and AP), and experimental manipulations were conducted exclusively at AP.

Photoquadrat surveys

We conducted photoquadrat surveys along 3 horizontal transects (10 m long) at each of five sites to characterize the major types of biogenic material associated with artificial structures (Figure 1). Transects were deployed haphazardly 10-20 m apart at the base of rocky artificial structures, such that they followed a relatively constant depth contour (5-7 m). Quadrats (0.09 m^2, 10 per transect) were positioned at random points within 3 m on either side of transects. This approach allowed us to collect photoquadrats of both hard and soft substrates. Hard-substrate quadrats were used to characterize epilithic composition and identify the major biomass

producers on artificial structures. Photoquadrats of surface sediments were used to characterize the composition of macroalgal drift in the immediate vicinity of artificial structures.

Quadrats were photographed using an Olympus C-8080 camera with an Ikelite strobe and an attached 36 × 25 cm aluminum framer. All photographs were analyzed for percent cover in ImageJ (NIH version 1.42) according to methods described by Dethier et al. (1993) and adapted by Elahi and Sebens (2012). Epilithic organisms and macroalgal drift were identified to the lowest taxonomic level possible (see Appendix 1). Specimens of the major macroalgal taxa observed in photos were also collected and pressed to confirm identification.

Due to the random positioning of quadrats and the placement of transects at the edge of artificial structure habitats, the sample size of hard- and soft-substrate quadrats was unbalanced between sites. This would have proved problematic for multivariate tests (Anderson and Walsh, 2013), and the data were therefore evaluated qualitatively by plotting the composition of epilithic organisms and of drift for each site. Appendix 1 provides a complete list of the species detected in photoquadrat surveys (Table S1) and a summary of sample sizes by substrate type (Table S2).

Sediment surveys

Sediment surveys were conducted to evaluate correlative relationships between sedimentary habitats and distance from artificial structures (causal linkages were evaluated through subsequent experiments, described below). Sediment cores were collected along 3 horizontal transects, placed perpendicularly to artificial structures along a constant depth contour at two sites (EBMB and SP). Though collected, cores from CP, DA, and SMB were not used because of rapidly deepening depth contours of sedimentary habitat at these locations. We did not collect cores from JBP because of the contamination history at this site (EPA, 2009).

Four replicate core samples were collected at each of three distances along horizontal transects: 1, 7, and 15 m. Core samples (8 cm deep × 10 cm wide) were transferred to plastic Ziploc bags underwater and brought to lab in coolers on ice. One of the replicate cores was frozen at -10 °C for grain size analysis at a later date. To analyze grain size, we dried sediments at 60 °C to a constant weight and sieved them through a stack of decreasing mesh sizes (4, 2, 1, 0.5, 0.25, 0.125, and 0.063 mm). The stack was dry sieved for 10 min using a RoTap shaker. The final mass in each size category is reported in Appendix 2 (Table S3). The other three samples were processed unfrozen for macroalgal detritus, shell composition, and macrofauna. For these, total sample volume was first quantified via displacement in a 1000 ml graduated cylinder. Sediments were then wet sieved through a 0.5 mm mesh, and the material caught in the sieve was sorted under a dissecting scope. All macroalgal material big enough to pick up with forceps was identified to major phyla based on color using a compound microscope.

Live macrofauna were extracted by sorting through all material retained by the 0.5 mm sieve and preserving them in 80% ethanol. Macrofaunal counts from this stage of the study were primarily useful as a means of providing context for subsequent field experiments. Numerous studies have documented gradients in macrofaunal composition with increasing distance from artificial structures (Ambrose and Anderson, 1990; Barros et al., 2001b; Davis et al., 1982; Wilding, 2006), and such patterns were anticipated across sites. Species composition also was anticipated to differ between sites, given the high spatial variation known to occur in estuarine soft sediment communities (Thrush et al., 1999). Since all subsequent field manipulations were performed at a site 50 m southeast of AP (see section 2.4), and macrofaunal counts were primarily used as a reference for these experiments, we only enumerated macrofauna in core survey samples collected at AP.

All particles retained by the 0.5 mm sieve (designated as “coarse particles” in subsequent sections) that were not macroalgal detritus or macrofauna were dried at 60 °C. The particles were then sorted under a dissecting scope into ten categories according to their origin: barnacles, *Pododesmus machrochisma* (bivalve), *Mytilus spp.*, clams, gastropods, serpulid tubes, chitons, other, unidentifiable organic, and inorganic (pebbles and small rocks). Dried material in each category was then weighed to provide the relative composition of each by weight.

Permutational multivariate analysis of variance (PERMANOVA) was used to test for differences in macrofaunal composition, sediment grain size, and the composition of coarse particles (≥ 0.5mm) with distance from artificial structures. We used ANOVA to test the effect of distance on the total dry weight of coarse particles, the proportion of coarse particles that were organic, and the proportion of organic particles that were derived from epilithic sources. All tests included distance from artificial structures as a continuous variable and sample volume as an offset. Site and transect (nested within site) were included as categorical factors.

The volume of macroalgal detritus in core samples was zero-inflated and was evaluated with a gamma hurdle (delta) approach involving two submodels: (1) a logistic regression for macroalgal detritus presence/absence, and (2) a generalized linear model (GLM) with gamma error for the volume of macroalgal detritus in core samples in which presence = 1. Both submodels were run using the glm() function in the base package of R (version 3.3.1, R Core Team 2016), with a binomial error distribution and logit link function for submodel (1) and gamma error (inverse link) for submodel (2).

Field experiments

We conducted field experiments to test the effect of biogenic material from artificial structures on infaunal communities. Separate experiments were conducted in the summers of 2013, 2014, and 2015, and are hereafter identified as Experiment 1, 2, and 3, respectively. All three experiments took place on a subtidal sandflat approximately 50 m southeast of AP, at a depth of 4-6 m. Methodology was based on methods described by Bishop et al., (2010), which we adapted for subtidal environments.

Experiment 1 – Experiment 1 tested the effect of both red macroalgal detritus and shell fragments on macrofaunal assemblages over an 8- and 16-week period. A grid of 49 circular plots (0.5 m diameter, 1.5 m apart) was established at the site in June 2013. Each plot was marked at the center with a small construction flag and assigned at random to one of seven treatments, including five types of material additions and two controls (Table 1). In the addition treatments, biogenic material was hand-churned into the top 5cm of sediment (Bishop et al., 2010). Addition treatments included two levels of red macroalgal additions (100 and 500 ml, designated as A1 and A2, respectively), two levels of shell fragment additions (100 and 500 ml, designated as S1 and S2, respectively), and a combined treatment of both 100 ml of red macroalgae and 100 ml of shell fragments (AS). Control treatments included an experimental control (CI), in which sediment was hand-churned without material additions, and an undisturbed control (CII).

Preparation of material additions was based on results from earlier survey work. Algal treatments comprised *Chondracanthus exasperatus, Polyneura latissima,* and *Sarcodiotheca gaudichaudii*. These were the three most common red macroalgal species found growing on artificial structures and in macroalgal drift surrounding structures in preliminary photoquadrat

surveys (Figure 2). Though *Ulva spp.* was also a large component of drift, numerous past studies have evaluated the effect of *Ulva spp.* on macrofaunal assemblages (Bolam et al., 2000; Franz and Friedman, 2002; Marsden and Bressington, 2009; Norkko and Bonsdorff, 1996; Rossi, 2006); sediment surveys we conducted also indicated that rhodophytes represented a far larger component of macroalgal detritus in sediments surrounding artificial structures than green macroalgae (Figure 3). Each macroalgal type was ground in a blender, with care taken to minimize the amount of exposure time to air. Mixtures of shredded macroalgae (consisting of 50% *C. exasperatus*, 30% *P. latissima*, and 20% *S. gaudichaudii* by volume) were prepared the day prior to deployment and were stored in closed zip-lock bags over ice. Shell fragment treatments were prepared from sediments that were retained by a 0.5 mm sieve approximately 1m from the artificial structure at AP.

Material addition and CI plots were modified only once, at the start of the experiment. Two core samples (10 cm diameter, 8 cm depth) were collected from each plot after 8 weeks, and again after 16 weeks. The core samples were stored in zip-lock bags and transported to the laboratory on ice. For Experiment 1 only, 2 ml of homogenized sediment from each sample was extracted for chlorophyll and phaeopigment analysis, and immediately frozen in a -20 °C freezer. (In subsequent experiments, these were collected separately in the field using oral syringes). The remaining sediment was then processed and analyzed for macrofauna using the same methodology described for sediment surveys (Section 2.3).

Sediments frozen for chlorophyll and phaeopigment analysis were inoculated with 10 ml of 90% acetone and stored in the dark for 24 hours at 4 °C. Each sample was then centrifuged for 10 minutes and 0.1 ml of the supernatant was transferred to a vial of 7 ml of acetone. We measured fluorescence of the mixture in a fluorometer before and after acidification (0.05 ml of

supernatant was used when dilutions were necessary). The mass of chlorophyll and phaeopigment was computed based on equations from Lorenzen (1967). Sediments used in chlorophyll extractions were retained and the remaining liquid was decanted, with remnants allowed to evaporate in a fume hood overnight. They were then dried in a drying oven at 60 °C for 24 hours and weighed to derive final estimates of chlorophyll and phaeopigment mass per gram of dry sediment.

Experiment 2 – In Experiment 2, we sought to test the effect of red macroalgal additions over two shorter time periods: 1 week and 4 weeks. A randomized grid of 15 0.5 m-diameter experimental plots was again established approximately 50 m southeast of AP. Experimental plots were randomly assigned to one of three treatments (n = 5): An addition of 120 ml of red macroalgae (A), a hand-churned control (CI), and an undisturbed control (CII) (Table 1).

Experiment 2 was unfortunately terminated ahead of schedule when a recreational diver or a local octopus (there was a large Giant Pacific Octopus, *Enteroctopus dofleini*, inhabiting the pipeline structure at the time) removed 12 of the 15 plot markers in week 3 and deposited them haphazardly throughout the experimental grid. The original plot location could not be determined definitively, and 4 week samples therefore were not available. We had collected two replicate core samples from each experimental plot in week 1, however, and macrofaunal composition from these samples were compared between treatments. In addition, sediment chlorophyll and phaeopigment samples collected frequently within the first week of the experiment provided insight into the rate change in pigment levels following algal additions. Two 3-ml oral syringes of sediment were collected from each plot prior to the addition of macroalgae, immediately following experimental manipulations, and again every other day for the first week (Day 3, Day

5, and Day 7). The oral syringes were immediately frozen to -20°C, transferred to lab in a dark cooler, and analyzed according the methods described in Section 2.4.1.

Experiment 3 – In Experiment 3, we tested the effect of weekly algal additions on macrofaunal assemblages over a 3- and 7-week period. To reduce lab processing time, undisturbed controls were excluded from this experiment and effects from algal additions were characterized based on differences from hand-churned controls only. We felt this was justified given the lack of differences between experimental and undisturbed controls in similar past studies in sandy habitats (Gladstone-Gallagher et al., 2014; Kelaher and Levinton, 2003; Olabarria et al., 2010), and because of the lack of intermediate- and short-term differences between control treatments in Experiments 1 and 2. In addition, to accommodate weekly algal additions, we modified protocol so that algae could be collected and treatments prepared underwater on the same dive. Prior to the start of Experiment 3 (in May 2015), we determined the approximate volume of ripped pieces of *C. exasperatus, P. latissima,* and *S. gaudichaudii* given their surface area. Collected algae were then ripped into standard-sized pieces to achieve the intended volume for addition treatments. Each standard-sized piece was further shredded into smaller pieces as it was hand-churned into experimental plots. Volume : surface area measurements from samples collected at the end of the experiment did not differ significantly from initial values. To ensure this protocol would not have altered the outcome of one-time addition treatments in Experiments 1 and 2, we included an initial algal addition and an initial hand-churned control treatment in Experiment 3.

Experiment 3 thus consisted of four treatments: Initial additions of red macroalgae at the start of the experiment (A1), initial hand-churning at the start of the experiment without material additions (C1), weekly additions of red macroalgae (A2), and weekly hand-churning of

sediments without material additions (C2) (Table 1). A grid of 28 0.5 m circular plots (n = 7) was again established at the same site, 50 m southeast of AP. Two replicate core samples were collected and analyzed for macrofauna after 3 and 7 weeks. Chlorophyll and phaeopigment levels were quantified from two replicate oral syringe samples (3 ml) collected from each plot prior to the start of the experiment, and after 3 and 7 weeks. We used the same protocol as in earlier experiments to analyze macrofaunal and pigment concentrations.

Statistical analyses

Experimental results were evaluated with a combination of univariate and multivariate tests. We used PERMANOVA to test for differences in macrofaunal composition between treatments. Differences in species richness, chlorophyll, and phaeopigments were evaluated via ANOVA, and individual species abundances were evaluated via GLMs (quasi-Poisson error to accommodate overdispersion). GLMs were also used for total macrofaunal abundance, Shannon diversity, and species evenness. In most cases, these metrics were right-skewed, and normal, lognormal, and gamma error distributions were compared via AIC and residual distribution patterns. In Experiments 2 and 3, left-skewed Shannon diversity and species evenness were inverted due to poor fits in all model alternatives. No other response variables were transformed in this study. For each variable, we performed a series of post-hoc tests to partition the variation from different types of materials, “dosage” levels, and frequency of additions. Data from each sampling date were analyzed separately to minimize model complexity. Residuals from all statistical tests and models were plotted against their spatial location in the experimental grid to check for spatial autocorrelation. We found no evidence of spatial autocorrelation in any of the tests performed, and residual plots are therefore not reported.

Pigment concentrations measured over the first week in Experiment 2 were compared between treatments using a generalized linear mixed model (GLMM), with treatment and sampling date as fixed effects and plot as a random effect. This was done using lmer() in the lme4 package in R. To characterize the rate at which algal additions were consumed or resuspended from sediments, we compared the fit of 7 alternative non-linear functions for data from algal-addition plots. These including a simple exponential decay formula, a 2- and 3-parameter exponential decay, logistic decay, two polynomial functions (quadratic and cubic), and a gaussian peak curve. The models were fit using the nls() in R and compared via AIC. The best performing model was then used to estimate the amount of time required for addition plots to return to baseline chlorophyll and phaeopigment levels.

Results

Photoquadrat surveys

We found 35 different epilithic taxa in photoquadrat surveys of artificial structures (Appendix 1). Total percent cover of epilithic organisms ranged from 80.2 ± 3.0% at AP to 99 ± 0.5% at CP. The most common occupier of space on artificial structures was a sediment-coated, low-lying (~ 1-3 cm height) matrix of stalks/filaments that we were not able to definitively assign to a single taxonomic group, but that appeared to include hydroids, bryozoans, filamentous macroalgae that were lacking in pigment (similar to complex (COMP) noted by (Sebens, 1986); hereafter abbreviated HBFS matrix). HBFS matrix was extensive at all sites, making up an average of 22.9 to 41.6% of total epilithic cover. Subsequent sediment surveys did not find evidence of HBFS matrix in surrounding sediments, presumably due to limited influx or/and rapid decomposition of this material, and we did not seek to characterize it further.

After HBFS matrix, the most common occupiers of space on artificial structures were the red foliose macroalgae, *C. exasperatus* and *P. latissima*, which represented an average of 9.9-30.0% and 6.9-13.2% of epilithic cover, respectively (minimum and maximum averages across sites; minimum-maximum standard deviations were 13.9-21.3% and 9.4-18.9%, respectively). Barnacles (*Balanus* spp.) were also common (8.8 ± 1.4% of epilithic cover), and were followed by the red macroalgae, *Callophyllis* spp. (7.1 ± 0.8%), crustose coralline algae (5.9 ± 1.0%), and *Ulva* spp. (4.8 ± 0.9%) (Appendix 1). Relative percent cover of these taxa varied among sites (Figure 2a). For instance, CP was largely dominated by red foliose macroalgae and HBFS matrix, while AP had higher relative cover by crustose coralline algae and other invertebrates, such as *Metridium farcimen* (9.1 ± 6.0% at AP) and *Pododesmus machrochisma* (1.3 ± 0.7% at AP).

The composition of macroalgal drift over surface sediments surrounding artificial structures was highly variable. *Ulva* spp. and *Sarcodiotheca gaudichaudii* were the most abundant components of drift on average (representing 26.2 ± 3.9% and 27.7 ± 4.2% of total macroalgal drift, respectively), and comprised > 50% of drift at three of the five sites sampled (Figure 2b). *C. exasperatus* (15.2 ± 3.3%) and *P. latissima* (9.9 ± 2.6%), were also common components of drift. Contributions of kelps (Laminariales) to drift were minimal (1.2 ± 0.5%).

Sediment surveys

Sediment surveys revealed major differences in macroalgal detritus load, sediment characteristics, and macrofaunal composition with increasing distance from artificial structures. The volume of macroalgal detritus decreased significantly with distance from artificial structures (Figure 3). Macroalgal detritus occurred in 93% of cores from AP, but only 67% of cores at

EBM, resulting in a significant site effect in the logistic regression component of the gamma hurdle model. There was no significant effect of distance on presence/absence of macroalgae (Table 2). Rhodophytes were the dominant component of macroalgal detritus at all distances from artificial structures, though chlorophyta also represented a substantial proportion of detrital material (Figure 3). Relative composition of different macroalgal types did not differ with distance or by site in multivariate tests (Appendix 2, Table S4).

Sediment grain size differed significantly with distance (Figure 3, Appendix 2), and tended to be coarser in core samples collected immediately adjacent to artificial structures (Table 2). Further analysis of coarse particles (≥ 0.5mm) suggested this was largely due to shell material from epilithic organisms. Both the proportion of coarse particles that were organic (i.e. made up of shell fragments) and the proportion of these organic particles that were epilithic in origin (derived from *Balanus* sp., *Pododesmus machrochisma*, serpulids, chitons, or mussels) were negatively correlated with distance (Table 2). Coarse organic particles at EBM contained a higher proportion of epilithic shell fragments than those at AP (Table 2); this may be due at least in part to a slightly steeper depth profile at EBM. The proportion of coarse particles that were organic was also significantly higher on Transect B at AP (Table 2). This transect extended from the pipeline structure in an east-west direction, perpendicular to the primary orientation of tidal currents, while the other two transects extended north and south from the structure, and covered a more limited depth range.

Macrofaunal assemblages were examined at AP to provide context for subsequent experiments conducted in the same area. There was a high degree of spatial variability in both univariate and multivariate metrics relating to macrofaunal assemblage structure and diversity (see Appendix 2). Despite this, we detected a significant negative correlation between total

macrofaunal abundance and distance from the pipeline structure (Table 3). This coincided with decreases in the abundance of several taxa with distance, including *Alvania* sp., *Parvilucina tenuisculpta*, *Spiochaetopterus costarum*, *Lirularia* sp., *Lacuna* sp., polynoids, and phyllodocids (Appendix 2). Abundance was found to increase with distance from the pipeline structure in *Euphilomedes* sp. (Figure 4).

Field experiments

We found few persistent effects from single additions of biogenic materials in field experiments. Slight differences in total macrofaunal abundance, Shannon diversity, and species evenness among treatments was observed after 8 weeks in Experiment 1. This was due primarily to differences in plots receiving 100ml of shredded red macroalgae, which had greater macrofaunal abundance, lower Shannon diversity, and lower species evenness than all other treatments in pairwise comparisons (Table 3). Material addition treatments had no effect on species richness (Table 3), multivariate dispersion (Permutation Test for homogeneity of dispersion, $df = 6$, $F = 0.721$, $p = 0.644$), or in PERMANOVA ($F = 1.026$, $R^2 = 0.063$, $p = 0.393$). While overall community composition was therefore unaltered by experimental treatments, there was a slight response among specific taxa. *Alvania* sp. was more abundant in plots receiving 100ml of macroalgae than in other treatments, while *Euphilomedes* sp. and goniadid polychaetes were most abundant in response to combined algae and shell additions (Figure 5).

After 16 weeks (Experiment 1), patterns observed earlier in the experiment were no longer evident. There were no differences in total abundance, diversity metrics (Table 3), or in multivariate tests (PERMANOVA: $F = 0.871$, $R^2 = 0.054$, $p = 0.656$; Permutation test for

homogeneity of dispersion, $df = 6$, $F = 1.592$, $p = 0.159$). There also were no differences in the abundances of major taxa. A clear temporal shift in species abundances and community composition did occur, with more *Alvania* sp., *Rochefortia tumida*, and *Tellina* sp., and fewer *Euphilomedes* sp., after 16 weeks. These changes were consistent across treatments (Appendix 3, Table S6), and presumably reflected ambient seasonal fluctuations in sandy bottom assemblages at that site, irrespective of experimental manipulations.

In Experiment 2, core samples collected 1 week after algal additions exhibited no differences in abundance, diversity, or community composition (Appendix for 3, Table S7). Among individual taxa, only goniadids differed between treatments. Goniadids were less abundant in hand-churned control plots. While this could potentially suggest a short-term negative effect for this taxon from physical disturbance to sediments, the lack of difference in goniadid abundance in plots receiving algal additions and those left undisturbed makes this outcome difficult to explain.

Though sediment cores from Experiment 2 demonstrated few patterns with respect to macrofauna, chlorophyll and phaeopgiment samples collected repeatedly throughout the first week were surprisingly informative. There were no differences in sediment chlorophyll or phaeopigment levels between plots before treatments were applied (ANOVA, $F = 0.559$, $p = 0.578$ and $F = 0.670$, $p = 0.519$ for chlorophyll and phaeopigments, respectively). Algal additions caused the concentrations of both photosynthetic pigments to increase significantly; Generalized linear mixed model results also indicated a significant treatment effect within the first week (Appendix 3, Table S8). Chlorophyll and phaeopigment concentrations from Experiment 2 are presented graphically in Figure 6. The best fit non-linear model for chlorophyll over time was an exponential curve with three parameters (Table 4, Figure 6). The model

suggested that chlorophyll concentrations began to decrease almost immediately following the addition of shredded red macroalgae to sediments, and returned to ambient levels within four days. For phaeopigments, a gaussian peak function provided the best fit of the data (Table 4, Figure 6), and indicated a lag between algal additions and peak phaeopigment concentrations of approximately 30 to 40 hours. Phaeopigments were estimated to return to ambient levels within 2 to 3 days based on this model. The Gaussian peak function did not converge for chlorophyll data, nor did the three parameter exponential model converge for phaeopigment data, underscoring the difference in pattern between the two metrics following algal additions.

In Experiment 3, we evaluated the effects of weekly additions of shredded red macroalgae in comparison to algal additions performed once, at the start of the experiment. Across all experimental plots, we extracted a total of 8,511 specimens from 47 taxa. Bivalves were the most common in Experiment 3 (3,697 individuals from 9 taxa), followed by gastropods (2,868 individuals from 10 taxa) and crustaceans (1,171 individuals from 5 taxa). Polychaetes were again the most diverse group, with 748 specimens from 19 families.

Plots receiving weekly additions of algae differed considerably from other treatments. After 3 weeks, they had lower macrofaunal abundance, lower species richness, and lower Shannon diversity, though species evenness was comparable to that in other treatments (Table 5). They also differed with respect to assemblage composition in multivariate tests (Table 6). Seven taxa were identified as particularly influential in the dissimilarity between treatments based on SIMPER analysis (Table 7). Three of these differed significantly between treatments and were less abundant in plots receiving weekly algal additions: *Alvania* sp., *Euphilomedes* sp., and amphipods (Table 8). In addition, *Tellina* sp. was less abundant in weekly addition plots after 3 weeks (Table 8 and Appendix 3, Table S9).

After 7 weeks, plots receiving weekly algal additions continued to have lower total macrofaunal abundance and species richness (Table 5), and differences in assemblage structure (Table 6). Interestingly, after 7 weeks, Shannon diversity was comparable between treatments, despite clear differences in 3-week samples. Species evenness also remained relatively consistent between treatments. The lack of significant treatment effects on Shannon diversity and species evenness, along with highly divergent patterns in macrofaunal abundance between treatment groups, was attributed to relatively widespread negative effects from weekly addition across taxa. Red macroalgae added weekly to experimental plots led to lower abundances in 6 of the 12 most common macrofaunal species, including *Alvania* sp., *Euphilomedes* sp., Goniadids, *Nutricola tantilla, Parvilucina tenuisculpta, Rochefortia tumida*, and *Tellina* sp. (Figure 7). We found only 1 amphipod in 7-week samples, and estimates of treatment effects thus are not provided for this taxonomic group. Among taxa that were sufficiently abundant for model estimates, we did not detect any positive responses to weekly algal additions (Table 8 and Appendix Table S9).

Discussion

We conducted both quantitative surveys and field experiments to evaluate the effect of material fluxes from artificial structures on macrofaunal assemblages. Results from our study suggest that detritus from epilithic organisms is a prominent component of sedimentary habitat within a few meters of artificial structures. Though macrofaunal assemblages were relatively resilient to one-time influx of epilithic detritus, the rapid decrease in algal content we observed following experimental manipulations suggests that repeated influx of macroalgal detritus may be common (since macroalgal pieces were consistently present in sediments close to artificial

structures). We found that repeated algal additions had considerable negative impacts on macrofauna, reducing densities of multiple taxa, and decreasing total macrofaunal abundance and richness. This finding is important from a conservation standpoint, as it suggests that material fluxes from artificial structures may limit biodiversity in sediments. It did not, however, support the prediction that material fluxes were a major driver of observed gradients in macrofaunal composition surrounding artificial structures. Experimental additions led to a low-diversity macrofaunal community that lacked several of the species most common immediately adjacent to structures. While material fluxes may therefore affect macrofauna, other mechanisms are likely more important in shaping macrofaunal assemblages surrounding artificial structures.

In past studies on the effect of phytodetritus on macrofaunal assemblages, slight to moderate negative effects of algal additions on total macrofaunal abundance have been common (Bishop et al., 2010; Bishop and Kelaher, 2007; Cardoso et al., 2004; Gladstone-Gallagher et al., 2014; Kelaher and Levinton, 2003; Olabarria et al., 2010; Rossi and Underwood, 2002; Taylor et al., 2010). Effects tend to differ between macroalgal types (Bishop et al., 2010) and also depend on sediment characteristics and macrofaunal community structure at the site where experimental additions are performed (Rossi and Underwood, 2002). However, in most cases where strong negative effects have been documented, there was a simultaneous positive response among one or more opportunistic species or functional groups (Kelaher and Levinton, 2003; Olabarria et al., 2010). Conversely, we observed negative effects of phytodetritus across numerous macrofaunal taxa, and among multiple functional groups. The species exhibiting the greatest and most rapid response to weekly additions were *Alvania* sp., an herbivorous gastropod (Light et al., 2007), *Euphilomedes* sp., a deposit-feeding ostracod (Speiser et al., 2013), and goniadid polychaetes, which are carnivorous (Fauchald and Jumars, 1979). Several deposit- and suspension-feeding

bivalves also decreased in abundance, particularly after 7 weeks of repeated algal additions, including *Tellina* sp., *Nutricola tantilla,* and *Rochefortia tumida*. We found no evidence of positive opportunistic responses to weekly algal additions among any taxa.

Differences in our results and past studies may be particularly influenced by three factors: (1) That phytodetritus in our study was comprised of Rhodophytes, (2) That we performed repeated, rather than one-time algal additions, and (3) That our experiment was conducted in a heavily urbanized marine environment. Given the regional dominance of laminarians in nearshore habitats, we were surprised by the dominance of red macroalgae on artificial structures, in drift, and in sediment cores. Past studies have considered effects of detritus from laminarians, fucoids, ulvoids, and members of the class Bryopsidophyceae (Bishop et al., 2010; Kelaher and Levinton, 2003; Olabarria et al., 2010; Taylor et al., 2010) on macrofauna, but there have been few experimental studies evaluating effects from red macroalgal detritus (though see Cardoso et al., 2004). Many species of red macroalgae are rich in chemically defensive compounds, including acetylene-containing lipids and halogenated secondary metabolites (Fenical, 1975; Pedersen et al., 1974), which could deter herbivores and secondary consumers directly, or reduce herbivore densities, with secondary effects on consumer composition and abundance. *C. exasperatus* has more than one known invertebrate consumer (Thornber et al., 2008) and may be among the more palatable red macroalgal species in the region, while *P. latissima* contains oxylipins (Jiang and Gerwick, 1997), which may inhibit grazing by herbivores (Nylund et al., 2011). However, Norkko et al. (2004) found that even a chemically defended red macroalgae (*Phyllophora antarctica*) entered infaunal food webs and had a structuring role on subtidal assemblages, though the process by which it broke down and was consumed was slow. It is therefore unclear

whether chemical defenses would be sufficiently toxic to decrease abundance across multiple infaunal taxa.

The present study also differed from past work in that phytodetritus was added repeatedly to experimental plots. In Experiment 2, we observed extremely fast reductions in sediment pigment concentrations within the first week. Presumably, this was due to a combination of degradation by bacteria (Ming-Yi et al., 1993; Szymczak-Zyla et al., 2008), subsurface deposit feeding activity (Bianchi et al., 2000, 1988; Furlong and Carpenter, 1988; Ingalls et al., 2000), and disturbance of mobile consumers, such as flatfish, which we frequently observed foraging around experimental plots. Assuming that the rate of decrease in pigment concentrations was comparable between experimental plots and sediments sampled nearby during observational surveys, the quantity of phytodetritus that was consistently observed in sediments adjacent to artificial structures suggests that macroalgal influx occurs frequently. The accumulation of macroalgal detritus might also be expected to lead to depletions in sediment oxygen levels. Anoxic conditions due to the decomposition of macroalgal detritus have been widely documented in sedimentary environments (Krause-Jensen et al., 1996; Norkko and Bonsdorff, 1996; Valiela et al., 1992), and can decrease abundances across multiple taxa (Kelaher and Levinton, 2003). The propensity for hypoxia in sedimentary environments depends on a variety of factors, including sediment porosity and bioturbation rates (Glud, 2008). Sediments away from artificial structures at AP were dominated by medium sands, with fine and coarse sands also present (Figure 3). While anoxic conditions were therefore less likely at AP than at sites with finer sediment grain size, we did not quantify porosity in this study directly, and are unable to further evaluate hypoxia as a potential mechanism for negative responses to repeated algal

additions. We did not observe obvious changes in the coloration of sediments receiving weekly algal additions.

Additionally, this study was conducted within a heavily urbanized waterway, where sediments are subject to a wide variety of heavy metals and other contaminants, which Rhodophytes absorb (Wang and Chen, 2009). Shifts in community composition could potentially be the result of higher concentrations of copper, nickel, and other contaminants. Studies on the extent to which biosorption by Rhodophytes influences marine trophic relationships are limited, and further manipulations and measurements would be needed to evaluate whether contaminants were a likely driver of the patterns we observed.

Our study demonstrates that macrofaunal responses to material influx depend on both the "dose" and type of material entering sedimentary environments. We found little evidence that shell material alters the composition of macrofauna, though this result may have differed if evaluated over a shorter time scale and in habitats with finer sediments. Conversely, red macroalgae may have uniquely negative impacts on macrofauna, though the extent to which this is generalizable and the mechanisms behind it are also uncertain. Macrofauna may be affected both directly, for instance via mechanisms we have discussed here, and indirectly, via interactions with meiofaunal and microbial communities (Alongi and Tenore, 1985). Examining both direct and indirect potential mechanisms for macrofaunal responses to red macroalgal additions will be an important component of future work and necessary to more fully characterize the effect of Rhodophyte detritus on sedimentary ecosystems. Further study is also needed to quantify the rates of red macroalgae influx in temperate sedimentary habitats.

We know from past studies that effects from artificial structures are complex and multifaceted. This study builds on our knowledge by suggesting that material fluxes are not

among the major drivers that alter macrofaunal communities surrounding artificial structures. Through studies such as this, we can begin prioritizing the many potential mechanisms by which artificial structures impact sedimentary ecosystems, and should eventually be able to identify design criteria that are most critical for preventing loss of ecosystem function as ocean sprawl proliferates. This will be ever more essential as climate change intensifies and poses greater risks to coastal communities, and the need for artificial structures that both protect shorelines from inundation while facilitating ecosystem goods and services grows.

Tables

Table 1. Summary of treatments in Experiments 1, 2, and 3. Table presents the year, treatment type (Addition: biogenic material added to the plot; Control: No material added to the plot), identity (+A: shredded red macroalgae, +S: Shell fragments, +A/+S: Combination of shredded red macroalgae and shell fragments, I: Hand-churned, II: Undisturbed), level (100ml or 500ml; controls receiving no additions are marked as (--)), and duration (in weeks) for each experiment. The timing of material additions is also provided (far right). All experiments involved single additions of biogenic materials at the start except for two treatments (2015: C and D), which received weekly additions or shredded red macroalgae (C) or were hand-churned without material additions on a weekly basis (D). Undisturbed control were excluded from Experiment 3 because they did not differ significantly from hand-churned controls in Experiments 1 and 2, or in past other studies (Bishop et al. 2010).

Year	Treatment		Identity	Level	Duration	Timing of Addition
2013	A1	Addition	algae	100ml	8 weeks 16 weeks	Start
	A2	Addition	algae	500ml		
	S1	Addition	shell	100ml		
	S2	Addition	shell	500ml		
	AS	Addition	algae / shell	100ml 100ml		
	CI	Control	hand-churned	--		
	CII	Control	undisturbed	--		
2014	A	Addition	algae	120ml	1 week 4 weeks*	Start
	CI	Control	hand-churned	--		
	CII	Control	undisturbed	--		
2015	A1	Addition	algae	120ml	3 weeks 7 weeks	Single Weekly
	C1	Control	hand-churned	--		
	A2	Addition	algae	120ml		
	C2	Control	hand-churned	--		

Table 2. Results of univariate analyses for sediment core samples collected 1, 7, and 15m from artificial structures at two sites in the Seattle Metropolitan Area: EBM and AP. Macroalgal detritus in sediments was evaluated using a Gamma Hurdle Model, which was comprised of a logistic regression for the presence/absence of macroalgae in core samples, and a Gamma GLM for the volume of macroalgae in non-zero core samples. While multivariate analyses of sediment grain size distribution are reported in Appendix 2 (Table S4), we conducted further univariate analyses (Gaussian error structure) of coarse particles (≥ 0.5mm), shown on the right-hand side of the table. These included the dry weight of coarse particles, the proportion of coarse particles that were organic (comprised of shell fragments), and the proportion of organic coarse particles that were epilithic in origin (produced by *Balanus sp.*, *Pododesmus machrochisma*, serpulids, chitons, or mussels).

		Macroalgal detritus				**Coarse particles (≥0.5mm)**					
		Presence / Absence		Volume (ml)		Total dry weight (g)		Proportion organic		Proportion epilithic	
Source	df	χ^2	*P*	*F*	*P*	*F*	*P*	*F*	*P*	*F*	*P*
Site	1	8.824	**0.003**	0.380	0.541	7.310	**0.010**	1.027	0.316	5.391	**0.024**
Distance	1	0.002	0.965	23.305	**<0.001**	20.134	**<0.001**	15.605	**<0.001**	18.054	**<0.001**
Transect (w/in Site)	4	2.275	0.685	0.922	0.462	1.393	0.251	2.787	**0.037**	0.892	0.476
Pairwise contrasts		*AP > EBM*				*EBM > AP*		*AP: B > A = C* *EBM: A = B = C*		*EBM > AP*	

Table 3. *F* and *p*-values from GLMs for total macrofaunal abundance, species richness, Shannon diversity, and species evenness in Experiment 1 after 8 weeks (top half of table) and 16 weeks (bottom half of table). Selected models used a gamma error structure for total macrofaunal abundance, for the inverse of Shannon diversity and for the inverse of species evenness. Species richness was modeled with Gaussian error. Previous work by Bishop et al. (2010), which influenced experimental design in this study, employed asymmetrical ANOVA and PERMANOVA to partition the variation from different types of material and different "dosage" levels while also accounting for overall treatment effects. Experiment 1 in our study was not fully orthogonal, as combined effects of macroalgae and shell material were only evaluated at one "dosage" level (100 ml of each). Non-normality in several response variables also prevented the specific post-hoc calculations (for mean sum of squares and traditional test statistics) that are required for asymmetrical ANOVA (Winer, 1971). We instead ran an overarching model for all treatments, followed by post-hoc analyses to compare the effect of material type and amount on the response of macrofaunal assemblages. For Experiment 1, this included four post-hoc models. Post-hoc model 1 tested for differences between the undisturbed control and other treatments. Post-hoc model 2 was applied only to orthogonal treatments, which included all plots receiving 100ml of one or both material types and the hand-churned control (+A, +S, +A/+S, I). Post-hoc models 3 and 4 compared the two levels of algal and shell additions, respectively, with the hand-churned control.

			Total Macrofaunal Abundance		**Species Richness**		**Shannon Diversity**		**Species Evenness**	
	Source	**df**	***F***	***P***	***F***	***P***	***F***	***P***	***F***	***P***
8-week samples	All Treatments	6	3.169	**0.007**	0.280	0.945	2.583	**0.023**	2.781	**0.016**
	Control vs Treatments	1	0.508	0.478	0.004	0.952	0.364	0.548	0.443	0.508
	Orthogonal Treatments	3	4.081	**0.011**	0.432	0.731	3.303	**0.027**	3.567	**0.020**
	Algae	1	8.603	**0.005**	0.104	0.748	4.700	**0.035**	5.299	**0.025**
	Shell	1	1.585	0.214	0.411	0.524	3.875	0.054	3.273	0.076
	Algae × Shell	1	2.056	0.158	0.781	0.381	1.333	0.254	2.130	0.150
	Level (+A)	2	7.558	**0.002**	0.387	0.682	2.885	0.068	3.193	0.052
	Level (+S)	2	0.223	0.801	0.900	0.415	0.466	0.631	0.118	0.889
16-week samples	All Treatments	6	0.335	0.917	0.963	0.455	0.836	0.545	0.791	0.579
	Control vs Treatments	1	0.108	0.743	1.552	0.216	0.180	0.672	0.574	0.451
	Orthogonal Treatments	3	0.261	0.853	2.125	0.108	1.094	0.360	1.146	0.339
	Algae	1	0.489	0.488	0.459	0.501	1.398	0.242	1.823	0.183
	Shell	1	0.007	0.935	3.776	0.057	1.385	0.245	0.333	0.567
	Algae × Shell	1	0.288	0.594	2.141	0.149	0.499	0.483	1.282	0.263
	Level (+A)	2	0.206	0.815	0.304	0.740	0.290	0.750	0.151	0.860
	Level (+S)	2	0.578	0.566	3.198	0.052	0.255	0.776	0.271	0.764

Table 4. Non-linear models and parameter estimates describing the decrease in chlorophyll and phaeopigment concentrations in sediments following the addition of shredded red macroalgae. Models were fit based on repeated measurements of chlorophyll and phaeopigments in Treatment A plots within the first week of Experiment 2.

Model	**Formula**	**Chlorophyll**		**Phaeopigments**	
		Corr.	**AIC**	**Corr.**	**AIC**
Simple exponential	e^{t}	0.32	131.8	0.49	109.9
2-par Exponential	$I_0 e^{-kt}$	0.53	127.3	0.56	107.9
3-par Exponential	$I_{max} + (I_0 - I_{max})e^{-kt}$	**0.54**	**128.9**	*no convergence*	
Logistic	$I_{max}/(1 + e^{-kt})$	0.54	128.9	0.66	105.8
Quadratic	$t + t^2$	0.52	127.7	0.59	106.9
Cubic	$t + t^2 + t^3$	0.52	127.7	0.59	106.9
Gaussian Peak	$I_0 + I_{max} e^{-(t/\beta)^2}$	*no convergence*		**0.78**	**100.6**

Table 5. *F* and *p*-value estimates from GLMs for total macrofaunal abundance, species richness, Shannon diversity, and species evenness in Experiment 3 after 3 weeks (top half of table) and 7 weeks (bottom half of table). Selected models used a gamma error structure for total macrofaunal abundance and for the inverse of Shannon diversity. Species richness and the inverse of species evenness were modeled with Gaussian error. The table presents results from an overarching model, labelled "All treatments", as well as those from post-hoc tests that partition variation associated with treatment type (addition versus control), frequency (single versus weekly), and the interaction between type and frequency.

			Total Macrofaunal Abundance		**Species Richness**		**Shannon Diversity**		**Species Evenness**	
	Source	**df**	***F***	***P***	***F***	***P***	***F***	***P***	***F***	***P***
3-week samples	All Treatments	3	7.904	**<0.001**	7.432	**<0.001**	6.080	**0.001**	0.116	0.951
	Type	1	19.269	**<0.001**	16.667	**<0.001**	14.648	**<0.001**	0.085	0.772
	Frequency	1	0.535	0.468	0.913	0.344	0.876	0.354	0.016	0.898
	Type × Frequency	1	3.908	0.053	4.716	**0.034**	2.715	0.105	0.246	0.622
7-week samples	All Treatments	3	4.629	**0.006**	6.478	**0.001**	1.688	0.181	1.258	0.298
	Type	1	12.305	**<0.001**	11.199	**0.002**	0.800	0.375	3.369	0.072
	Frequency	1	0.200	0.656	4.884	0.032	3.359	0.073	0.002	0.961
	Type × Frequency	1	1.383	0.245	3.353	0.073	0.904	0.346	0.403	0.528

Table 6. PERMANOVA results for 3-week and 7-week samples in Experiment 3. Experiment 3 involved four treatments: an algal addition and coinciding control treatment that were modified only once at the start of the experiment, and an algal addition and control treatment that were modified on a weekly basis for the duration of the experiment.

	Source	df	MS	*F*	R2	*P*	Contrasts
3-week samples	All Treatments	3	0.239	2.655	0.133	**0.001**	A2 ≠ C2 ≠
	Type	1	0.373	4.147	0.069	**0.002**	A1 = C1)
	Frequency	1	0.123	1.365	0.023	0.199	
	Type × Frequency	1	0.221	2.452	0.041	**0.017**	
	Residuals	52	0.090		0.867		
	Total	55			1.000		
7-week samples	All Treatments	3	0.420	4.208	0.195	**0.001**	A2 ≠ C2 ≠
	Type	1	0.680	6.815	0.105	**0.001**	A1 = C1)
	Frequency	1	0.280	2.802	0.043	**0.017**	
	Type × Frequency	1	0.300	3.006	0.047	**0.012**	
	Residuals	52	0.100		0.805		
	Total	55			1		

Table 7. Results from SIMPER analysis conducted for 3-week and 7-week samples in Experiment 3. SIMPER comparisons are reported only for combinations of treatments that differed significantly in PERMANOVA tests (Table 6). A1 and C1 represent algal addition and control plots that were modified only once, at the start of the experiment. A2 and C2 represent algal addition and control plots that were modified on a weekly basis for the duration of Experiment 3.

		Average Abundance				**Dissimilarity**			
	Species	**A1**	**C1**	**A2**	**C2**	**A2:C2** (Avg ± SD)		**A1:A2** (Avg ± SD)	
3-week samples	*Alvania* sp.	15	15	5	18	0.088	0.060	0.093	0.096
	Rochefortia tumida	13	18	17	19	0.100	0.058	0.087	0.051
	Euphilomedes sp.	9	14	6	14	0.061	0.049	0.059	0.057
	Nutricola tantilla	14	19	14	18	0.046	0.035	0.039	0.033
	Lirularia sp.	5	5	4	5	0.020	0.016	0.024	0.019
	Clinocardium sp.	3	3	3	3	0.017	0.013	0.021	0.017
	Amphipods	2	2	0	3	0.020	0.020	0.014	0.015
			Overall Dissimilarity:			0.467		0.453	
7-week samples	*Alvania* sp.	19	28	12	29	0.171	0.119	0.137	0.097
	Euphilomedes sp.	9	12	2	9	0.053	0.036	0.069	0.048
	Nutricola tantilla	10	15	11	19	0.084	0.066	0.051	0.039
	Lirularia sp.	5	7	8	7	0.033	0.026	0.048	0.033
	Rochefortia tumida	6	6	3	6	0.032	0.023	0.043	0.033
	Lacuna sp.	1	1	4	2	0.020	0.033	0.024	0.042
			Overall Dissimilarity:			0.528		0.506	

Table 8. Comparison of the response of the 12 most common species across all experiments to the addition of algae on either a weekly or one-time (single) basis. The first two lines of the table designate the frequency of algal additions and the time until core samples were collected. The bottom row of the table details from which experiment the information is derived (E1: Experiment 1, E2: Experiment 2, E3: Experiment 3). The table summarizes results (0 no change, - significant negative change, + significant positive change) from only the low dosage (100-120ml) algal treatments and experimental controls (and does not include the combined algae and shell addition treatment in E1). Insufficient numbers of amphipods across all treatments in 7-week samples from Experiment 3 prevented us from discerning the effect of either weekly or single algal additions on this taxa and sampling period.

Frequency of algal additions:		**Weekly**		**Single**			
Time until collection:	**1wk**	**3wks**	**7wks**	**3wks**	**7wks**	**8wks**	**16wks**
Alvania sp.	0	-	-	0	0	+	0
Amphipods	0	-	*na*	0	*na*	0	0
Clinocardium sp.	0	0	0	0	0	0	0
Euphilomedes sp.	0	-	-	0	0	0	0
Goniadids	0	-	-	0	0	0	0
Lacuna sp.	0	0	0	0	0	0	0
Lirularia sp.	0	0	0	0	0	0	0
Nutricola tantilla	0	0	-	0	0	0	0
Parvilucina tenuisculpta	0	0	-	0	0	0	0
Rochefortia tumida	0	0	-	0	0	0	0
Spiochaetopterus costarum	0	0	0	0	0	0	0
Tellina sp.	0	-	-	0	0	0	0
Experiment	*E2*	*E3*	*E3*	*E3*	*E3*	*E1*	*E1*

Figures

Figure 1. Map of field sites for photoquadrat and sediment surveys. Photoquadrats were collected from all sites marked by a circle. At the two sites marked with triangles, sediment surveys were also conducted. All field experiments took place in a subtidal sand flat approximately 50m southeast of the artificial reef at Alki Pipeline (AP).

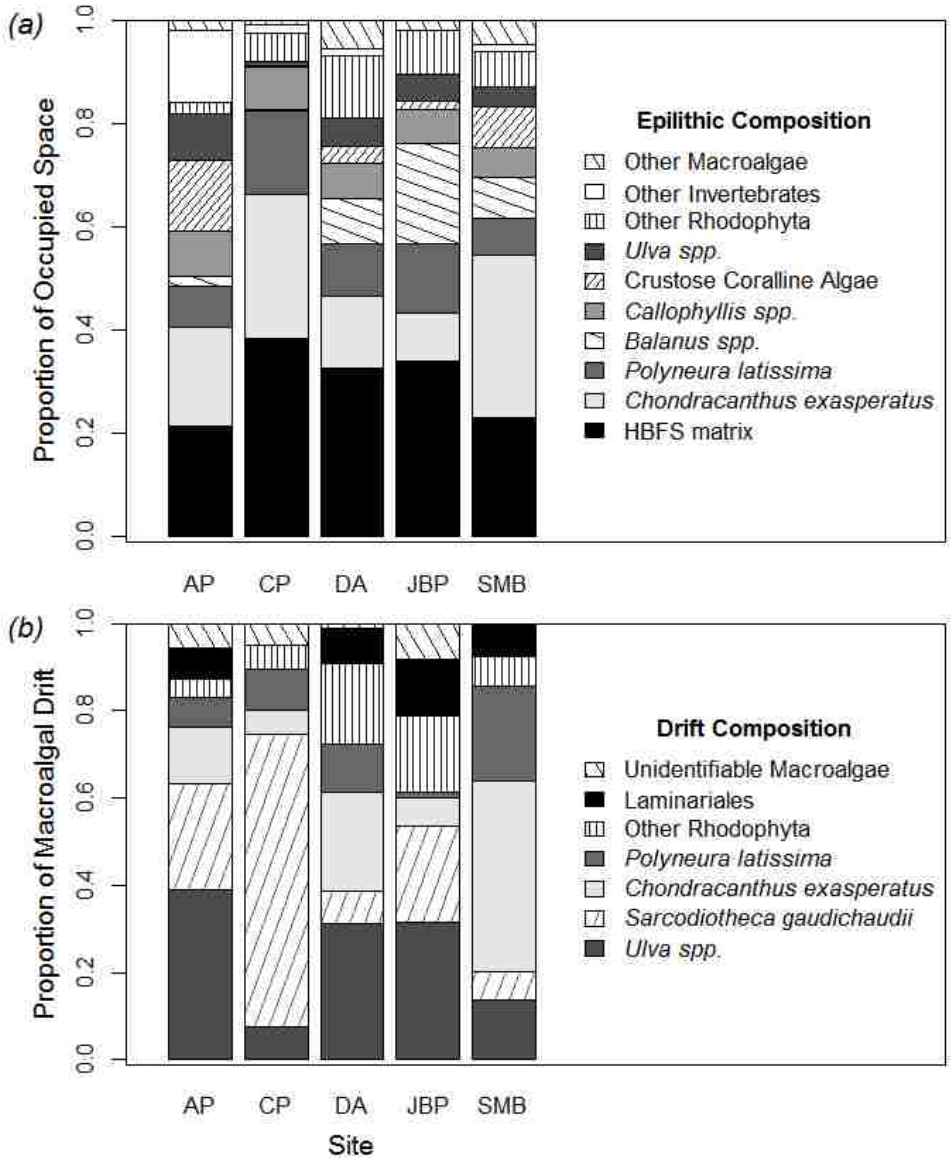

Figure 2. Epilithic composition on artificial structures (*a*) and the composition of drift macroalgae in surrounding sediments (*b*) from photoquadrats collected at five sites (AP: Alki Pipeline, CP: Centennial Park, DA: Don Armeni Boat Ramp, JBP: Jack Block Park, and SMB: Shilshole Marina Breakwater). Proportions were computed as the average relative percent cover from all transects within a site. On artificial structures, the most common space occupier was a low-lying matrix comprised of hydroids, bryozoans, filamentous macroalgae, or some combination of these groups, which was covered in fine sediments (abbreviated as HBFS matrix, and shown in black).

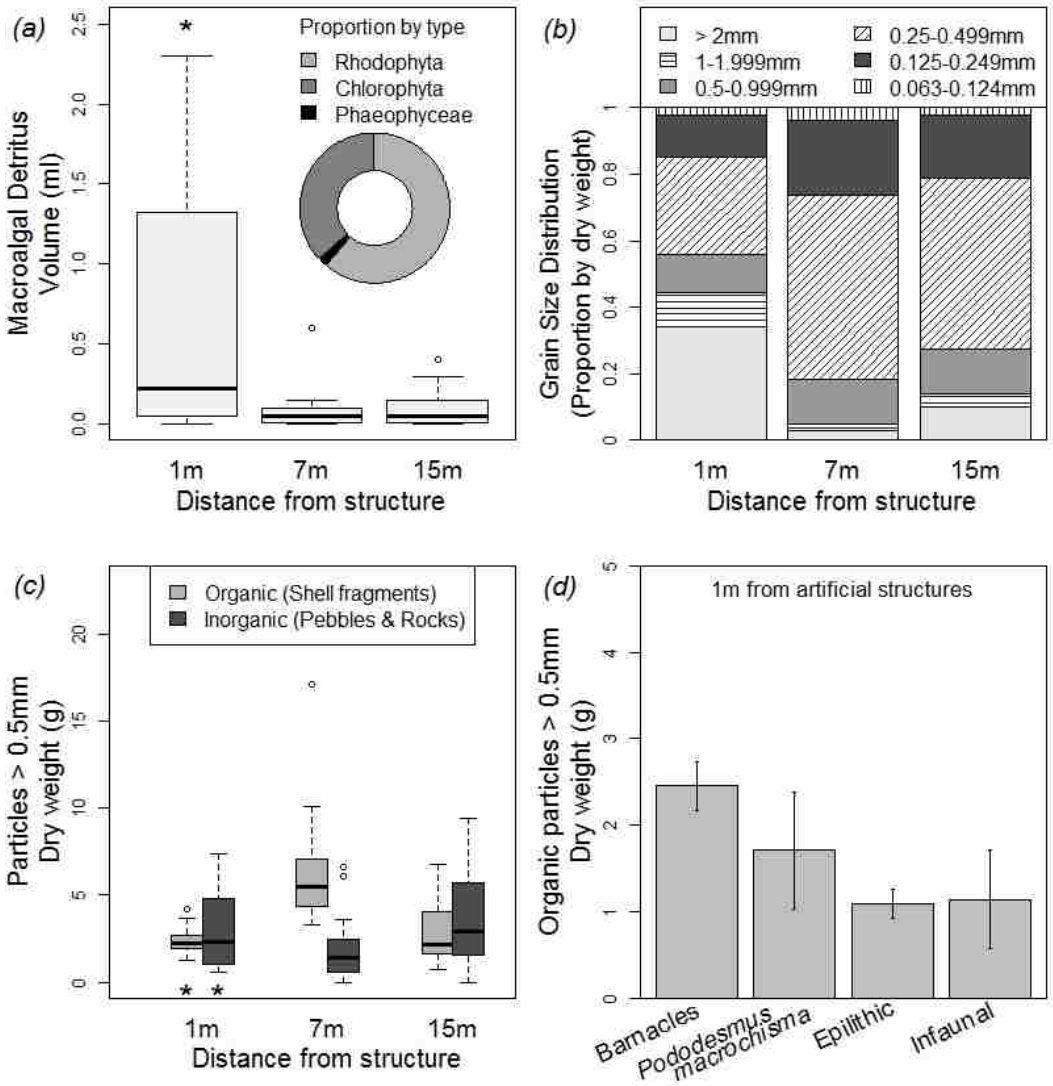

Figure 3. Macroalgal detritus load and sediment characteristics from core samples collected 1, 7, and 15m from artificial structures. (*a*) Volume of macroalgal detritus (ml per core) versus distance from artificial structures. In the upper right hand corner of (*a*), we present the proportion of total volume identified as originating from Rhodophyta, Chlorophyta, and Phaeophyceae. (*b*) Grain size distribution of sediment core samples collected at each distance from artificial structures. (c) Dry weight (g per core) of coarse particles (> 0.5mm) that comprised organic material, such as fragments from shells and calcareous tubes, and inorganic material, such as pebbles and rocks, at each distance from artificial structures. (*d*) The composition of organic coarse particles (>0.5mm) in core samples collected 1m from artificial structures. Chlorophyll and phaeopigment concentrations were not evaluated from core samples.

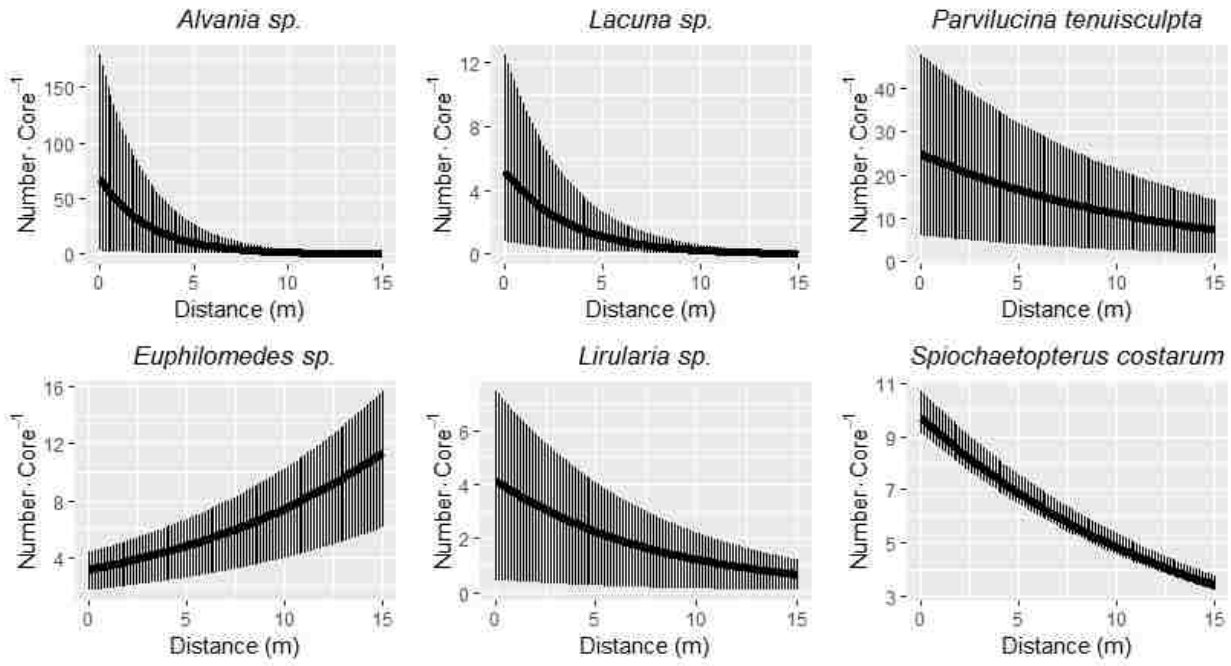

Figure 4. Abundance of macrofaunal with increasing distance from the artificial structure at AP: gastropods *Alvania sp.*, *Lacuna sp.*, and *Lirularia sp.*, ostracods, *Euphilomedes sp.*, bivalves, *Parvilucina tenuisculpta*, and polychaetes, *Spiochaetopterus costarum*. These were the six most abundant species in sediment surveys for which there was a significant relationship between abundance and distance in quasi-Poisson GLM models (Appendix 2). Solid lines represent the mean estimate; The area between the first and third quantiles of model estimates is shaded with vertical lines.

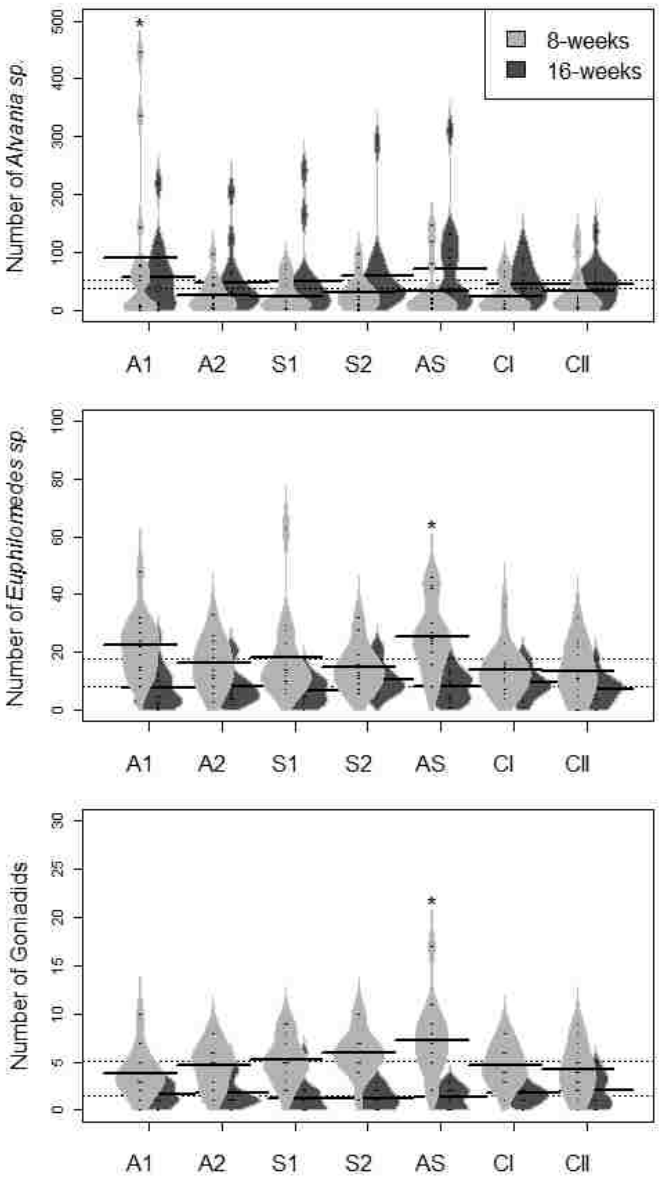

Figure 5. Abundance of the gastropod, *Alvania* sp., *Euphilomedes* sp. ostracods, and goniad polychaetes by treatment after 8 weeks (light gray) and 16 weeks (dark gray), the three species for which there were significant differences between experimental treatments in Experiment 1; treatments that differed significantly from at least one of the others in post-hoc tests are marked on the graphs by (*). Treatment codes are provided in Table 1. 'A' represented algal additions, 'S' represented additions of shell fragments, and CI and CII were the hand-churned and undisturbed controls, respectively.

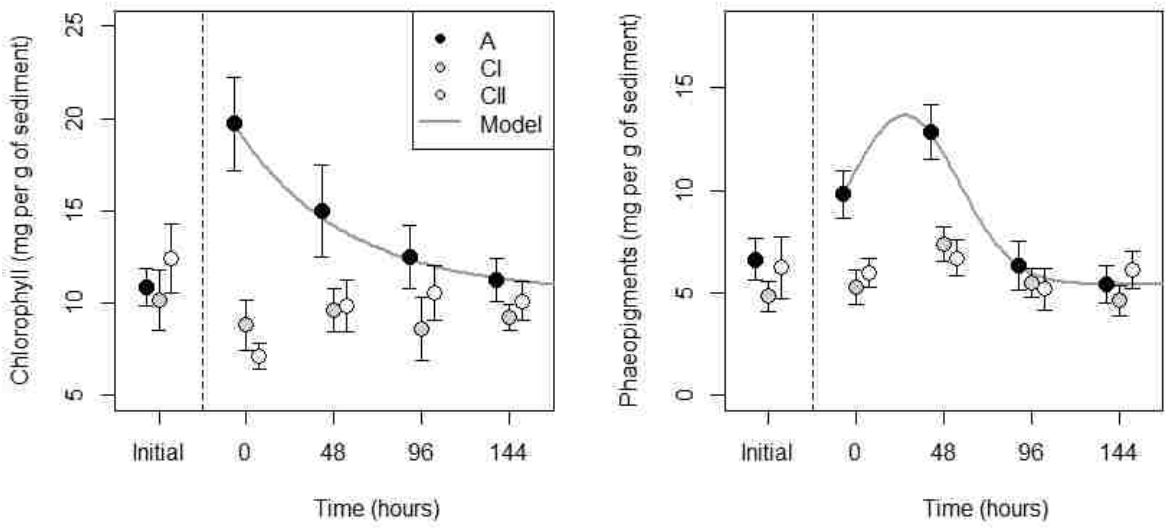

Figure 6. Sediment chlorophyll and phaeopigment concentrations in plots receiving algal additions (A, black circles), hand-churned controls (CI, gray circles), and undisturbed controls (CII, white circles) over the first week following the start of Experiment 2. Gray lines represent the mean estimates from best-fit non-linear models applied to treatment A data and selected based on AIC. The best fit non-linear model was an exponential curve with three parameters for chlorophyll (parameter estimates: I_0 = 10.492, I_{max} = 19.7, ln(c) = -4.098) and a gaussian peak function with four parameters for phaeopigments (I = 5.412, I_{max} = 8.50, t_0 = 33.446, β = 42.174).

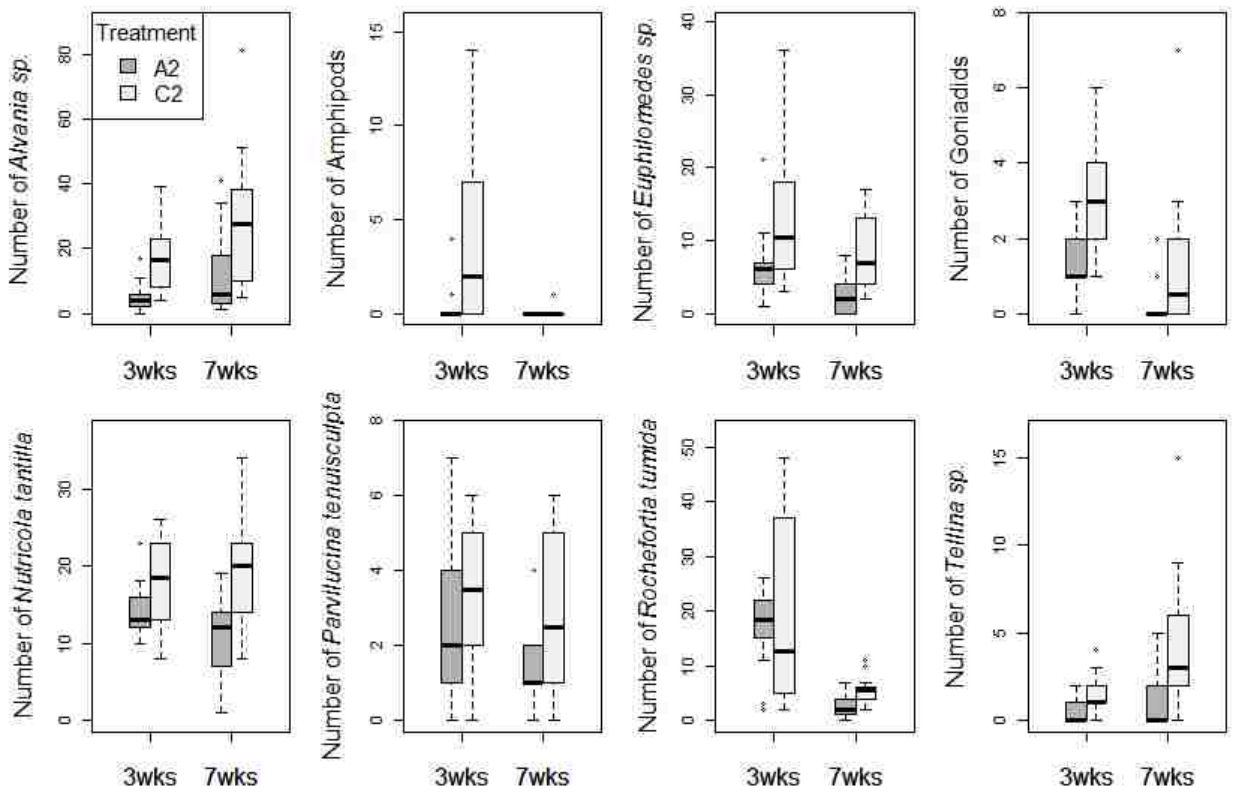

Figure 7. Abundance of eight taxa after 3 and 7 weeks in plots receiving weekly algal additions (A2, dark gray) and in weekly hand-churned control plots (C2, light gray) in Experiment 3. Species included in the plot are those for which there was a significant effect from weekly algal additions (see Table 8). Treatments A1 and C1 (see Table 1), for which there were no significant differences in macrofaunal abundances, are excluded from the plot to conserve space.

Supplementary material

APPENDIX 1. Detailed summary of findings from photoquadrat surveys conducted at five sites in the Seattle Metropolitan Area.

Table S1. Taxanomic group, species, percent cover (mean and standard deviation), and proportion of epilithic cover (i.e. – not including bare space; mean and standard deviation) from photoquadrat surveys. Taxa are listed from highest to lowest percent cover. Data are summarized across all sites and transects.

Species	Phylum / Taxonomic Group	Total Percent Cover		Proportion of Epilithic Cover	
		Mean	SD	Mean	SD
Hydroid-Bryozoan-Filament Matrix	Multiple	20.43%	8.27%	30.68%	13.47%
Chondracanthus exasperatus	Rhodophyta	14.12%	15.24%	19.43%	19.70%
Polyneura latissima	Rhodophyta	7.42%	12.24%	9.98%	14.71%
Balanus glandula	Arthropoda	5.76%	8.39%	8.82%	13.11%
Callophyllis spp.	Rhodophyta	4.94%	4.81%	7.14%	6.88%
Crustose Coralline Algae	Rhodophyta	3.80%	5.66%	5.90%	9.46%
Ulva spp.	Chlorophyta	3.39%	6.21%	4.76%	7.73%
Sarcodiotheca gaudichaudii	Rhodophyta	1.45%	3.87%	2.29%	5.93%
Mazzaella splendens	Rhodophyta	1.24%	4.11%	1.65%	5.25%
Metridium farcimen	Cnidaria	1.22%	7.99%	1.74%	10.93%
Unidentified encrusting red algae	Rhodophyta	0.96%	3.85%	1.35%	5.06%
Kelp (unidentifed Laminariales)	Phaeophyta	0.95%	5.25%	1.13%	6.00%
Agarum fimbriatum	Phaeophyta	0.70%	5.18%	0.77%	5.39%
Plocamium cartilagineum	Rhodophyta	0.63%	1.74%	0.94%	2.65%
Serpulidae	Annelida	0.36%	1.18%	0.58%	1.95%
Unidentified red filamentous algae	Rhodophyta	0.30%	2.77%	0.34%	3.13%
Rhodymenia spp.	Rhodophyta	0.29%	2.06%	0.37%	2.63%
Unidentified macroalgae	Unknown	0.28%	1.16%	0.42%	1.79%
Pododesmus machrochisma	Mollusca	0.22%	0.94%	0.36%	1.48%
Hydroids	Cnidaria	0.20%	0.77%	0.27%	0.99%
Saccharina latissima	Phaeophyceae	0.18%	1.67%	0.25%	2.31%
Gloiocladia laciniata	Rhodophyta	0.12%	0.81%	0.13%	0.96%
Sponge unidentified	Porifera	0.09%	0.32%	0.13%	0.48%
Fucus distichus	Phaeophyceae	0.07%	0.66%	0.09%	0.86%
Encrusting bryozoans (unidentified)	Bryozoa	0.05%	0.20%	0.07%	0.28%
Branching Bryozoan	Bryozoa	0.04%	0.19%	0.06%	0.29%
Unidentified red foliose algae	Rhodophyta	0.04%	0.36%	0.06%	0.51%
Bugula californica	Bryozoa	0.04%	0.20%	0.06%	0.31%
Thelepus/Neoamphitrite	Annelida	0.04%	0.25%	0.05%	0.34%
Psolus chitonodes	Echinodermata	0.03%	0.29%	0.04%	0.40%

Table S1 (*continued*). Taxanomic group, species, percent cover (mean and standard deviation), and proportion of epilithic cover (i.e. – not including bare space; mean and standard deviation) from photoquadrat surveys. Taxa are listed from highest to lowest percent cover. Data are summarized across all sites and transects.

Species	Phylum / Taxonomic Group	Total Percent Cover		Proportion of Epilithic Cover	
		Mean	SD	Mean	SD
Crucigera zygophora	Annelida	0.03%	0.26%	0.05%	0.42%
Cnemidocarpa finmarkiensis	Chordata	0.02%	0.18%	0.03%	0.28%
Branching Coralline Algae	Rhodophyta	0.01%	0.12%	0.02%	0.15%
Dodecaceria concharum	Annelida	0.01%	0.11%	0.02%	0.17%
Chelyosoma columbianum	Chordata	0.01%	0.07%	0.01%	0.10%

Table S2. Number of photoquadrats collected on hard-substrate and soft-substrate at each site. Sample sizes are presented separately for transect 1, 2, and 3 (separated by commas). Single quadrats from transects 1 and 2 at Don Armeni Boat Ramp (DA) were excluded from data due to poor camera focus.

		Hard Substrate		**Soft Substrate**		**Total # Quadrats**
Site name	**Abbrev.**	Total	By Transect	Total	By Transect	
Alki Pipeline	AP	16	4, 6, 6	14	6, 4, 4	30
Centennial Park	CP	13	4, 4, 5	17	6, 6, 5	30
Don Armeni Boat Ramp	DA	14	2, 6, 6	14	7, 3, 4	28
Jack Block Park	JBP	20	4, 7, 9	10	6, 3, 1	30
Shilshole Marina Breakwater	SMB	20	6, 7, 7	10	4, 3, 3	30

APPENDIX 2. Supplementary statistical analyses for macroalgal detritus and sediment characteristics from sediment surveys conducted at AP and EBM.

Table S3. Average percentage (± standard error) of particles in each size category at three different distances from artificial structures (1, 7, and 15m) in sediment surveys conducted at AP and EBM.

		Distance from structure								
	Particle Size	1m			7m			15m		
AP	>2mm	41.7%	±	13.0%	1.0%	±	0.5%	3.3%	±	2.0%
	1-1.999mm	8.1%	±	2.1%	2.5%	±	1.2%	2.7%	±	1.0%
	0.5-0.999mm	7.9%	±	2.2%	10.1%	±	2.8%	8.7%	±	1.6%
	0.25-0.499mm	27.4%	±	7.1%	61.6%	±	1.2%	57.6%	±	2.3%
	0.125-0.249mm	13.4%	±	4.7%	24.3%	±	3.9%	26.9%	±	2.1%
EBM	>2mm	26.7%	±	4.7%	18.9%	±	9.2%	2.4%	±	0.6%
	1-1.999mm	12.5%	±	1.6%	5.4%	±	1.2%	1.7%	±	0.3%
	0.5-0.999mm	14.6%	±	1.8%	17.1%	±	2.1%	18.1%	±	1.2%
	0.25-0.499mm	31.0%	±	2.9%	40.6%	±	6.1%	52.5%	±	0.8%
	0.125-0.249mm	12.4%	±	3.7%	13.8%	±	1.8%	18.8%	±	1.0%
	>0.1249mm	2.9%	±	0.2%	4.1%	±	0.8%	6.5%	±	0.5%

Table S4. Multivariate analyses from sediment core surveys. (*a*) PERMANOVA results for the relative composition of macroalgal detritus in core samples collected at 1, 7, and 15m from artificial structures. Macroalgae were extracted from sediment cores, examined under the dissecting scope and placed in the following categories based on color: Rhodophyta, Chlorophyta, Phaeophyceae, Unknown. PERMANOVA was performed only on core samples where macroalgal detritus were present; samples lacking macroalgal detritus were excluded from this analysis. (b) PERMANOVA results for sediment grain size distribution, showing significant effects from Site, Distance, and Transect. (c) Results from a PERMANOVA for the composition of organic coarse particles. (d) PERMANOVA results for macrofaunal composition across three transects and with increasing distance from the artificial structure at AP.

Source	df	SS	MS	Pseudo-F	R^2	P
(a) Composition of macroalgal detritus						
Site	1	0.188	0.188	2.197	0.050	0.134
Distance	1	0.229	0.229	2.669	0.061	0.101
Transect (w/in Site)	4	0.158	0.039	0.461	0.042	0.807
Residuals	37	3.167	0.086		0.846	
Total	43	3.742			1.000	
(c) Grain Size Distribution						
Site	1	0.367	0.367	6.771	0.074	0.001
Distance	1	1.321	1.321	24.346	0.266	0.001
Transect (w/in Site)	4	0.730	0.183	3.366	0.147	0.008
Residuals	47	2.550	0.054		0.513	
Total	53	4.968			1.000	
(c) Composition of shell fragments						
Site	1	0.956	0.956	11.412	0.145	0.001
Distance	1	0.807	0.807	9.636	0.122	0.001
Transect (w/in Site)	4	0.744	0.186	2.220	0.112	0.006
Residuals	49	4.104	0.084		0.621	
Total	55	6.610			1.000	
(d) Macrofaunal composition						
Transect	2	0.7111	0.3555	2.3705	0.1520	0.0070
Distance	1	0.5165	0.5165	3.4439	0.1104	0.0020
Residuals	23	3.4495	0.1500		0.7375	
Total	26	4.6771			1.0000	

Table S5. Model F and P statistics for total macrofaunal abundance, diversity metrics, and the abundances of the twelve most abundant taxa in core samples collected during observation surveys at AP. Model output is provided with respect to two factors: Transect (3 levels: A, B, C) and Distance from the pipeline structure. The nature of significant relationships between individual species abundances and distance from the structure are presented in Figure 4.

		Transect		Distance	
Variable	**Distribution**	***F***	***P***	***F***	***P***
Total Macrofaunal Abundance	Gamma	13.589	**0.000**	13.155	**0.001**
Species Richness	Gaussian	2.936	0.073	1.822	0.190
Shannon Diversity	Gamma	0.663	0.525	0.530	0.474
Species Evenness	Gaussian	0.850	0.441	3.930	0.060
Individual Species Abundances					
Alvania sp.	quasi-Poisson	27.261	**<0.001**	30.842	**<0.001**
Amphipods	quasi-Poisson	8.823	**0.012**	0.001	0.976
Euphilomedes sp.	quasi-Poisson	3.737	0.154	6.528	**0.011**
Goniadids	quasi-Poisson	0.270	0.874	3.260	0.071
Lacuna sp.	quasi-Poisson	7.920	**0.019**	10.570	**0.001**
Lirularia sp.	quasi-Poisson	8.084	**0.018**	5.090	**0.024**
Nutricola tantilla	quasi-Poisson	16.723	**<0.001**	3.641	0.056
Parvilucina tenuisculpta	quasi-Poisson	20.658	**<0.001**	7.604	**0.006**
Pectinariids	quasi-Poisson	2.537	0.281	2.447	0.118
Rochefortia tumida	quasi-Poisson	1.945	0.378	0.885	0.347
Spiochaetopterus costarum	quasi-Poisson	0.331	0.847	9.094	**0.003**
Tellina sp.	quasi-Poisson	2.842	0.242	0.309	0.578

APPENDIX 3. Additional statistical analyses for Experiments 1, 2, and 3.

Table S6. Results from supplementary PERMANOVA and SIMPER analyses performed to evaluate temporal patterns in community composition in Experiment 1. Macrofauna abundances were determined 8 and 16 weeks after the addition of shredded red macroalgae and/or shell fragments to experimental plots.

PERMANOVA						
Source	***df***	**SS**	**MS**	***F***	***R2***	***P***
Treatment	6	0.719035	0.119839	1.048394	0.027933	0.374
Date	7	4.218875	0.602696	5.272593	0.163892	0.001
Residuals	182	20.80395	0.114307		0.808176	
Total	195	25.74186			1	

SIMPER	**Abundance**		**Contribution to Dissimilarity**		
Species	8 weeks	16 weeks	Avg	SD	Cumulative
Alvania sp.	37.06	52.96	0.18	0.15	0.35
Rochefortia tumida	4.83	17.15	0.06	0.05	0.46
Euphilomedes sp.	17.78	8.38	0.05	0.05	0.55
Nutricola tantilla	20.60	16.19	0.05	0.05	0.65
Tellina sp.	1.33	9.71	0.04	0.03	0.72

Table S7. Univariate and multivariate analyses for macrofauna in algal addition versus control plots after 1 week in Experiment 2. Only F/Pseudo-F statistics and p-values are presented to conserve space.

Variable	Model	*F*	*P*	Contrasts
Total Macrofaunal Abundance	ANOVA	0.414	0.665	
Species Richness	ANOVA	2.331	0.116	
Shannon Diversity	Gamma	1.725	0.197	
Species Evenness	Gamma	0.029	0.971	
Multivariate Dispersion	ANOVA	1.603	0.220	
Multivariate Composition	PERMANOVA	1.086	0.364	
Individual Species Abundances				
Alvania sp.	quasi-Poisson	0.406	0.671	
Amphipods	quasi-Poisson	0.048	0.953	
Clinocardium sp.	quasi-Poisson	0.342	0.713	
Euphilomedes sp.	quasi-Poisson	1.757	0.192	
Goniadids	quasi-Poisson	3.693	**0.038**	CI < CII = A
Leitoscoloplos/Scoloplos (Orbiniid)	quasi-Poisson	0.083	0.921	
Lirularia sp.	quasi-Poisson	0.896	0.420	
Nephtyids	quasi-Poisson	1.790	0.186	
Nereids	quasi-Poisson	1.468	0.248	
Nutricola tantilla	quasi-Poisson	0.264	0.770	
Rochefortia tumida	quasi-Poisson	0.081	0.922	
Tellina sp.	quasi-Poisson	1.213	0.313	

Table S8. Results from the mixed effects linear model used to compare chlorophyll and phaeopigment levels between treatments in Experiment 2. Oral syringes of sediment were collected on Day 1, 3, 5, and 7 following algal additions and evaluated for chlorophyll and phaeopigment concentrations using fluorometric analysis.

Source	df	SS	MS	F	P	Contrasts
(a) Chlorophyll						
Treatment	2	369.881	184.941	11.254	**<0.001**	A > CI = CII
Date	3	194.892	64.964	3.953	0.008	
(b) Phaeopigments						
Treatment	2	111.590	55.795	8.356	**<0.001**	A > CI = CII
Date	3	64.793	21.598	3.235	0.021	

Table S9. Quasi-Poisson GLM results for the 12 most common species in Experiment 3. The table presents the degrees of freedom (df), estimated F statistic (*F*), and p-value (*P*) for a model with one parameter ("All Treatments"), and a two-parameter post-hoc comparison in which variation is partitioned by Treatment Type (algal addition versus control), Treatment Frequency (Single or Weekly), and the interaction between Type and Frequency.

			Alvania sp.		*Clinocardium* sp.		*Euphilomedes* sp.		Goniadids	
	Source	**df**	***F***	***P***	***F***	***P***	***F***	***P***	***F***	***P***
3-week samples	All Treatments	3	4.836	**0.005**	0.008	0.999	4.409	**0.008**	4.505	**0.007**
	Type	1	4.927	**0.031**	0.013	0.911	11.294	**0.001**	2.357	0.131
	Frequency	1	1.264	0.266	0.013	0.911	0.965	0.330	4.773	**0.033**
	Type × Frequency	1	8.316	**0.006**	0.000	0.999	0.967	0.330	6.385	**0.015**
7-week samples	All Treatments	3	2.800	**0.049**	2.203	0.099	10.921	**<0.001**	3.470	**0.023**
	Type	1	7.028	**0.011**	0.448	0.506	12.584	**0.001**	1.947	0.169
	Frequency	1	0.346	0.559	0.000	1.000	12.987	**0.001**	3.351	0.073
	Type × Frequency	1	1.026	0.316	6.160	**0.016**	7.192	**0.010**	5.112	**0.028**

			Lacuna sp.		*Lirularia* sp.		*Nutricola tantilla*		*Parvilucina tenuisculpta*	
	Source	**df**	***F***	***P***	***F***	***P***	***F***	***P***	***F***	***P***
3-week samples	All Treatments	3	1.062	0.373	0.431	0.732	3.259	**0.029**	1.153	0.337
	Type	1	0.061	0.806	0.180	0.673	9.670	**0.003**	3.298	0.075
	Frequency	1	0.976	0.328	0.109	0.743	0.023	0.879	0.035	0.852
	Type × Frequency	1	2.148	0.149	1.004	0.321	0.082	0.775	0.125	0.725
7-week samples	All Treatments	3	3.652	**0.018**	2.175	0.102	6.052	**0.001**	4.531	**0.007**
	Type	1	1.818	0.183	0.254	0.616	14.267	**<0.001**	9.563	**0.003**
	Frequency	1	7.614	**0.008**	3.247	0.077	3.339	0.073	1.870	0.177
	Type × Frequency	1	1.524	0.223	3.023	0.088	0.549	0.462	2.161	0.148

			Pectinariids		*Rochefortia tumida*		*Spiochaetopterus costarum*		*Tellina* sp.	
	Source	**df**	***F***	***P***	***F***	***P***	***F***	***P***	***F***	***P***
3-week samples	All Treatments	3	3.075	**0.036**	0.703	0.555	3.063	**0.036**	4.176	**0.010**
	Type	1	7.926	**0.007**	1.201	0.278	7.908	**0.007**	2.511	0.119
	Frequency	1	0.062	0.805	0.684	0.412	1.270	0.265	4.171	**0.046**
	Type × Frequency	1	1.239	0.271	0.223	0.639	0.009	0.923	5.846	**0.019**
7-week samples	All Treatments	3	0.627	0.601	4.334	**0.008**	0.273	0.845	4.547	**0.007**
	Type	1	0.181	0.672	3.786	0.057	0.539	0.466	12.904	**0.001**
	Frequency	1	0.020	0.888	4.508	**0.039**	0.040	0.842	0.010	0.920
	Type × Frequency	1	1.680	0.201	4.710	**0.035**	0.240	0.626	0.726	0.398

CHAPTER 2: Urbanization-related distribution patterns and habitat-use by giant Pacific octopus (*Enteroctopus dofleini*)

Abstract

Urbanization is a process that heavily alters marine and terrestrial environments, though terrestrial urban ecosystems have been studied far more intensively. Terrestrial studies suggest that urbanization can facilitate mesopredators by enhancing food and shelter resources and reducing predation pressure from apex consumers. This in turn has considerable consequences for ecological communities. Characterizing marine mesopredator response to urbanization is important for understanding ecological structure and processes in urban marine ecosystems, and for anticipating how marine organisms will respond as urbanization increases in coastal zones. We evaluated spatial distribution patterns and habitat-use of the marine mesopredator, giant Pacific octopus (*Enteroctopus dofleini*), relative to terrestrial urbanization intensity in Puget Sound, Washington, USA. Using a combination of citizen-contributed REEF data and field surveys, we examined: (1) Whether the distribution of *E. dofleini* was related to urbanization, (2) Whether *E. dofleini* abundance related to the extent of anthropogenic debris in benthic habitats, and (3) Whether *E. dofleini* diets (as reflected by shell middens) differed as a function of urbanization and den habitat. Our results suggest that urbanization impacts may differ with depth. A mixed-effects logistic regression estimated greater probability of occurrence of *E. dofleini* as urbanization increased in deep-water habitats (> 24 m), and lower probability of occurrence in shallow habitats (< 18 m). Accompanying field surveys indicated that *E. dofleini* abundance was correlated with the number of benthic anthropogenic debris items, and that *E. dofleini* diets were not affected by urbanization intensity or den habitat. Though *E. dofleini* may be synanthropic within certain urban habitats, the mechanisms driving this pattern likely differ from those affecting common urban mesopredators on land, with den provisioning from man-made structures being more important than altered food resources. Further, experimental work is

needed to test these and alternative potential mechanisms behind octopus distribution patterns in urban areas. This study and future research it facilitates will build much needed knowledge of ecological responses to urbanization in the marine environment.

Introduction

Urbanization alters ecosystems globally, and is particularly intense in coastal regions, where more than half of the world's population resides and population growth rates are most rapid (Neumann et al., 2015). Most of what is known about the effects of urbanization on ecosystems is based on studies in terrestrial systems (Alberti et al., 2017; Aronson et al., 2014; Shochat et al., 2006). Knowledge of urban impacts in marine ecosystems is more limited (Beger et al., 2010; Bulleri, 2006), and much work is needed to discern whether urban ecology paradigms developed in terrestrial systems are applicable to the marine environment.

Effects from urbanization vary widely across terrestrial taxa (McKinney, 2002), and particularly across mid and high trophic consumers (Gehrt et al., 2010). For some consumer species, habitat degradation, landscape fragmentation, and other anthropogenic disturbances associated with urbanization lead to reduced gene flow, behavioral shifts, increased disease risk, and population declines (George and Crooks, 2006; Riley et al., 2007, 2006). For others, particularly certain mid-sized consumers, or "mesopredators", urbanization instead provides ecological benefits that increase population density, survivorship, and reproductive success (Bateman and Fleming, 2012; Prange and Gehrt, 2004). These so-called "synanthropic" mesopredators, such as raccoons, are commonly generalists, with broad dietary and habitat requirements (McKinney, 2002) that allow them to exploit food and shelter resources provided by human activities (Bateman and Fleming, 2012). Further, mesopredator dominance has considerable implications for ecosystem structure, function, and services (Prugh et al., 2009), potentially contributing to ecosystem homogenization in built environments.

Understanding the distribution and habitat use patterns of marine mesopredators relative to urbanization is important for anticipating how these organisms will respond to future

anthropogenic change. Marine urbanization changes natural habitats in ways that are both similar and distinct from changes on land (Dafforn et al., 2015). The introduction of marine artificial structures in urban areas fragments coastal habitats, potentially altering the connectivity of marine populations (Bishop et al., in press). Artificial structures support distinct assemblages of flora and fauna (F Bulleri and Chapman, 2010), and are commonly added to historically soft sediment environments, thus altering habitat heterogeneity (Heery et al., 2017). Urban waters tend to be nutrient-rich due to influx of organic material from human sources, and this can alter the abundance and composition of primary producers (Savage et al., 2010; Yasuhara et al., 2012). Further, marine urbanization leads to higher levels of chemical contaminants (Dafforn et al., 2013), noise pollution (Williams et al., 2015), and light pollution, which can cause behavioral changes in fish and sea turtles (Bolton et al., 2017; Gaston et al., 2012) and alter benthic community structure (Inglis and Kross, 2000). Each of these factors could potentially influence marine mesopredator dominance, which could in turn have ecosystem-level consequences. Few studies have directly evaluated marine mesopredator distribution patterns relative to urbanization (though see Miller et al., 2010; Vargas-Fonseca et al., 2016), and the extent to which marine urbanization may influence mesopredator population dynamics is presently unknown.

The purpose of this study was to identify whether there is a relationship between urbanization intensity and the distribution and habitat use of giant Pacific octopus, *Enteroctopus dofleini*. *E. dofleini* is the largest known octopod, with a maximum radial arm span of over 9 m (McClain et al., 2015), and is a prominent generalist mesopredator in nearshore habitats of the northeast Pacific (Hartwick et al., 1984). It has several traits in common with terrestrial synanthropic mesopredators (Bateman and Fleming, 2012), including behavioral flexibility, a high capacity for learning (Anderson and Mather, 2010), and the ability to utilize anthropogenic structures as

shelter, as has been documented among other octopods (Aronson, 1986; Katsanevakis and Verriopoulos, 2004). Conversely, *E. dofleini* are subject to bioaccumulation of urban contaminants (Anderson, 2003; Mann et al., 1988), may be heavily influenced by their acoustic environment (André et al., 2011), and could be negatively impacted by urbanization in ways that are yet unknown.

We evaluated *E. dofleini* distribution and habitat use across a gradient of urbanization in Puget Sound, Washington, USA. The Puget Sound region has undergone rapid growth and development over the last century, with a nearly 6-fold increase in population size, and 4 million people currently living within 20 km of the shoreline (Kelly et al., 2016). This has manifest in extensive artificial structures (Dethier et al., 2016), sediment contamination (Long et al., 2013; Long and Chapman, 1985), localized eutrophication (McDonald et al., 2015), and other marine habitat changes, particularly in the urban centers of Seattle and Tacoma. We addressed the following questions: (1) Is *E. dofleini* presence/absence related to urbanization intensity? (2) Is *E. dofleini* abundance related to the quantity of anthropogenic debris? and (3) Do *E. dofleini* diets (reflected by shell debris, or "midden" piles left outside of octopus dens) vary relative to urbanization intensity and den habitat? To pursue these objectives, we utilized a combination of citizen science data, quantitative modeling, spatial analyses, video transect surveys, and midden collections. Based on anecdotal observations during preliminary surveys, we hypothesized that urbanization-related distribution patterns would be depth-dependent, with more octopus sightings in deep sedimentary environments near cities. Additionally, we expected that octopus abundance would correlate with the density and extent of anthropogenic debris items in video surveys. Finally, we hypothesized that octopus diets would be less diverse in heavily urban areas.

Methods

Study Area

Puget Sound is a 2,642 km^2 fjordal system with estuarine circulation, located in Washington State, USA (Figure 1), at the Southern end of the Salish Sea. The Puget Sound region supports a population of over 4 million people (Puget Sound Partnership, 2015), with high density centers in Seattle and Tacoma. Subtidal benthic habitat in Puget Sound is largely sedimentary, though natural rocky outcrops also occur in some locations (Burns, 1985; Shipman, 2008). Artificial structures, such as large artificial reefs and anthropogenic debris objects, are also common (Buckley and Hueckel, 1989). Data included in this study spanned from Olympia to Admiralty Inlet, WA, and were collected from relatively shallow subtidal habitats (< 50 m) via SCUBA.

Spatial/Temporal Distribution Patterns

REEF Data – We evaluated *E. dofleini* distribution patterns using citizen-contributed data from the Reef Environmental Education Foundation (REEF). Since 2000, REEF has trained recreational divers and overseen a subtidal data collection program in the Puget Sound region. Trained divers rove dive sites and count marine organisms using an order-of-magnitude scoring system (1: single individual, 2: 2-10 individuals, 3: 11-100 individuals, 4: > 100 individuals). For this analysis, only data from REEF divers designated as "experts" (REEF Experience Levels 4 and 5) were used. Between January 1, 2000 and January 10, 2016, expert REEF divers conducted 5792 surveys across 176 sites throughout Puget Sound. The maximum depth of survey dives ranged from 3 to 45 m, with a mean of approximately 20 m.

E. dofleini tends to have relatively large home ranges and low densities (Scheel et al., 2007), and REEF data for *E. dofleini* were zero-inflated, with most sightings (63%) receiving an order-

of-magnitude score of 1 (single individual observed). Though past studies have used REEF's order-of-magnitude data to derive estimates of abundance for other mobile invertebrates and for demersal fish (Cooper, 2014; Schultz et al., 2016; Wolfe and Pattengill-Semmens, 2013), the structure of the data for *E. dofleini* made it difficult to produce abundance estimates with a sufficient level of certainty. We instead derived presence/absence for each REEF survey, with surveys with an octopus sighting (order-of-magnitude abundance scores 1-4) recorded as 1 and surveys without octopus sightings recorded as 0.

Model predictors – E. dofleini presence/absence was evaluated with respect to three types of predictor variables: (1) Survey-specific variables, (2) Temporal variables, and (3) Urbanization-related variables. Survey-specific variables included bottom time, bottom temperature, visibility, maximum depth, and habitat type (Appendix 1). Temporal variables included the month, year, and two temperature-related indices previously found to correlate with *E. dofleini* abundance (Scheel 2015): Optimum Interpolation Sea Surface Temperature (SST; NOAA, 2016) and monthly Pacific Decadal Oscillation (PDO) index (NOAA, 2016b).

Urbanization intensity can be represented by a variety of different metrics and proxies, which have been discussed extensively in the literature (for examples, see Alberti et al., 2007; Deng et al., 2009; Luck and Wu, 2002). We considered two separate urbanization indices and one metric for the level of shoreline armoring as predictor variables. Urbanization indices included a Population Proximity Index (PPI), which was calculated within a 20 km radius of each site (Feist and Levin, 2016), and an index derived via Principal Component Analysis (PCA) (Alberti, 2008; Spirandelli, 2014). Five geospatial data layers were used in the PCA: human population density (U.S. Census Bureau, 2010), imperviousness (USGS, 2014; Xian et al., 2011), proportion of

intertidal shoreline armored with coastal defense structures (PSNERP, 2010), road density (HSIP, 2013), and proportion of adjacent land characterized by NOAA's Coastal Change Analysis Program (C-CAP) as High Intensity Developed (NOAA, 2013; Supplementary Table S1). These data layers were summarized at the level of riverine basin, as designated by the Puget Sound Nearshore Restoration Project (PSNERP, 2010), and normalized to prevent their having a disproportionate effect on the resulting urbanization index. PCA was performed using the function prcomp in R (Version 3.3.1, R Development Core Team 2016). Lastly, the proportion of shoreline armoring (PSNERP, 2010) in the nearest PSNERP basin to each REEF site was used as an additional model predictor (average distance from REEF sites to the closest PSNERP basin polygon was 164.2 ± 19.5 m). All predictor variables were checked for collinearity; the models considered included only variables with Spearman's rank correlation coefficients between -0.5 and 0.5 (Rhodes et al., 2006).

Model – We tested whether urbanization was related to *E. dofleini* presence/absence using generalized linear mixed-effects models (GLMM) with a binomial error distribution and a logit link function. Site was included as a random effect. We developed a set of candidate models from alternative combinations of fixed effects and from a "null" model, consisting of only an intercept. Relative support for candidate models was evaluated using Akaike's Information Criterion (AIC). Model fit was evaluated based on the percentage of deviance explained and on Cohen's κ statistic (Cohen, 1960), as derived through a 10-fold cross validation. We evaluated spatial correlation among model residuals graphically relative to their geographic coordinates, and by plotting estimates of semivariance against between-site distances (Fortin and Dale, 2005).

Candidate models were developed in two stages. In Stage I, we derived a suite of "background" models by including variables unrelated to urbanization (survey-specific and temporal predictors). Variables selected in Stage I were then included in an expanded model (Stage II) that also contained an urban-related metric. Three types of Stage II models were considered: (1) Models with PPI, (2) Models with PC1 and/or PC2, and (3) Models with Armoring as the only urbanization-related predictor. The latter evaluated whether octopus occurrence was related to shoreline armoring specifically. In the (1) and (2) Stage II models, Depth × Urbanization (PC or PPI) interaction terms were also included to reflect the hypothesis that *E. dofleini* sightings were more common at depth in urban areas, where we had observed extensive amounts of anthropogenic debris in preliminary surveys.

Video transect surveys

We conducted video transect surveys at four sets of paired sites to the west and southwest of the Seattle Metropolitan Area in January and May 2015 (Figure 1). These sites represented all known locations in the region at which there were adjacent areas with a consistent bottom profile and with high and low densities of anthropogenic debris. A 20m transect tape was deployed horizontally at two depths within each site pair (14m and 20m). Digital video was recorded with a Canon S110 in an Ikelite underwater housing. Two lasers mounted 9cm apart at the base of the camera allowed for measurements of debris items. Lasers were positioned over all artificial structures larger than $0.0625m^2$ for subsequent measurement. The number of octopus from each survey was also recorded, and used in final analyses. *E. dofleini* do not flee their dens or swim away from divers unless molested. All *E. dofleini* found in the survey were observed in their dens and remained in dens for the duration of transect sampling.

The horizontal area ("footprint") and maximum height of anthropogenic debris was measured from still frames from each video transect using ImageJ (NIH version 1.42). The scale was set based on the known distance between the laser points in each frame. For objects that tapered at the base, horizontal area was determined as at the point of maximum width. Most objects were captured from multiple angles, providing sufficient data to compute the total structure footprint. However, assumptions about unmeasured dimensions were occasionally required. We sought to make conservative estimates in all cases, with lower values of structure height and horizontal area wherever measurements were in doubt.

We modeled both the presence/absence of octopus via mixed effects logistic regression, as well as the number of octopus observed via a GLMM with negative binomial error. In both approaches, site pair was included as a random effect. We considered five alternative models, each containing either depth, survey month, the number of debris structures, the total horizontal area of structures, or the maximum height of anthropogenic debris as a fixed effect. Alternative models were compared with a null model (only an intercept) via AIC and model fit was evaluated graphically, by examining dispersion (for negative binomial GLMMs only) and the percentage of deviance explained.

Midden Composition

To determine whether the trophic resources utilized by *E. dofleini* in urban areas differed from those in more rural, natural environments, we collected octopus middens at 24 sites in Puget Sound in January through May 2014 (Figure 1) (Scheel and Anderson, 2012). Selection of midden survey sites was non-random, and included all locations where *E. dofleini* had been observed previously, as well as locations listed on Seattle Aquarium's annual "Octopus Census"

(www.seattleaquarium.org/octopus-census). Sites with high flow were not included in the survey, as high current speed tends to disperse midden contents (Ambrose, 1983). In surveys conducted at slack tide, SCUBA divers visually searched for octopus dens or middens. Middens were recognized by octopus presence, den excavation in characteristic fashion, or large piles of shell remains (Scheel and Anderson, 2012). Midden contents were collected into gallon ziploc bags for later analysis in the lab. Only shell remains within a 1 m radius of the den were collected. Midden depth, location, den material, and surrounding substrate remains were recorded. Multiple middens were found at some sites, resulting in 46 collected middens in total.

Midden composition was analyzed in the lab by identifying shell remains to species and recording the number of individuals they represented (Scheel and Anderson, 2012). Crabs were counted by carapace and/or matching chelae, gastropods were counted by the number of shells, and bivalve shells were matched when possible. Unmatched chelae and valves were counted as individuals. Prey with obvious signs of predation by other organisms, such as the moon snail, *Neverita lewisii*, were excluded; octopus drill and bite marks were identified in accordance with descriptions from Dodge and Scheel (1999). Prey size was evaluated from all intact shells, by measuring the carapace at the widest point and across bivalve shells from the anterior to posterior end. We used length-weight relationships and conversion factors from multiple sources (detailed in Supplementary Table S3) to estimate Ash-Free Dry Mass (AFDM) and Shell-Free Dry Mass (SFDM).

We looked for patterns in trophic utilization based on several univariate metrics. Individual specialization was examined by calculating proportional similarity (PS_i) (Bolnick et al., 2002):

$$PS_i = 1 - 0.5 \sum_j |p_{ij} - q_j|$$

where p_{ij} is the proportion of prey items of species j in midden i, and q_j is the proportion species j comprises across all middens. Though individual specialization ($PS_i < 0.5$) can result from a variety of mechanisms, systematic differences in PS_i can signal distinct conditions with respect to resource availability and intraspecific interactions (Bolnick et al., 2002). We also calculated the total number of prey items, the total estimated tissue weight of prey, the number and estimated tissue weight of decapods, and separately heterodont clams, and the number of unique prey types in each midden. GLMMs with site as a random effect and with different fixed effects (PC1, PPI, depth, den material, surrounding substrate, latitude, longitude, or collection date) were compared with null models for each metric. A negative binomial error structure was used for the number of total prey items, heterodonts, and decapods, while log-normal error was used for estimated weights. Poisson error provided the best fit for the number of unique prey types, and PS_i was approximately normally distributed. Model fit was examined graphically and compared for each response variable via AIC.

We performed a redundancy analysis (RDA) to determine whether the composition of prey in octopus middens differed with urbanization (PC1 and PPI) and with depth (Legendre and Anderson, 1999). Site was included as a condition in the analysis, which we performed using the 'vegan' package in R. ANOVA permutation tests with 999 permutations were used to evaluate significance level of global model and canonical axes.

Results

Spatial/temporal distribution patterns

E. dofleini were observed on 2158 of the 5790 REEF surveys included in our analysis. From 2000 to the beginning of 2016, octopus were sighted at 52.8% of the sites surveyed; sightings

occurred at an average of 35.0% ± 1.3% of sites in any given year. *E. dofleini* was found throughout the study area, from as far south as Steilacoom, Washington (47°10′12″N, 122°35′40″W) to as north as Coupeville, Washington (48°13′6″N, 122°41′1″W), near the boundary of our study area at Admiralty Inlet.

In the PCA used to reduce the dimensionality of urbanization-related spatial data layers, PC1 explained 61% of the variation in urban metrics (Figure 1), with roughly equal weight attributed to population density, imperviousness, road density, and high intensity development (Table 1). An additional 16% of the variation was explained by PC2, which corresponded primarily with the extent of shoreline armoring. PC3 represented 11.5% of the variation and correlated most strongly with the density of roadways. PC3 was also excluded as a model predictor, however, because it correlated with PC1 (Spearman's rank correlation, $r_S = 0.56$). The fourth and fifth principal components were also excluded as model predictors because they explained little of the variation (Table 1).

The best fit mixed effects logistic regression model had only moderate statistical support, yet clearly provided a better fit of octopus presence/absence data than alternative model configurations (*w*AIC = 0.99, Table 2). The selected model included parameters related to both spatial and temporal distribution patterns and to detection probability. The probability of encountering octopus increased with bottom time and visibility, and tended to be greater in rocky habitats and artificial reefs than in soft sediment environments (Figure 2). Octopus occurrence was also negatively correlated with temperature-related oceanographic indices, which is consistent with previous studies (Scheel, 2015). Specifically, PDO averaged over the previous 50 months (4.2 years) was favored in model selection, and outperformed diver-recorded bottom temperature and finer resolution SST indices. Logistic regression models also revealed a strong

effect from depth, with a higher chance of octopus sightings on deeper dives. The magnitude and direction of model coefficients is shown in Figure 2 (also see Supplement Figure S1).

We found evidence that octopus presence was associated with urbanization mainly through interactions with other variables. The level of urbanization (PC1) alone did not strongly impact estimates of the probability of occurrence (Figure 2, Supplement Figure S1). Rather, there was a strong depth-dependent effect from PC1, manifest in improved model fit with the inclusion of a Depth×PC1 interaction term (Table 2). On deeper surveys (maximum depth > 24 m), the probability of encountering octopus increased with urbanization intensity (Figure 3). Conversely, urbanization appeared to decrease octopus occurrence on dive surveys conducted at shallower depths (< 18 m). Sample size was within a comparable range in each depth interval (Shallow (< 12m): 812 surveys, Shallow-Intermediate (12-18m): 1554 surveys, Intermediate-Deep (18-24m): 1762 surveys, and Deep (>24m): 1662 surveys), we found no evidence in model residuals to suggest the pattern was an artifact of the model itself. The number of surveys and the number of sites sampled were also comparable across most values of PC1, through few dive surveys were conducted at sites with a PC1 > 7. However, we found the same depth-dependent effects from urbanization when we reran the analysis excluding PC1 > 7 sites.

Despite being clearly favored, the best-fit model explained only 6.7% of deviance, and its κ statistic (0.4) indicated only fair model performance (Cohen, 1960). We found no evidence of spatial autocorrelation in model residuals, though there did appear to be more overestimates of occurrence probability early in the time series (2006 and earlier). Reasons for this pattern of temporal autocorrelation were unclear, though likely related to more patchy and limited sampling in earlier years of the REEF program. The conclusions from the model were unchanged when we

reran the analysis without selected sites that were sampled more or less in early years, as well as when we reran the analysis without data prior to 2007.

Video transect surveys

In video surveys, octopus were found at two of the four survey sites with large amounts of anthropogenic debris and were absent from all four (paired) survey sites with little anthropogenic debris. Debris items included hulls and other boats, concrete slabs, tires, and other structures, and are summarized in Supplementary Table S4. Model comparisons indicated that the number of anthropogenic debris items was the best predictor for both octopus presence/absence and the number of octopus observed (Table 3). The horizontal area and average height of debris structures also had moderate support as model predictors of octopus abundance and presence/absence (Supplement Table S4), but were secondary to the number of debris items. Overall, more anthropogenic debris coincided with more octopus, though there were considerable site-specific differences in octopus abundance (Figure 4).

Midden Composition

Across all 46 middens, we identified a total of 890 prey items representing 29 different taxa. The mean count of prey items per midden was 19.7 (SE ± 3.83). Middens were found at a range of depths, from 3.3 to 23.7 m, and were associated with dens made of anthropogenic debris (54.3%), natural rock (15.2%), and quarried boulders that were part of artificial reefs or shoreline defense structures (30.3%). Benthic habitat surrounding collected middens included sand (30.4%), mud (23.9%), cobble (15.2%), and rock (30.4%). The most common prey included *Pododesmus macrochisma, Cancer productus, Saxidomus gigantea, Clinocardium nuttalli,*

Pugettia producta and *Metacarcinus magister* (Figure 5, Supplement Table S6). Only two species, *Pododesmus macrochisma* and *Cancer productus*, were present in over 50% of the middens. *Clinocardium nuttalli, Saxidomus gigantea*, and *Pugettia productus* were the next most common species, and were present in at least 30% of middens.

Proportional Similarity Index was highly variable and showed no clear patterns relative to latitude, longitude, date, urbanization metrics (PC1 and PPI), or the type of habitat in which the midden was found (artificial structure, continuous rock, or natural rock piles). Though the most specialized middens were found relatively shallow (6-7m), linear mixed-effects models with depth as an explanatory variable performed worse than the null model for proportional similarity (Supplement Table S5). Overall, the amount of variability in the proportional similarity index within sites was large relative to variability across sites, suggesting that specialization occurs on an individual basis, and may be more the result of individual preference or niche partitioning than of site-specific prey availability.

Comparable results were found for other univariate metrics of midden composition. Predictor variables performed worse than null models for the number of unique prey items, the number and estimated tissue weight of prey items, and the number and estimated tissue weight of crabs. PPI and longitude were favored in model comparisons for the number and estimated weight of heterodont clams. For the set of sites used in midden surveys, longitude and PPI were correlated (Spearman rank correlation coefficient = 0.61). The number and weight of heterodonts in middens tended to be higher on the eastern shores of Puget Sound, where there was also greater urbanization. While PPI provided a superior fit than longitude, the extent to which urbanization versus natural spatial gradients drive this pattern cannot be discerned from our data.

Similarly, RDA results indicated no effect from the explanatory variables we considered. When partitioning variation between urbanization and site, neither urbanization index (PC1 or PPI) explained a significant proportion of the variation in midden composition. Conditional (partial) effects from site were significant, however, explaining 11.6% and 12.2% of the variation in models with PC1 and PPI, respectively ($P = 0.034$ and $P = 0.033$). Depth was also inadequate as a model predictor (-2.2% adjusted R^2); Adjusted R^2 values for den material, surrounding substrate, latitude, longitude, and date were all less than 0.005.

Discussion

This study is among of the first to characterize the distribution and habitat use patterns of a marine mesopredator with respect to urbanization. Our findings suggest that urbanization-related patterns in giant Pacific octopus occurrence are depth-dependent. Octopus were predicted to occur more frequently at depth (> 24m) in highly urban areas, and less frequently at depth along more rural shorelines. Though our final model accounted for a small amount of the total variation in octopus sightings, there was strong statistical support for depth-specific patterns. Accompanying data from our field surveys further suggested that octopus abundance may be related to the extent of anthropogenic debris in benthic habitats, and that patterns in octopus occurrence across an urban gradient were not likely driven by trophic dynamics.

Our findings suggest that giant Pacific octopus may be synanthropic within certain urban marine habitats, however, the primary mechanisms driving these patterns likely differ from those in urban terrestrial environments. Though many terrestrial synanthropes utilize man-made structures as shelter (Duduś et al., 2014; Prange et al., 2003), they typically also benefit either directly or indirectly from enhanced food resources provided by human activities (Bateman and

Fleming, 2012; McKinney, 2006). We found no evidence that urbanization altered or subsidized the diets of octopus. However, octopus did utilize man-made structures as den sites, and were more likely to occur in locations with greater amounts of anthropogenic debris. Anthropogenic debris often results from localized, land-based human activities (Galgani et al., 2015; Ioakeimidis et al., 2014; Thiel et al., 2013; Zhou et al., 2011), and tends to be particularly extensive in urban areas and at depth (Galgani et al., 2000; Leite et al., 2014). If den provisioning from urbanization is a major driver in octopus distribution patterns, it does not appear to be accompanied by greater food availability. It may, however, coincide with other urban drivers we did not evaluate that are known to benefit some terrestrial mesopredators, such as release from predation pressure by apex predators (Crooks and Soulé, 1999; Prugh et al., 2009).

Depth-specific effects from urbanization may be influenced by abiotic conditions. *E. dofleini* distribution patterns are thought to be negatively correlated with temperature (Scheel, 2015) and positively correlated with salinity (Hartwick et al., 1984). Major cities in the Puget Sound region are located at the mouths of rivers and may have localized patches of low surface salinity at certain times of year (Krishnakumar et al., 1994; Toft et al., 2007). Biotic conditions may also vary with depth and urbanization intensity. For instance, *E. dofleini* serve as prey for pinnipeds, such as harbor seals (*Phoca vitulina*), California Sea Lions (*Zalophus californianus*), and others, which utilize man-made structures at the surface as haul-out sites. Given the size of adult *E. dofleini* (McClain et al., 2015), the risks to mammalian predators of hunting this species at depth may outweigh the benefits, effectively providing a depth refuge for giant Pacific octopus in urban areas.

Further, depth-dependent effects we observed could also be influenced by differences in octopus dispersion and diver search patterns in deep- versus shallow-water habitats. Presumably,

divers covered a larger search area on deep dives, as getting to deeper habitats requires traveling farther underwater. If octopus were more uniformly distributed in urban areas and patchier in rural areas, deep dives would yield more octopus sightings at urban sites, as was observed. Presently, we know of no empirical evidence suggesting that octopus dispersion differs with urbanization. Thus, strong support we found for a *Depth* × *PC1* interaction term may either suggest that *E. dofleini* is more common at depth in cities, or more uniformly distributed in cities, and thus more likely to be detected by divers covering a broader survey area. Future studies should identify whether octopus dispersion patterns differ with urbanization intensity, and are needed before this alternative hypothesis can be excluded.

Ultimately, knowledge of urban marine ecosystems is so limited (Bulleri, 2006) that few external data sources exist that would allow us to prioritize the suite of potential hypotheses behind the depth-dependent effects of urbanization we observed for *E. dofleini*. Evaluating mechanisms that drive urbanization-related distribution patterns for this species is further complicated by the limited number of effective tagging and experimental techniques available for octopods (Scheel and Bisson, 2012; Semmens et al., 2007). While large-scale additions or removals of man-made structures could help determine the extent to which anthropogenic debris is an important driver, such manipulations involve considerable logistical challenges and present ethical dilemmas, as man-made debris items alter marine ecosystems considerably (Rochman et al., 2016; Heery et al., in press). Despite the large size of *E. dofleini*, experiments in an aquarium setting may therefore provide the best means of evaluating causal linkages between urbanization and *E. dofleini* abundance. Mesocosm experiments with smaller octopods that have similar urbanization-related distribution patterns might also serve as useful model species, and could be coordinated with existing shoreline development and restoration projects that serve as a natural

experiment. While mesocosms are likely needed to understand octopus responses to water conditions, contaminants, noise and light pollution, and benthic habitat modification, expanded observational surveys will also be essential in order to better characterize the physical, chemical, and biotic effects of urbanization for octopus, as well as other marine taxa.

This study suggests that urbanization may influence the distribution and dynamics of marine mesopredators. Though giant Pacific octopus may be synthanthropic within certain habitats, our results should be interpreted cautiously. Until the mechanisms underlying observational patterns in octopus populations are better understood, concluding that *E. dofleini* benefits from urbanization in any of the habitats it utilizes would be misguided. The dynamics of well-documented synanthropic species are non-linear, depend on urbanization intensity, and influenced by a wide variety of variables (Kelly et al., 2016; Magle et al., 2016, 2014). *E. dofleini* responses to urbanization are therefore likely to be complex. However, since mesopredators have considerable impacts on lower trophic levels and on ecosystem processes more broadly (Prugh et al., 2009), characterizing the dynamics of marine mesopredators, such as *E. dofleini*, in heavily developed coastal areas is essential for understanding how marine ecosystems are impacted by urbanization. Our study demonstrates the utility of both localized surveys and broad-scale citizen-contributed data for examining marine mesopredator distribution and habitat-use patterns in coastal cities. Further observational surveys and experimental studies will provide valuable insights into the dynamics of octopods and other urban marine taxa. Such insights will be ever more critical as urbanization in coastal regions intensifies and marine habitats are subject to greater modification and disturbance.

Tables

Table 1. Principal Component (PC) loadings for five urbanization-related metrics and the cumulative proportion of the variance explained by each PC (bottom row). Principal Component Analysis (PCA) was performed to reduce the dimensionality of urbanization metrics. PC1 and PC2 were subsequently included as potential explanatory variables in mixed effects linear regression models of octopus presence/absence.

Variable	**PC1**	**PC2**	**PC3**	**PC4**	**PC5**
Population Density	0.49	-0.05	0.17	0.77	0.37
Imperviousness	0.53	-0.14	0.01	0.06	-0.84
Armoring	0.35	0.72	-0.58	-0.09	0.09
Road Density	0.44	0.22	0.67	-0.52	0.22
High Intensity Development	0.40	-0.64	-0.44	-0.36	0.33
Cumulative Proportion	61%	77%	89%	96%	100%

Table 2. Summary of the mixed effects logistic regression models relating the probability of octopus occurrence to diver bottom time (BT), visibility (Vis), maximum depth (Depth), month (Mn), year (Yr), habitat type (Hab2: Artificial Reef, Rocky, Sedimentary), Pacific Decadal Oscillation (PDO) index averaged over the previous 50 months (PDO50), the first principle component from PCA (PC1), the population proximity index (PPI), and the proportion shoreline armoring (Armoring). The table presents delta values and weights of Akaike's Information Criterion (ΔAIC and wAIC), percentage of deviance explained (%Dev), and Cohen's Kappa statistic (κ) for each in the suite of selected models. Models are listed by decreasing %Dev explained and go from best to worst fit.

Model	ΔAIC	wAIC	%Dev	κ
BT + Vis + Depth + Mn + Yr + Hab2 + PDO50 + PC1 + Depth:PC1	0.0	0.9893	6.68	0.4 ± 0.04
BT + Vis + Depth + Mn + Yr + Hab2 + PDO50 + PPI + Depth:PPI	10.2	0.0061	6.53	0.4 ± 0.04
BT + Vis + Depth + Mn + Yr + Hab2 + PDO50 + PC1 + PC2	14.5	0.0007	6.41	0.4 ± 0.04
BT + Vis + Depth + Mn + Yr + Hab2 + PDO50 + PC2	13.0	0.0015	6.40	0.4 ± 0.04
BT + Vis + Depth + Mn + Yr + Hab2 + PDO50 + PPI	15.5	0.0004	6.37	0.4 ± 0.04
BT + Vis + Depth + Mn + Yr + Hab2 + PDO50 + PC1	15.5	0.0004	6.37	0.4 ± 0.04
BT + Vis + Depth + Mn + Yr + Hab2 + PDO50 + Armoring	15.6	0.0004	6.37	0.4 ± 0.04
BT + Vis + Depth + Mn + Yr + Hab2 + PDO50	13.6	0.0011	6.36	0.4 ± 0.04
BT + Vis + Depth + PDO50	76.8	0.0000	5.34	0.3 ± 0.04
BT + Vis + Depth + Mn + Yr	88.7	0.0000	5.20	0.4 ± 0.04
BT + Vis + Hab2 + PDO 50	115.4	0.0000	4.76	0.3 ± 0.04
BT + Vis + Depth + Hab2	215.2	0.0000	3.38	0.3 ± 0.04
BT + Vis + Depth	233.7	0.0000	3.06	0.3 ± 0.04
BT + Vis + Hab2	279.4	0.0000	2.38	0.3 ± 0.04
BT + Vis	300.8	0.0000	2.01	0.3 ± 0.04
BT	354.7	0.0000	1.21	0.3 ± 0.04
Depth	360.4	0.0000	1.18	0.3 ± 0.04
Vis	371.5	0.0000	0.97	0.3 ± 0.04

Table 3. Best fit models for each of the univariate responses considered from video transect surveys (*a*) and midden collections (*b*). For all response variables where a model predictor provided a better fit than the null, AIC weights and the percentage of deviation explained by that predictor are provided. Complete model results are also available in Supplement Table S5.

Response Variable	Best Model
(a) Video Transect Surveys	
Octopus counts	*Number of structures (wAIC = 0.520, %Dev = 22.4%)*
Octopus presence/absence	*Number of structures (wAIC = 0.790, %Dev = 78.3%)*
(b) Midden Collections	
Estimated tissue weight of all prey	*Null*
Estimated tissue weight of Heterodonts	*PPI (wAIC = 0.773, %Dev = 1.72%)*
Estimated tissue weight of Decapods	*Null*
Number of Heterodonts	*Longitude (wAIC = 0.527, %Dev = 4.28%)*
Number of Decapods	*Null*
Number of unique prey types	*Null*
Proportional Similarity (PS)	*Null*
Total number of prey items	*Null*

Figures

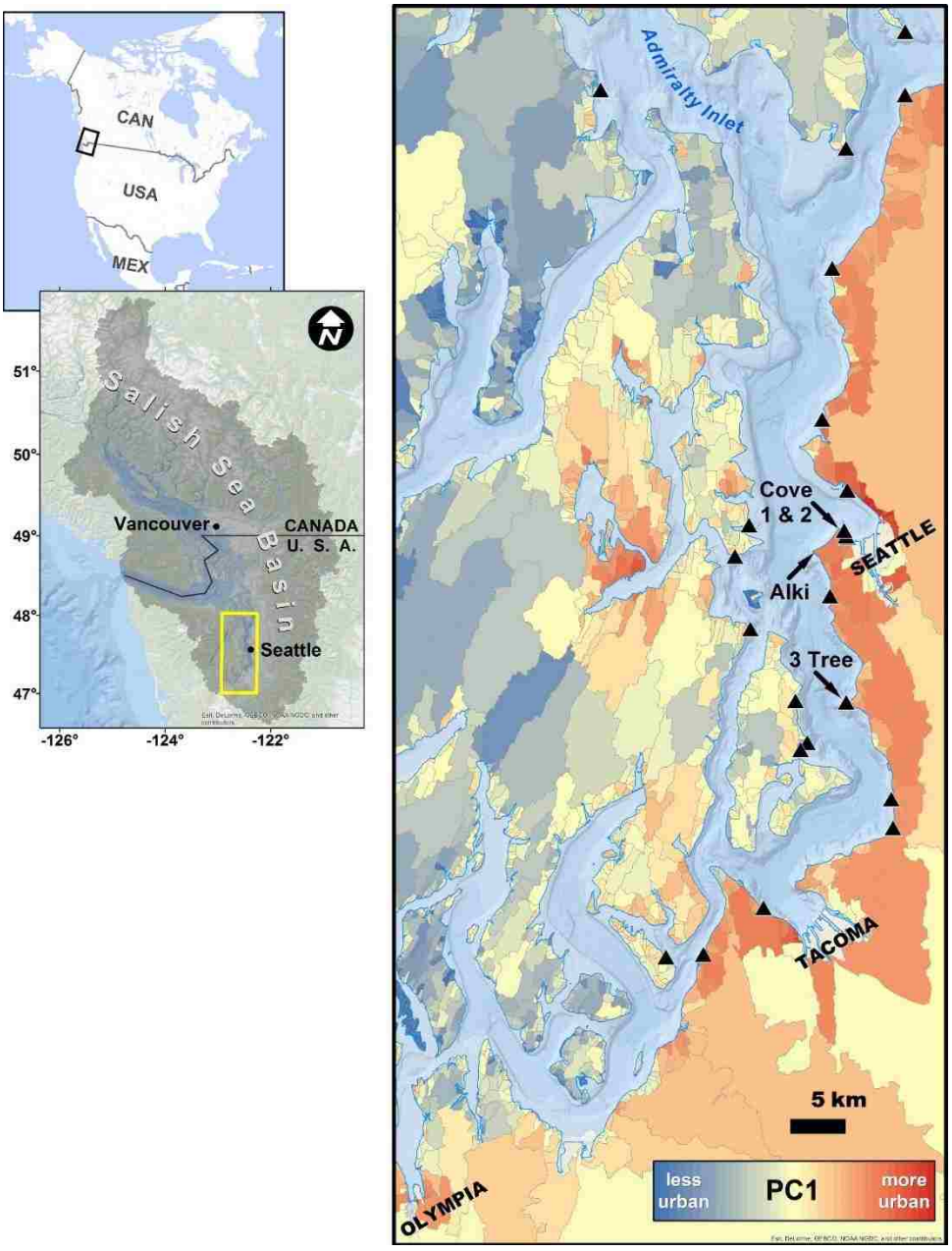

Figure 1. Map of the study area in Puget Sound. Riverine basins derived by the Puget Sound Nearshore Restoration Project (PSNERP) are shaded according to their score from the first axis of the Principal Component Analysis (PCA). Black triangles mark the locations where we collected octopus middens and the areas where we conducted paired-site video transect surveys are labeled and marked with a white arrow. Courtesy of Dr. Blake Feist (NWFSC/NOAA).

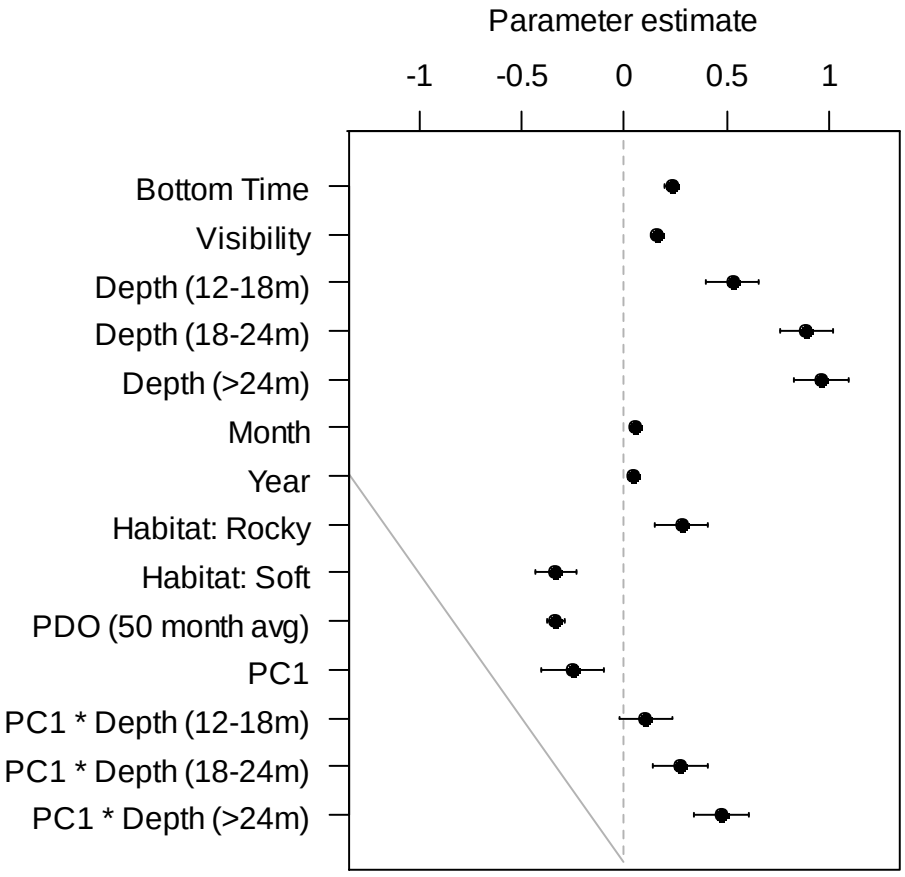

Figure 2. Estimated coefficients (SE) from the best-fit mixed effects logistic regression model of octopus presence/absence.

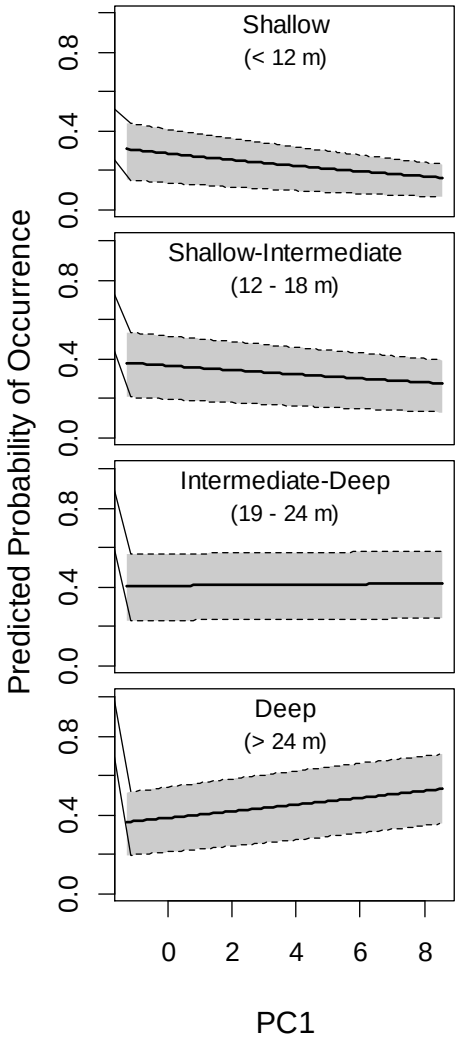

Figure 3. Predicted probability of occurrence vs PC1 within in each of the four intervals for diver bottom depth: Shallow (< 12m), Shallow-Intermediate (12-18m), Intermediate-Deep (18-24m), and Deep (>24m). Mean (solid lines) and quartile (dashed lines) estimates were generated based on parameter estimates from the best fit mixed-effects logistic regression for octopus presence/absence.

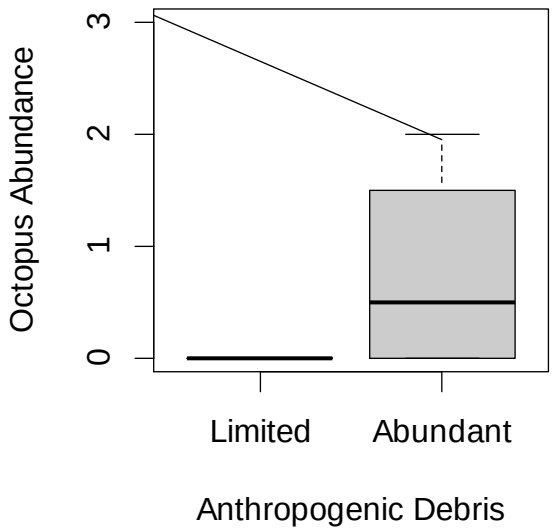

Figure 4. Boxplot of octopus abundance from video transect surveys, at site pairs with limited anthropogenic debris versus site pairs with abundant anthropogenic debris. Note that octopus were observed at only two of the four sites surveyed (Cove 2 and 3 Tree); octopus abundance was zero at both site pairs at Alki and Cove 1 (Figure 1).

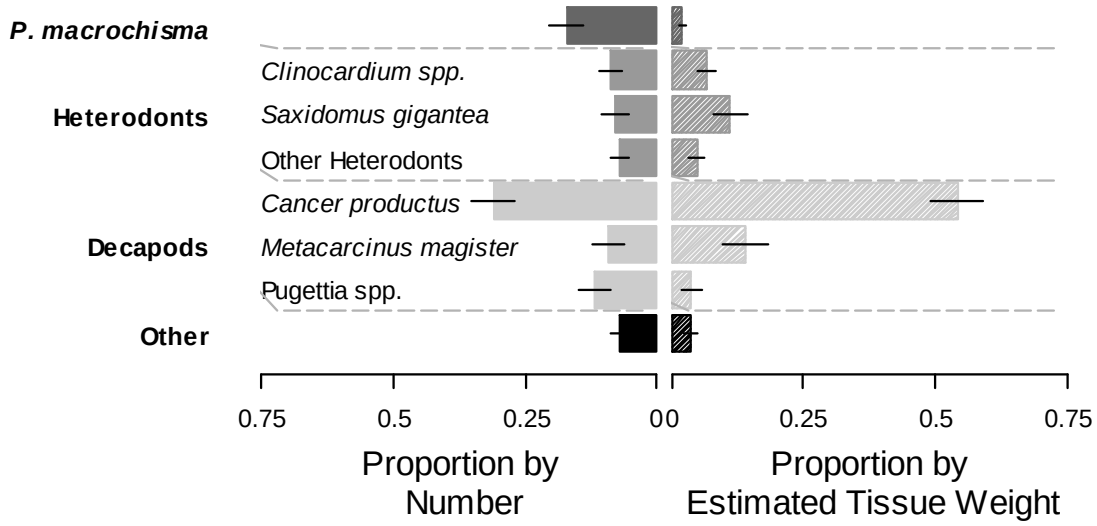

Figure 5. The proportion of prey (Mean ± SE) in octopus middens, calculated both in terms of the number of prey items (left) and the estimated tissue weight of prey (right). Bars are color-coded by prey type, with *Pododesmus machrochisma* in dark gray, heterodont clams in medium grey, decapods in light gray, and other prey types in black. Midden composition varied considerably between individual octopus; More comprehensive summary statistics are provided in Supplement Table S6.

Supplementary material

APPENDIX 1: Model predictors and spatial data layers.

Table S1. Variables considered in mixed effects logistic regression models of octopus presence/absence. A brief description, the level of aggregation, and the source of each variable is provided.

Variable	Description	Aggregation	Source
Bottom Temperature	Bottom temperature in Farenheit as recorded by diver	Survey	REEF Program (visit www.reef.org)
Bottom Time	Bottom time in minutes as recorded by diver	Survey	REEF Program
Visibility	Visibility as estimated by diver	Survey	REEF Program
Max Depth	Maximum diving depth in 10ft intervals (<10', 10-19', 20-29', etc)	Survey	REEF Program
Habitat	Habitat type; One of eleven possible categories (see ***1.2* Table S2**) selected by diver	Survey	REEF Program
Date	Month, day, and year on which the survey took place	Survey	REEF Program
Start Time	Hour (0-24) when survey started	Survey	REEF Program
Area Depth	Estimated water depth in meters relative to mean high water (MHW), as extracted from NOAA NGDC tsunami inundation grids and NOS hydrographic survey data	Site	Shelton et al. (2016)
Wave Exposure	Index of wave exposure, incorporating 30 year wind patterns and fetch (see ***1.3* Wave Exposure** below)	Site	Arguez et al. (2010); USGS (Various)
PPI	Population Proximity Index (PPI) within a 20 km radius	Site	Feist and Levin (2016)
Armoring	Proportion of basin classified as armored	PSNERP basin*	PSNERP (2010)
Population Density	Density (people/km^2) of humans living in given PSNERP basin	PSNERP basin*	U.S. Census Bureau (2010)
Imperviousness	Area weighted mean imperviousness	PSNERP basin*	USGS (2014); Xian et al. (2011)
Road Density	Density (m of road/km2) of roads in al NAVTEQ functional classes	PSNERP basin*	HSIP (2013)
High Intensity Development	Proportion of basin designated as high intensity development (a land use and land cover category in NOAA's Coastal Change Analysis Program)	PSNERP basin*	NOAA (2013)
SST	Optimum Interpolated (OI) Sea Surface Temperature	Variable**	NOAA (2016a)
PDO	Monthly Pacific Decadal Oscillation Index	Variable***	NOAA (2016b)

** Puget Sound Nearshore Ecosystem Restoration Project (PSNERP) riverine basins (PSNERP 2010)*

*** Weekly mean SST, monthly mean SST, and mean SST from the past three months for the NOAA_OI_SST_V2 grid cell at 42°N, -122°W were compared as potential explanatory variables using AIC*

**** Mean PDO values in the month of sampling and aggregated means from the past 6, 12, 24, 30, 40, 50, 60, 70, 80, 90, 100, and 120 months were compared as potential explanatory variables using AIC*

Table S2. Habitat types and codes used by survey divers in the REEF program (see www.reef.org) and two alternative aggregations of diver-recorded habitat designations that were considered as explanatory variables in mixed effects logistic regression models of octopus presence/absence. The alternative aggregations were used because the 12-level habitat code did not allow for model convergence.

Habitat Type	REEF Habitat Code	Habitat Variable 1 (Hab1)	Habitat Variable 2 (Hab2)
Kelp Forest	1	Kelp Bed	Rocky
Rock/Shale Reef	2	Natural Rock	Rocky
Artificial Reef	3	Artificial	Artificial Reef
Sandy Bottom	4	Sediment	Sedimentary
Open Ocean	5	--	--
Eel Grass	6	Seagrass	Sedimentary
Surf Grass	7	Seagrass	Sedimentary
Pinnacle	8	Natural Rock	Rocky
Bull Kelp Bed	9	Kelp Bed	Rocky
Mud/Silt	10	Sediment	Sedimentary
Cobblestone/Boulder Field	11	Cobble / Boulder	Sedimentary
Vertical Walls	12	Natural Rock	Rocky

APPENDIX 2: Data summaries and model estimates.

Table S3. Length-weight relationship parameters (α,β) and mass conversion factors used to estimated Ash-Free Dry Mass (AFDM) and Shell-Free Dry Mass (SFDM) from measured shells in octopus middens. Regression coefficients α and β are for the form $W = \alpha L^{\beta}$, where L is the shell measurements (carapace width or shell length in mm) and W is the estimated weight (wet mass in grams). Wet mass (WM) was then converted to AFDM and SFDM using the conversion factors shown.

	Wet Mass (WM) Estimates			Mass Conversion Factors		
Species/Genus	**α**	**β**	**Source**	**AFDM**	**SFDM**	**Source**
Cancer productus	0.00005	2.790	[1] - *Metacarcinus magister*	*NA**	0.71*	[1] - *M. magister*
Chlamys spp.	0.00016	2.986	[2] - *Aequipecten opercularis*	5.8	8.7	[3] - bivalves
Clinocardium spp.**	0.00062	2.848	[4] - *Clinocardium spp.*	5.8	8.7	[3] - bivalves
Crassostrea gigas	0.00030	2.653	[5] - *Crassostrea gigas*	5.8	8.7	[3] - bivalves
Gari californica	0.00001	3.475	[2] - *Gari fervensis*	5.8	8.7	[3] - bivalves
Humilaria kennerlyi	0.00062	2.848	[2] - *Timoclea ovata*	5.8	8.7	[3] - bivalves
Macoma sp.	0.00029	2.846	[6] - *Macoma balthica*	5.8	8.7	[3] - bivalves
Mactromeris polynyma	0.00017	3.012	[2] - *Spisula elliptica*	5.8	8.7	[3] - bivalves
Metacarcinus magister	0.00005	2.790	[1] - *Metacarcinus magister*	*NA**	0.71*	[1] - *M. magister*
Modiolus rectus	0.00014	2.847	[2] - *Modiolus modiolus*	5.8	8.7	[3] - bivalves
Nemocardium centifilosum	0.00042	2.961	[2] - *Acanthocardia echinata*	5.8	8.7	[3] - bivalves
Neptunea sp.	0.00020	2.840	[2] - *Buccinum undatum*	7.5	10.6	[3] - gastropods
Neverita lewisii	0.00132	2.639	[2] - *Euspira catena*	7.5	10.6	[3] - gastropods
Penitella penita	0.00020	2.973	[7] - *Tresus capax*	5.8	8.7	[3] - bivalves
Pododesmus macrochisma	0.00010	2.870	[2] - *Pododesmus patelliformis*	5.8	8.7	[3] - bivalves
Protothaca spp.***	0.00062	2.848	[1] - *Timoclea ovata*	5.8	8.7	[3] - bivalves
Pugettia spp.****	0.00100	2.510	[8] - *Pugettia producta*	8.9	11.4	[8] - *P. producta*
Saxidomus gigantea	0.00013	3.169	[3] - *Saxidomus gigantea*	5.8	8.7	[3] - bivalves
Simomactra falcata	0.00017	3.012	[2] - *Spisula elliptica*	5.8	8.7	[3] - bivalves
Telmessus cheiragonus	0.00035	3.004	[2] - *Atelecyclus rotundatus*	8.9	11.4	[8] - *P. producta*
Terebratalia transversa	0.00008	3.297	[2] - *Terebratulina retusa*	2.1	33.3	[9] - *T. transversa*
Tresus capax	0.00020	2.973	[7] - *Tresus capax*	5.8	8.7	[3] - bivalves

* Length-weight parameters for this *Metacarcinus* magister estimated AFDM directly, rather than WM. No AFDM/WM conversion was therefore required. The value included under SFDM/WM is the ratio of SFDM:AFDM.

** *Clinocardium* species included *C. ciliatum*, *C. fucanum*, and *C. nuttalli*. The same values were used for all *Clinocardium* species due to a lack of species-specific estimates in the literature.

*** *Protothaca* species included *P. staminea* and *P. tenerrima*. The same values were used for both species due to a lack of species-specific estimates in the literature.

**** Though *Pugettia producta* was the primary species from this genus in octopus middens, *P. foliata*, *P. gracilis*, and *P. richii* were also found. The same values were used for all *Pugettia* species due to a lack of species-specific estimates in the literature.

[1] Holsman et al. (2003) *Estuaries* 26(4): 1155-1173

[2] Robinson et al. (2010) *J. of the Marine Biological Association of the United Kingdom* 90(1): 95-104

[3] Ricciardi and Bourget (1998) *Marine Ecology Progress Series* 163: 245-251

[4] Bradbury et al. (2006) Washington Department of Fish and Wildlife FPT 05-15

[5] Kobayashi et al. (1997) *Aquaculture* 149: 285-321

[6] Chambers and Milne (1975) *Estuarine and Coastal Marine Science* 3: 443-455

[7] Lauzier et al. (1998) Canadian Stock Assessment Secretariat Research Document 98/88

[8] Reed et al. (2016) *Marine Biology* 163: 101-107

[9] Ballanti et al. (2012) *Paleobiology* 38(4): 525-537

Table S4. Summary of anthropogenic debris items observed on video transect surveys. The table provides the total number of objects within each debris type at adjacent site pairs with abundant versus limited debris, and separates these totals out by each site, represented by lower-case letters: *a*: 3 Tree, *b*: Alki, *c*: Cove 1, *d*: Cove 2 (see Figure 1). The average horizontal area and maximum height of objects in each debris category are presented in the last two columns.

	Site Pair					
	Abundant Debris		***Limited Debris***		**Average horizontal area (m^2)**	**Average maximum height (m)**
Debris Type	Number	(by site)	Number	(by site)		
Boat hulls & boat trailers	4	(*a* - 2; *d* - 2)	0		8.09	1.17
Boat parts	7	(*a* - 3; *d* - 4)	0		0.38	0.26
Buckets, barrels, drums	4	(*a* - 3; *d* - 1)	0		0.34	0.27
Car and bicycle parts	2	(*a* - 1; *d* - 1)	0		0.32	1.03
Concrete slabs & rubble (incl. cinderblocks)	13	(*d*)	10	(*a* - 2; *d* - 8)	0.34	0.16
Fiberglass containers & plastic objects	7	(*b* - 1; *d* - 6)	0		0.31	0.36
Metal and concrete pipes	6	(*b* - 3; *c* - 1; *d* - 2)	0		0.13	0.23
Sheet metal & metal grating	10	(*a* - 2; *b* - 2; *d* - 6)	3	(*a* - 1; *d* - 2)	0.59	0.27
Tires	4	(*a* - 2; *c* - 1; *d* - 1)	2	(*c* - 1; *d* - 1)	0.14	0.08
Wooden & steel beams	17	(*d*)	1	(*d* - 1)	0.63	0.37
Other miscellaneous (*bricks, burlap bags, flower pots, garden hoses, etc.*)	3	(*a* - 2; *d* - 1)	3	(*b* - 1; *d* - 2)	0.26	0.09

Table S5. Summary of generalized linear mixed effects models of video transect survey data (I) and midden survey data (II). Tables of the delta values and weights of Akaike's Information Criterion (ΔAIC and wAIC), percentage of deviance explained (%Dev), and Cohen's Kappa statistic (κ) are provided for each response variable considered (labeled *a* through *h*).

(I) Video Transect Surveys	**ΔAIC**	**wAIC**	**%Dev**		**ΔAIC**	**wAIC**	**%Dev**
(a) Count Data				*(b) Presence/Absence*			
Num. of structures	**0.0**	**0.520**	**22.36**	**Num. of structures**	**0.0**	**0.790**	**78.29**
Average height	1.8	0.206	15.18	Horizontal area	2.7	0.202	62.95
Horizontal area	2.8	0.129	11.56	Average height	10.6	0.004	18.48
Depth	5.4	0.036	1.52	Date	13.9	0.001	0.00
Date	5.8	0.029	0.00	Depth	13.9	0.001	0.00
Null	3.8	0.080	0.00	Null	11.9	0.002	0.00

(II) Midden Composition	**ΔAIC**	**wAIC**	**%Dev**		**ΔAIC**	**wAIC**	**%Dev**
(a) Proportional Similarity				*(b) Number of Unique Prey Types*			
Null Model	2.8	0.111	0.00	Surrounding	2.4	0.068	1.83
PPI	4.8	0.041	0.00	Longitude	0.8	0.148	0.59
PC1	4.8	0.042	-0.08	Date	1.0	0.133	0.49
Den Material	6.4	0.018	-0.73	Latitude	1.3	0.119	0.37
Longitude	4.4	0.051	-0.81	Den Material	3.5	0.039	0.27
Date	3.4	0.082	-2.60	Depth	1.7	0.093	0.13
Surrounding	6.8	0.015	-3.73	PC1	1.8	0.093	0.12
Latitude	1.8	0.187	-5.71	PPI	2.0	0.084	0.02
Depth	0.0	0.454	-9.06	Null Model	0.0	0.223	0.00
(c) Number: Heterodonts				*(d) Estimated Tissue Weight: Heterodonts*			
Longitude	**0.0**	**0.527**	**4.28**	**PPI**	**0.0**	**0.773**	**1.72**
PPI	0.6	0.382	4.01	Longitude	3.1	0.164	1.29
PC1	4.3	0.063	2.47	Depth	6.4	0.032	0.85
Den Material	10.2	0.003	0.80	Den Material	9.2	0.008	0.72
Depth	8.8	0.006	0.55	PC1	8.1	0.014	0.61
Latitude	8.9	0.006	0.50	Surrounding	12.3	0.002	0.58
Surrounding	12.9	0.001	0.49	Date	12.0	0.002	0.07
Date	10.1	0.003	0.01	Latitude	12.5	0.002	0.01
Null Model	8.1	0.009	0.00	Null Model	10.5	0.004	0.00

Table S5 (cont).

(II) Midden Composition	ΔAIC	wAIC	%Dev		ΔAIC	wAIC	%Dev
(e) Number: Decapods				*(f) Estimated Tissue Weight: Decapods*			
Surrounding	4.0	0.031	0.83	Surrounding	2.9	0.049	0.57
Depth	0.7	0.168	0.57	Den Material	1.7	0.090	0.42
Den Material	3.2	0.047	0.34	Depth	0.4	0.173	0.29
Latitude	1.3	0.124	0.32	PC1	1.3	0.110	0.13
Date	1.4	0.117	0.27	Latitude	1.4	0.106	0.11
PC1	1.6	0.106	0.18	PPI	1.7	0.089	0.05
PPI	1.9	0.088	0.03	Longitude	1.8	0.089	0.05
Longitude	2.0	0.087	0.02	Date	2.0	0.080	0.01
Null Model	0.0	0.232	0.00	Null Model	0.0	0.213	0.00
(g) Number: All Species				*(h) Estimated Tissue Weight: All Species*			
Surrounding	3.5	0.045	0.72	Surrounding	2.7	0.061	0.40
PPI	1.1	0.147	0.25	PPI	0.7	0.169	0.16
Depth	1.7	0.112	0.09	PC1	1.3	0.122	0.08
Den Material	3.8	0.039	0.07	Den Material	3.5	0.041	0.06
PC1	1.8	0.104	0.05	Depth	1.7	0.102	0.04
Date	1.9	0.099	0.02	Latitude	1.8	0.095	0.02
Longitude	2.0	0.098	0.01	Date	2.0	0.088	0.00
Latitude	2.0	0.096	0.00	Longitude	2.0	0.088	0.00
Null Model	0.0	0.260	0.00	Null Model	0.0	0.235	0.00

Table S6. Summary statistics across all middens collected from octopus dens in Puget Sound. 46 middens were collected in total, from 24 sites (see Figure 1).

	Number			Estimated Tissue Weight		
Species	**Total**	**Mean**	**SE**	**Total**	**Mean**	**SE**
Cancer productus	169	3.8	3.8	5038.2	112.0	112.0
Chlamys hastata	9	0.2	0.2	13.4	0.3	0.3
Chlamys rubida	23	0.5	0.5	14.4	0.3	0.3
Clinocardium ciliatum	13	0.3	0.3	249.2	5.5	5.5
Clinocardium fucanum	6	0.1	0.1	23.1	0.5	0.5
Clinocardium nuttalli	75	1.7	1.7	616.4	13.7	13.7
Crassostrea gigas	2	0.0	0.0	3.7	0.1	0.1
Gari californica	8	0.2	0.2	3.0	0.1	0.1
Humilaria kennerlyi	14	0.3	0.3	165.8	3.7	3.7
Macoma spp.	21	0.5	0.5	23.3	0.5	0.5
Mactromeris polynyma	1	0.0	0.0	1.3	0.0	0.0
Metacarcinus magister	36	0.8	0.8	1292.5	28.7	28.7
Modiolus rectus	1	0.0	0.0	17.2	0.4	0.4
Nemocardium centifilosum	19	0.4	0.4	34.8	0.8	0.8
Neptunea spp.	1	0.0	0.0	0.5	0.0	0.0
Neverita lewisii	4	0.1	0.1	15.5	0.3	0.3
Penitella penita	1	0.0	0.0	8.0	0.2	0.2
Pododesmus macrochisma	293	6.5	6.5	157.5	3.5	3.5
Protothaca staminea	3	0.1	0.1	11.8	0.3	0.3
Protothaca tenerrima	1	0.0	0.0	4.1	0.1	0.1
Pugettia foliata	1	0.0	0.0	0.0	0.0	0.0
Pugettia gracilis	9	0.2	0.2	2.1	0.0	0.0
Pugettia producta	38	0.8	0.8	79.5	1.8	1.8
Pugettia richii	1	0.0	0.0	0.2	0.0	0.0
Saxidomus gigantea	91	2.0	2.0	1631.4	36.3	36.3
Simomactra falcata	5	0.1	0.1	7.6	0.2	0.2
Telmessus cheiragonus	6	0.1	0.1	75.4	1.7	1.7
Terebratalia transversa	18	0.4	0.4	75.7	1.7	1.7
Tresus capax	18	0.4	0.4	351.1	7.8	7.8

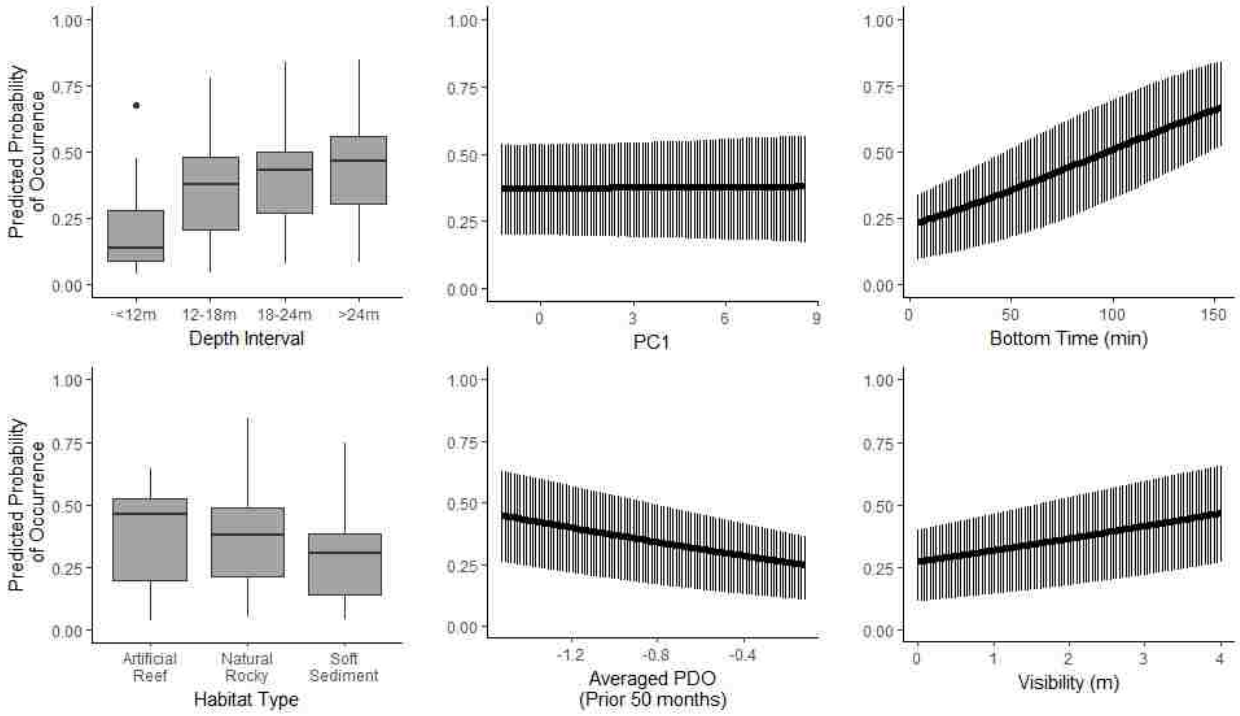

Figure S1. Estimated probability of occurrence based on parameter estimates from the best-fit mixed-effects logistic regression model (model coefficients are shown in Figure 2).

CHAPTER 3: Benthic subtidal assemblages vary across an urban gradient in Puget Sound, Washington, USA

Abstract

Coastal zones through much of the world are currently undergoing rapid urbanization, causing substantial changes to marine habitats. Past studies suggest that artificial structures and other factors associated with urbanization coincide with distinct patterns in benthic marine assemblages. We used subtidal surveys across 36 sites in Puget Sound, Washington, USA to: (1) Determine whether artificial and natural rocky habitats supported distinct benthic assemblages; (2) Identify whether macroalgal composition and abundance varied with land-based urbanization intensity; and (3) Compare the importance of urbanization metrics relative to natural environmental variables as correlates of macroalgal and community composition. Benthic communities in artificial rocky habitats were distinct from, and were more variable than those in natural environments. Additionally, kelp and red filamentous algal turf varied relative to land-based urbanization intensity, with fewer kelps and more red filamentous algal turf at urban sites. Though urbanization metrics correlated strongly with benthic community composition, they were collinear with surface salinity and flow, making it difficult to discern whether urbanization processes or naturally occurring flow and salinity gradients that overlapped with urbanization were most important. Collinearity in explanatory variables will likely be a persistent problem for future studies evaluating urban effects in marine environments, as coastal cities tend to be located in protected bays and at the mouths of rivers, where surface salinity and flow are relatively low. However, observation studies such as this, combined with experimental work that addresses mechanism, are essential for building a framework for understanding and anticipating the effects of future urbanization on marine ecosystem structure and function.

Introduction

The number of people living in coastal regions worldwide is growing rapidly as a result of global population increase and coastward migration (Hugo, 2011; Small and Nicholls, 2003). Much of this growth is taking place in coastal cities (Seto et al., 2011), where urbanization causes substantial changes to the marine landscape (Dafforn et al., 2015). Recent studies in terrestrial environments have found differences in community composition, biotic processes, and abundance of ecologically important and non-native species along urban-to-rural gradients (Aronson et al., 2015; Bates et al., 2011; Evans et al., 2015; Faeth et al., 2011; Uno et al., 2010). However, whether such patterns also occur in urban marine environments and what this may mean for marine ecosystem functioning is presently unknown (Bulleri, 2006). Improved understanding of how marine communities are structured along urban gradients will be important for maintaining ecosystem services to human populations as coastal zones become increasingly urbanized in the coming decades (Neumann et al., 2015; Spalding et al., 2014).

Urbanization alters marine habitats by introducing artificial structures to the seafloor (Dafforn et al., 2015), and by changing nutrient influx, sedimentation rates, and other water quality parameters (Airoldi and Beck, 2007). Urban artificial structures provide hard substrate in both intertidal and subtidal habitats. Past studies indicate that intertidal artificial structures do not serve as effective surrogates for natural rocky environments; Intertidal assemblages differ between artificial and natural rocky substrates (Aguilera et al., 2014; Bulleri et al., 2005; Chapman, 2003; Ferrario et al., 2016; Lam et al., 2009; Martins et al., 2016; Moschella et al., 2005; Musetta-Lambert et al., 2015; Strayer et al., 2012). However, comparable studies on subtidal urban rocky structures have been limited (though see Burt et al., 2011, 2009).

Modified water quality parameters in urban areas tend to be particularly important for macroalgae (Airoldi, 2003; Krause-Jensen et al., 2008). The nutrient-rich, high-sedimentation conditions in urban settings are thought to support opportunistic, turf-forming algal species and macroalgal epiphytes, while limiting the recruitment and survival of kelps (Gorgula and Connell, 2004; Gorman and Connell, 2009; Russell et al., 2005), which are important primary producers and ecosystem engineers (Teagle et al., 2017). Urbanization-related patterns in macroalgal communities have been best documented in urban marine environments in Australia (Gorman et al., 2009) and Europe (Airoldi, 2003), but may also be important drivers of community dynamics in other regions, particularly those where kelps are essential components of nearshore ecosystems.

Puget Sound, in the southern part of the Salish Sea, Washington State, USA, is an ideal system in which to evaluate benthic communities relative to an urban gradient because it has a relatively high degree of patchiness with respect to urbanization intensity compared with other urbanized estuaries. The Puget Sound region supports a population of approximately 4 million (Kelly et al., 2016). High density areas (> 1000 per km^2) are limited to a handful of urban centers, the largest of which are Seattle, Tacoma, and Everett. Though these urban centers occur primarily on the eastern shore of the estuary, Puget Sound is a narrow, fjordal system with complex bathymetry, circulation, and shoreline configuration in which natural longitudinal gradients in benthic composition are unlikely. Further, Puget Sound is located in a biogeographic region that has been relatively well characterized with respect to subtidal benthic species composition and diversity (Elahi et al., 2014; Witman et al., 2004), providing ample context for evaluating urbanization-related patterns in benthic composition.

In this study, we sought to improve knowledge of the effects of marine urbanization by characterizing subtidal benthic communities on artificial and natural rocky habitats across an urban gradient in Puget Sound. Our study was performed with three overarching objectives: (1) Determine whether artificial and natural rocky habitats supported distinct benthic assemblages; (2) Identify whether macroalgal composition and abundance varied with land-based urbanization intensity; and (3) Compare the importance of urbanization metrics relative to natural environmental variables as predictors of macroalgal and community composition. This paper provides a summary of benthic composition patterns relative to urbanization across a temperate estuary with unusually variable degrees of land-based urbanization intensity compared with other populated coastal regions. Findings from the study will contribute to a growing body of literature on the effects of urbanization in marine ecosystems.

Methods

Site selection

Sites were selected throughout the Whidbey, Central, and South Basins of Puget Sound. Potential sites were identified by examining nautical charts from NOAA's Office of Coast Survey for these areas. All locations with sewer pipelines, "ruins", "fish havens" (artificial reefs), breakwaters, reefs, emergent rocks, or steep bathymetric profiles at less than 13 m depth were marked on nautical charts and their coordinates recorded. The locations of sewer pipelines were compared with records of Combined Sewer Overflow (CSO) outfalls from Washington Department of Ecology (www.ecy.wa.gov) to eliminate active CSOs from the list of potential sites in order to ensure the safety of divers. Sites within the jurisdiction of the U.S. Department of Homeland Security (downtown shorelines of Seattle, Tacoma, and Everett) were also eliminated due to accessibility and security concerns.

This process resulted in a total of 60 potential sites (Fig. 1). Each potential site was visited by boat or from shore between January and May 2014, and explored on SCUBA. Photoquadrat surveys were performed at all sites that were found to have extensive rocky substrate (either artificial or natural) between 3 and 12 m depth. Of the 60 sites visited, 36 met these criteria (Fig. 1), and are henceforth referred to as "selected sites".

Photoquadrat surveys and analysis

At each selected site, photoquadrat surveys were conducted along three 10-m horizontal transects, deployed along a constant depth contour of rocky substrate. At most sites, rocky habitat was present only within a range of 3-5 m depth and transect depth was therefore relatively consistent. At sites where rocky habitat extended over a broader depth range, 1 to 2 additional horizontal transects were deployed where sufficient additional hard substrate existed. In all cases, transects were separated by at least 15 m horizontally and at least 5 m vertically. Quadrats (10 per transect) were positioned at every meter along each transect, over the closest gradually sloping rocky substrate. Horizontal and vertical rock surfaces were not used. When the sampling point on the transect fell on a horizontal or vertical surfaces, the closest sloping surface (within 1 m in all cases) was instead surveyed. Quadrats were photographed using a Canon S110 digital camera with an Ikelite underwater housing attached to a 45 × 34 cm (0.153 m^2) PVC framer. Divers also recorded the substrate type (artificial or natural) and depth of each transect.

Photoquadrat data were enumerated using the online repository and annotation tool, CoralNet (coralnet.ucsd.edu). In CoralNet, percent cover is estimated based on the proportion of random annotation points characterized in each species or species group. Based on preliminary species accumulation curves (Supplementary Fig. S1), we applied 200 random annotation points to each photo. Species designations and species groupings are provided in Supplementary Table S1.

CoralNet uses computer vision algorithms and machine-learning to automate the annotation of random points (Beijbom et al., 2015). In the present study, CoralNet's annotation predictions were accurate 54% of the time. Even when CoralNet's "confidence threshold" was set to 78% (coinciding with a 5% drop in label accuracy as suggested by Beijbom et al. (2016)), CoralNet's automated annotations provided limited alleviation of workload. We therefore relied only upon human-annotated photos and used a subset of collected photoquadrats in our final analysis.

To limit bias associated with using only a subset of photoquadrat data, photoquadrats were selected for inclusion in our analysis through several steps. First, we annotated all quadrats from one transect per site and extracted percent cover data. Community composition was then averaged at the transect-level based on all quadrats in the transect (T_Q), and based on 1, 2, 3, and 4 randomly selected quadrats, producing five separate community data matrices (T_Q, $T_{q=1}$, $T_{q=2}$, $T_{q=3}$, and $T_{q=4}$, respectively). Percent cover was compared graphically between transect averages generated from subsets of quadrats versus averages generated from all quadrats. We compared percent cover estimates between T_Q and T_1, T_2, T_3, or T_4 for each benthic cover type using scatterplots and regression statistics, and for the overall community composition using NMDS ordinations and Procrustes analysis. Methods and results for this analysis are presented in further detail in Supplementary Material (Appendix 2). Findings from the analysis led us to conclude that a minimum of three quadrats per transect was adequate to produce representative data for each transect. For the remaining transects in our study, we therefore completed annotations on a minimum of 3 quadrats. All statistical analyses (described below) were performed on transect-level averages of percent cover.

Predictor variables

The predictor variables of primary interest in this study were subtidal habitat type (artificial versus natural rocky habitat) and land-based urbanization intensity. Habitat type was recorded in preliminary examination of nautical charts and confirmed by divers during field surveys. Urbanization was characterized using two separate indices: a Population Proximity Index (PPI), which was calculated within a 20 km radius of each site (Feist and Levin, 2016), and an index derived from five spatial data layers (Table 1) via Principal Component Analysis (PCA) (Alberti, 2008; Spirandelli, 2014). Principal Component Analysis (PCA) was performed to reduce the dimensionality of urbanization metrics and generate an index of urbanization. Spatial data layers used in PCA included human population density (U.S. Census Bureau, 2010), area weighted mean imperviousness (USGS, 2014; Xian et al., 2011), proportion of intertidal shoreline armored with coastal defense structures (PSNERP, 2010), road density (HSIP, 2013), and proportion of adjacent land characterized by NOAA's Coastal Change Analysis Program (C-CAP; NOAA, 2013) as High Intensity Developed (Table 1). These data layers were summarized at the level of riverine basin, as designated by the Puget Sound Nearshore Restoration Project, and normalized to prevent their having a disproportionate effect on the resulting urbanization index. PCA was performed using the function *prcomp* in R (Version 3.3.1, R Development Core Team 2016). The first principal component (PC1), which explained 61% of the variation in urbanization metrics and corresponded with population density, imperviousness, road density, and high intensity development, was subsequently used as an explanatory variable of macroalgal and community composition (Table S4). PC2, which explained 16% of the variation and corresponded primarily with shoreline armoring, was not considered further, as habitat type (artificial versus natural rocky substrate) was already accounted for as a predictor. PC3 was also excluded as a model predictor, however, because it correlated with PC1 (Spearman’s rank

correlation, rS = 0.56). The fourth and fifth principal components were also excluded as model predictors because they explained little of the variation (Table S4).

To contextualize the relative magnitude of effects from urbanization and artificial structures, we also compiled a suite of marine environmental variables for comparison (Table 2). Depth for each transect was recorded by divers during field surveys. Estimates of flow, salinity, and temperature were derived from a hindcast simulation model of the Salish Sea, which is summarized in Sutherland et al. (2011). We also generated an index of relative wave (and wind) exposure at each of our study sites using the Waves (v. 2012) tool (Rohweder et al., 2008). We used ArcGIS to calculate a wind speed and direction weighted fetch distance for Puget Sound. We ran our model over a spatial domain spanning 47.0° to 50.0° N latitude and -122.2° to -124.6° W longitude, with a spatial grain or resolution of 50 m. The tool used two input geospatial data layers: shoreline and wind. For the Canadian and the US portions of the shoreline (converted from vector to 50 m grid), we used NASA's world surface water body data (downloaded from http://gis.ess.washington.edu/data/vector/worldshore/index.html) and USGS digital line graph (DLG, USGS Various), respectively. For the wind data, we used "normal" hourly wind direction and velocity for the Sea-Tac International Airport weather station (Arguez et al., 2010), based on data from 1980 – 2010. We used this wind station because it was central to modeling domain had a complete data record from 1980 – 2010. We used the SPM-Restricted option in the Waves tool to generate wind direction and speed weighted fetch distances for all of the 50 m grid cells in the modeled area. Finally, we overlaid the point locations for each of our study sites with the resulting weighted fetch distance grid and captured the relative wave exposure value for each site.

Statistical analyses

To determine whether artificial and natural rocky habitats supported distinct benthic assemblages, we used multivariate permutational analysis of variance (PERMANOVA, Anderson, 2001) based on Bray-Curtis dissimilarities of square-root transformed percent cover data that had been aggregated to the transect level. Square-root transformations were performed to reduce the contribution of dominant space-occupiers to multivariate patterns. PERMANOVA was performed in R using the function *adonis2()* in the vegan package (Oksanen, 2015), with site specified in the function's *strata* argument. In order to evaluate whether data dispersion was homogenous between habitat types (an assumption of PERMANOVA), an analysis of multivariate dispersion (PERMDISP) (Anderson, 2006) was also performed using the vegan function *betadisper()*. Non-metric multidimensional scaling (NMDS) was used to visualize the results, and a SIMPER analysis was performed to identify the benthic cover types that contributed most to differences between habitat types.

We conducted a series of additional procedures to evaluate the relative importance of habitat type and other environmental predictors for benthic composition. First, a Mantel test was performed to determine how well environmental predictors corresponded with differences in community composition. Partial Mantel tests were then used to evaluate spatial autocorrelation and control for geographic distance in correlations between dissimilarity of community composition and environmental predictors. To compare the importance of environmental predictors, we used canonical correspondence analysis (CCA) with backward stepwise fitting. Specifically, a partial CCA was used to account for spatial autocorrelation, and incorporated a third conditioning matrix of geographic coordinates in addition to species percent cover and environmental predictor matrices. Only predictor variables that met the assumption of multicollinearity were used in a given partial CCA model; collinearity was assessed both based

on Spearman correlation coefficients of predictor variables and on variance inflation factors in the final partial CCA model. These analyses were also performed in R using the vegan package.

We examined macroalgal composition and abundance relative to urbanization using percent cover of the three most abundant macroalgal groups: red foliose macroalgae, red filamentous algal turf, and kelps. Percent cover data were non-normally distributed and fit poorly to generalized linear models with binomial and beta error distributions. We instead tested for correlations with urbanization and environmental variables using PERMANOVA with Euclidean distances and 999 permutations. Univariate PERMANOVA is similar to traditional ANOVA, but avoids distributional assumptions by using permutations. Percent cover of the three macroalgal groups was assessed relative to urbanization in two separate models, each with PC1 or PPI as the sole predictor variable. To evaluate the relative importance of urbanization effects, additional models were run for each of the environmental variables listed in Table 2 and compared based on their respective PERMANOVA test statistics. Univariate PERMANOVA tests were performed in R, with site specified as strata in the function *adonis2()*.

Results

Benthic Composition

Rocky subtidal habitats surveyed in this study were dominated by red foliose macroalgae and red filamentous algal turf (Fig. 2a). Red foliose macroalgae consisted of *Chondracanthus exasperatus, Polyneura latissima, Plocamium cartilagineum, Cryptopleura ruprechtiana*, and others. Red filamentous algal turf was likely comprised of a variety of filamentous species, which could not be identified from photos. We observed these filamentous turfs in a range of states from fresh, pigmented growth with a height of up to 5 cm, to heavily sedimented forms that lacked obvious pigment and ranged in height from 1 to 3 cm.

Kelps (Laminariales) were the eighth most common occupiers of space, with a mean percent cover of 3.7% (SE ± 0.7%). This group was dominated by the subtidal Laminarian *Agarum fimbriatum*, though *Saccharina latissima*, *Costaria costata*, and others were also found. No major canopy-forming kelps (ie - *Nereocystis luetkeana*) were observed in photoquadrats. Other common benthic cover types were bare substrate (13.1 ± 1.6%), *Balanus* spp. (7.8 ± 1.3%), and crustose coralline algae (3.9 ± 0.7 %). *Metridium* spp., which included two species (*M. farcimen* and *M. senile*), had a mean percent cover of 6.5% (SE ± 1.6%), but were found at only 18 of 36 sites. Conversely, red foliose macroalgae, red filamentous algal turf, bare substrate, *Balanus* spp., and crustose coralline algae were observed at > 90% of sites. Kelp was present at 21 of the 36 sites (58%).

Macroalgal groups exhibited distinct depth distributions (Fig. 2b). Red macroalgae was especially dominant in shallow water habitats (< 9 m depth) while cover of crustose coralline algae increased with depth. Red filamentous algal turf tended to occur across the depth range surveyed. Kelps were most common in moderate depths, from 5 to 10 m depth (Fig. 2b).

Artificial versus natural rocky habitat

Benthic community composition was more variable in artificial rocky habitat than in natural rocky habitat. We observed significant differences in multivariate dispersion between habitat types (PERMDISP, $F = 5.56$, $P = 0.03$). The NMDS ordination showed overlap in artificial and natural rocky habitat communities, with greater clustering among natural habitat sites (Fig. 3a). For unbalanced designs, PERMANOVA tends to be conservative when there is greater dispersion in the larger group (Anderson and Walsh 2013), as was the case in this study; PERMANOVA was therefore performed.

PERMANOVA indicated differences in community composition between artificial and natural rocky habitats (df = 1, 34, F = 39.671, $P < 0.0001$). These differences were attributed to eight benthic cover types based on SIMPER results (Table 3): red foliose macroalgae, red filamentous algal turf, *Balanus* spp., kelp, bare substrate, *Metridium* anemones, colonial diatoms, and crustose coralline algae. Natural rocky habitats tended to have slightly more bare substate, greater cover by kelps, crustose coralline algae, and red foliose macroalgae, and less cover by red filamentous algal turf than artificial rocky habitats (Table 3).

Numerous environmental variables corresponded significantly with benthic composition (Mantel r = 0.299, P < 0.0001). In partial CCA, the first two axes accounted for 40.6% and 24.4% of the association between environmental variables and community dissimilarity, and there were six significant canonical axes in total. Most of the explanatory variables tested were found to coincide significantly with the community dissimilarity matrix, regardless of the number of total variables that were included or the order in which they were removed in stepwise selection. However, the variables that tended to be eliminated first and had consistently low permutational p-values in partial CCA were depth, habitat type, date, and wave exposure (Fig. 3b). Depth, date, and wave exposure were also the most significantly correlated with benthic composition in partial Mantel tests, though mobile fauna cover and surface salinity were also significant (Table 4).

Urbanization intensity and macroalgal cover

Cover by filamentous algal turf was positively correlated with the urbanization metrics, PPI and PC1 (Table 5, Fig. 4). Univariate PERMANOVA also revealed an inverse relationship between turf cover and both surface salinity and flow, which varied collinearly with urbanization metrics (flow and surface salinity tended to be lower at urban sites). Whether filamentous algal

turf was associated with urbanization or natural environmental gradients could not, therefore, be determined based on our data. In addition to these patterns, red filamentous algal turf cover was slightly negatively correlated with date.

Kelp showed the opposite trend relative to surface salinity, flow, PC1, and PPI. Kelp cover was highest in rural areas, where surface salinity and flow were also relatively high (Table 5, Fig. 4). Kelp cover also varied systematically with sampling date and habitat type. Kelps increased over the sampling period, and tended to be more abundant in natural rocky habitats, as was discussed previously. There was no relationship between kelp cover and bottom salinity, temperature, mobile fauna, or other environmental variables.

Benthic cover by red foliose macroalgae was unrelated to urbanization intensity, but did correlate significantly with surface salinity, with lower red foliose macroalgal cover in areas with freshwater surface layers. Red foliose species were inversely related to wave exposure, though not flow. Shoreline wave exposure may be a better proxy of water movement compared with bottom flow velocity due to the shallow depth zone they tended to inhabit (Fig. 2b). Further, red foliose macroalgae was negatively correlated with percent cover of mobile fauna (Table 5).

Discussion

Urban estuaries serve as an experiment in progress and a natural laboratory in which to evaluate how ecosystems shift as marine habitats become integrated into human-dominated landscapes. This study characterized benthic subtidal assemblages across an urban gradient, compared assemblage structure in artificial and natural rocky habitats, and evaluated spatial patterns in macroalgal cover relative to land-based urbanization intensity across Puget Sound. Communities inhabiting artificial and natural rocky habitats differed, despite similar substrate

materials and benthic profile. Though kelp and red filamentous algal turf did vary relative to land-based urbanization intensity, collinear relationships between urbanization metrics, surface salinity, and flow make it difficult to discern between the potential mechanisms driving this pattern. This will likely be a persistent problem in studies evaluating urban effects, as coastal cities tend to be located in protected bays and at the mouths of rivers, where surface salinity and flow are relatively low. Nonetheless, the patterns we documented in kelp and filamentous algal turf relative to co-varying urban/environmental variables is a necessary first step towards characterizing urban gradients and developing testable mechanistic hypotheses relating to the effects of urbanization in marine ecosystems. It also underscores the importance of accounting for confounding variables.

Responses of subtidal communities to artificial rocky substrates

Findings from this study indicate that rocky subtidal artificial structures frequently support distinct benthic assemblages from natural rocky substrate in Puget Sound. This is consistent with past work in the intertidal zone, which documented differences in sessile flora and fauna in natural and artificial hard-substrate environments in several regions (Aguilera et al., 2014; Bulleri et al., 2005; Chapman, 2003; Ferrario et al., 2016; Lam et al., 2009; Martins et al., 2016; Moschella et al., 2005; Musetta-Lambert et al., 2015; Strayer et al., 2012), but may include the age, construction material, and physical characteristics (vertical relief, size, spatial configuration, etc.) of artificial structures (Burt et al., 2009; Granneman and Steele, 2015). Artificial structures may also differ from natural habitats with respect to connectivity and isolation (Airoldi et al., 2015), biotic interactions (Bulleri et al., 2006; Marzinelli et al., 2011), and the frequency with which they are subject to anthropogenic disturbance (Airoldi and Bulleri, 2011). These and other

factors may have influenced results with respect to natural versus artificial rocky habitats, yet experimental work is needed to discern mechanisms.

Additionally, community composition on artificial structures was more variable than that on natural rocky substrate. This may have been indicative of artifacts from the study design. Though we visited all known artificial and natural rocky sites in the study area, there were fewer natural rocky habitats to sample than artificial structures, which made for unbalanced comparisons. Natural habitats also tended to occur in more rural locations (with relatively high flow and surface salinity) while artificial structures occurred throughout the study area. This may have influenced differences for several taxa, particularly kelp and red filamentous algal turf. In future observational studies, these limitations could potentially be addressed by expanding spatial scope or adjusting survey design to include only sets of similar, adjacent natural/artificial site pairs. Both of these approaches may prove challenging because of the inherent challenges in studying marine urbanization observationally (discussed further in Section 4.3).

Effects of urbanization on space-dominant macroalgae

Kelp and red filamentous algal turf varied relative to land-based urbanization intensity in a manner that was consistent with marine urbanization literature. Urban sites tended to support fewer kelps and more red filamentous algal turf than more rural sites. Importantly, sites with high urbanization intensity in our study tended to have lower mean surface salinity and lower estimated flow. Whether the patterns observed in kelp and algal turf cover were the result of urbanization processes or naturally occurring flow and salinity gradients that overlap with urbanization is therefore uncertain.

Kelps are limited by several of the environmental variables associated with marine urbanization, including increased sedimentation, light limitation, and altered hydrodynamic

conditions (Airoldi, 2003; Dayton, 1985). These factors may be limiting at multiple life stages. In the present study, population proximity index (PPI) was the best correlate of kelp cover. This is consistent with recent work from Feist and Levin (2016), who found negative correlations between canopy-forming kelp (primarily *Macrocystis pyrifera* and *Nereocystis luetkeana*) and PPI on the West Coast of the US. The present analysis quantified understory kelp cover over a smaller spatial range, and suggests that further work on the sensitivity of understory kelp species to urbanization is needed.

The opposite pattern was exhibited by red filamentous algal turf relative to urbanization intensity and is also consistent with predictions from the literature. Dominance by algal turfs in response to anthropogenic disturbance has been documented in several regions (Airoldi et al., 2008; Connell, 2007; McCook, 2001). Though experimental work discerning mechanism has been limited, increased nutrient and sediment loads may be important factors supporting greater turf cover in urban areas (Gorgula and Connell, 2004). These factors were not explicitly incorporated into our analysis, though they are closely related with flow and water column stratification. Connell et al. (2014) noted the importance of defining algal turf more comprehensively, and morphological, physiological, and ecological characteristics of algal turfs may influence their response to anthropogenic stressors. We have provided a basic summary of the red filamentous algal turf that is a dominant component of Puget Sound rocky subtidal communities, but there is still need to identify species composition and epifaunal interactions, characterize spatial patterns over time, and understand temporal dynamics relative to environmental variables.

Challenges and future directions for marine urban ecology

Our ability to draw firm conclusions about the effects of urbanization was limited by the fact that urban and naturally-occurring environmental gradients co-vary; that is also indicative of the broader challenges of characterizing the effects of urbanization on marine ecosystems. Because of the placement of most coastal cities, it is difficult to discern whether ecological patterns along urban gradients are in fact attributable to urbanization, or are the result of naturally occurring gradients in environmental factors that overlap with urbanization intensity, such as freshwater influx, water-column stratification, and current speed. For this reason, there is considerable need both for studies that improve our understanding of these relationships, and for experimental studies that test alternative mechanisms by which urbanization may be impacting important species groups, such as kelps. Unraveling these interactions will be complicated by the fact that marine urbanization occurs over multiple scales, with localized modification of factors such as bathymetry, sediment influx, effluent and waste water inputs, and point-source pollutants (Epstein et al., 2016; Firth et al., 2016; Von Glasow et al., 2013), as well as regional changes in factors such as nutrient load, oxygen availability, and pCO_2 and pH (Feely et al., 2010; Hawkins et al., in press). Local and regional scale anthropogenic stressors likely have differential effects on marine ecosystems (Elahi et al., 2015; Hawkins et al., in press; Strain et al., 2014). Expanded study at both local and regional scales, and in a manner that integrates across spatial scales, is thus ever more critical as nearshore habitats become increasingly urbanized.

Though correlation between urbanization intensity and naturally occurring environmental variables make it difficult to discern between potential mechanistic hypotheses based on observational studies alone, observational patterns of marine communities over urban gradients are nevertheless informative. We conclude that urban areas do appear to support distinct marine assemblages, and this is an important consideration for nearshore ecosystem management

regardless of whether anthropogenic or natural drivers are the primary cause. The present study contributes to a growing body of literature documenting patterns in marine ecosystems relative to urban gradients globally. These studies combined with experimental work in the field are critical steps towards building a framework for understanding and anticipating the effects of future urbanization on marine ecosystem structure and function.

Tables

Table 1. Urbanization-related variables used in Principal Component Analysis (PCA). All metrics were summarized at the level of riverine basins, as designated by the Puget Sound Nearshore Ecosystem Restoration Project (PSNERP, 2010).

Variable	Description	Source
Armoring	Proportion of basin classified as armored	(PSNERP, 2010)
Population Density	Density (people/km2) of humans living in given PSNERP basin	(U.S. Census Bureau, 2010)
Imperviousness	Area weighted mean imperviousness	(USGS, 2014; Xian et al., 2011)
Road Density	Density (m of road/km2) of roads in al NAVTEQ functional classes	(HSIP, 2013)
High Intensity Development	Proportion of basin designated as high intensity development (a land use and land cover category in NOAA's Coastal Change Analysis Program)	(NOAA, 2013)

Table 2. Predictor variables used in both univariate and multivariate response variables. Univariate responses (percent cover of red foliose macroalgae, red filamentous algal turf, and kelp) were assessed via univariate PERMANOVA. Multivariate community composition evaluated relative to each variable below via one-way multivariate PERMANOVA.

Variable	Description	Level of Aggregation / Scale	Source
Area Depth	Estimated water depth in meters relative to mean high water (MHW), as extracted from NOAA NGDC tsunami inundation grids and NOS hydrographic survey data	Site	Shelton et al. (2017)
Date	Month, day, and year on which the survey took place	Site	Recorded in the field
Depth	Transect depth in meters	Transect	Recorded in the field
Flow	Mean estimated bottom flow from the Salish Sea hindcast simulation model (computed from model outputs *u* and *v* as sqrt($u^2 + v^2$)	Model grid	Sutherland et al. (2011)
Habitat	Type of rocky habitat (artificial or natural)	Site	Recorded in the field
PC1	The first principal component (corresponding with population density, imperviousness, road density, and high density development)	PSNERP basin*	Principle Component Analysis
PPI	Population Proximity Index (PPI) within a 20 km radius	Site	Feist and Levin (2016)
Salinity	Mean estimated bottom salinity from the Salish Sea hindcast simulation model	Model grid (300 m cells)	Sutherland et al. (2011)
Surface Salinity	Mean estimated surface salinity from the Salish Sea hindcast simulation model	Model grid	Sutherland et al. (2011)
Temperature	Mean estimated bottom temperature from the Salish Sea hindcast simulation model	Model grid	Sutherland et al. (2011)
Wave Exposure	Index of wave exposure, incorporating 30 year wind patterns and fetch	Site	Arguez et al. (2010); USGS (Various)

** Puget Sound Nearshore Ecosystem Restoration Project (PSNERP) riverine basins (PSNERP, 2010)*

Table 3. Mean cover, average (and standard deviation of) dissimilarity, and cumulative percent contributions of 8 benthic cover types highlighted in SIMPER analysis as being particularly important in shaping differences between artificial and natural rocky habitat communities.

	Mean Cover		**Dissimilarity**		**Cumulative**
Benthic Cover Type	*Artificial*	*Natural*	*Avg*	*SD*	**%**
Red foliose macroalgae	0.505	0.595	0.066	0.052	0.453
Red filamentous algal turf	0.451	0.389	0.048	0.038	0.355
Balanus spp.	0.187	0.196	0.047	0.043	0.963
Kelp	0.050	0.199	0.045	0.039	0.551
Bare substrate	0.317	0.308	0.044	0.034	0.146
Metridium spp.	0.169	0.007	0.038	0.061	0.936
Colonial diatoms	0.121	0.097	0.035	0.039	0.252
Crustose coralline algae	0.114	0.205	0.034	0.030	1.000

Table 4. Results from partial Mantel tests for each urbanization-related and environmental predictor variable. Partial Mantel tests were based on Pearson's product-moment correlation using 9999 permutations, and tested for correlations between benthic composition and each variable while controlling for geographic distance. The table presents the Mantel statistic (*r*) and the empirical significance based on permutations (*P*).

Variable	*r*	*P*
Date	0.1281	0.0001
Depth	0.3399	0.0001
Flow	0.0775	0.0564
Mobile fauna	0.1056	0.0170
PC1	0.0396	0.1082
PPI	0.0478	0.0714
Salinity	-0.0046	0.5275
Surface salinity	0.0924	0.0219
Temperature	0.0367	0.1250
Wave exposure	0.0769	0.0110

Table 5. Summary of univariate PERMANOVA tests used to detect significant relationships between environmental predictors and three response variables: percent cover of (1) red foliose macroalgae, (2) red filamentous algal turf, and (3) kelp.

		Red Foliose Macroalgae		*Red Filamentous Algal Turf*		*Kelp*	
Variable	df	F	Pseudo-P	F	Pseudo-P	F	Pseudo-P
Date	1	2.810	0.088	13.479	0.001	13.648	0.001
Depth	1	46.460	0.001	0.776	0.382	0.265	0.625
Flow	1	1.833	0.171	6.164	0.011	40.066	0.001
Habitat	1	3.216	0.073	2.970	0.108	28.449	0.001
Mobile fauna	1	30.841	0.001	4.229	0.043	0.051	0.831
PC1	1	0.272	0.608	14.350	0.001	14.795	0.001
PPI	1	0.339	0.556	6.462	0.016	79.714	0.001
Salinity	1	0.008	0.935	0.337	0.549	2.882	0.090
Surface salinity	1	15.834	0.001	18.177	0.001	27.708	0.001
Temperature	1	5.207	0.024	1.959	0.181	0.200	0.663
Wave exposure	1	26.415	0.001	0.786	0.381	2.087	0.164

Figures

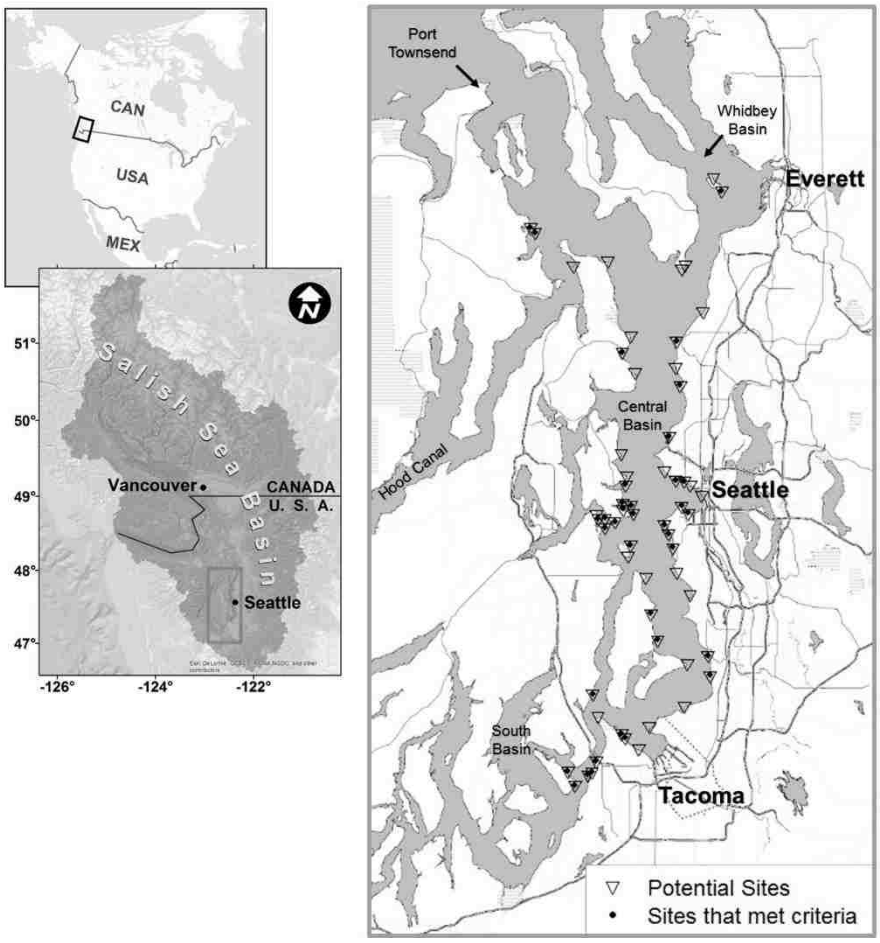

Figure 1. Map of study area in Puget Sound, the southern part of the Salish Sea. Potential sites identified from nautical charts and explored via SCUBA are shown as triangles. Sites that met the criteria of having extensive rocky substrate (either artificial or natural) between 3 and 12 m depth, and that were surveyed using benthic photoquadrats, are shown as black circles. Some components of this figure were provided by Blake Feist (NOAA/NWFSC).

(*a*)

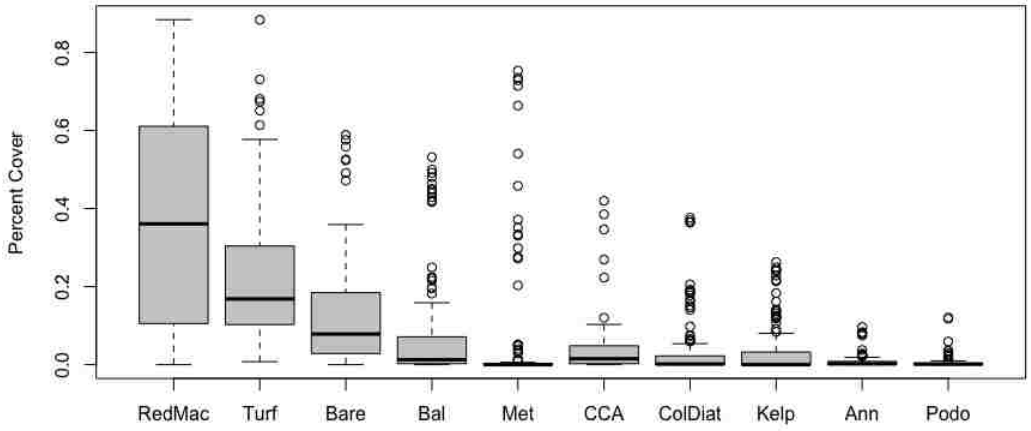

(*b*)

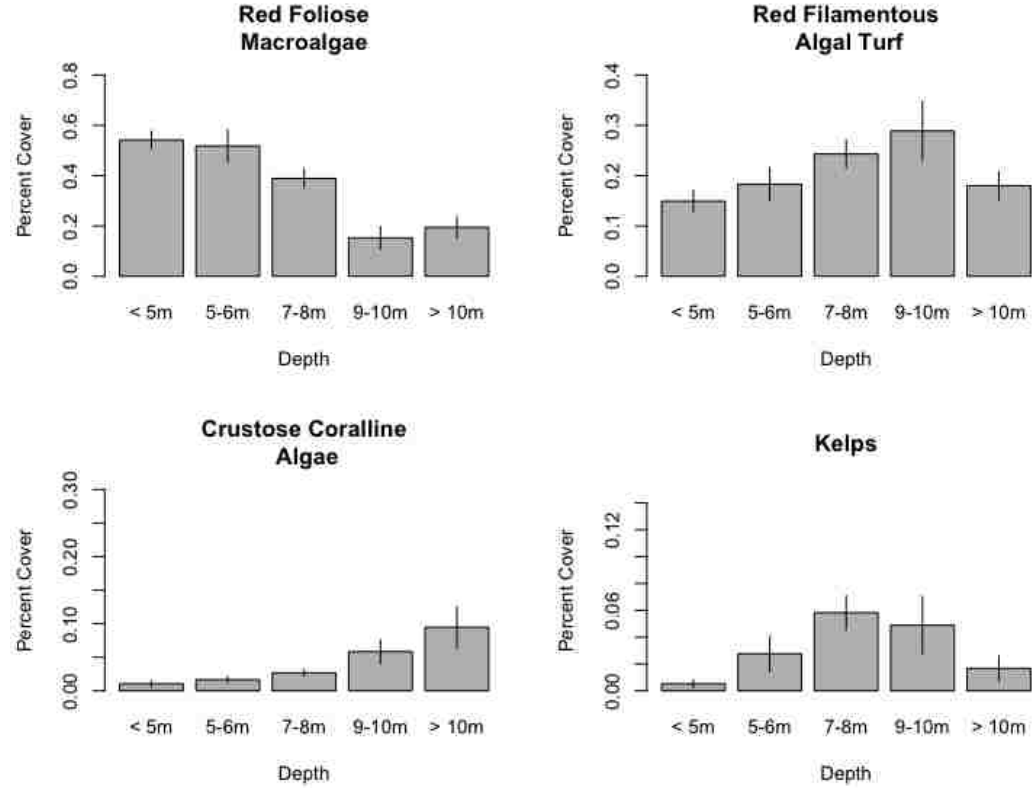

Figure 2. (*a*) Boxplot of the percent cover of the 10 most common benthic cover types observed in rocky subtidal habitats (both artificial and natural) in Puget Sound. Abbreviations on the x-axis stand for the following - RedMac: red foliose macroalgae, Turf: red filamentous algal turf, Bare: bare substrate, Bal: *Balanus spp*., Met: *Metridium spp*., CCA: Crustose coralline algae, Kelp: Laminariales, ColDiat: Colonial Diatoms, Ann: Annelids, Podo: *Pododesmus machrochisma*. (*b*) Average percent cover vs depth of the major macroalgal groups observed in subtidal surveys of Puget Sound (red foliose macroalgae, red filamentous algal turf, crustose coralline algae, and kelps). Note the differences in y-axis range between species groups.

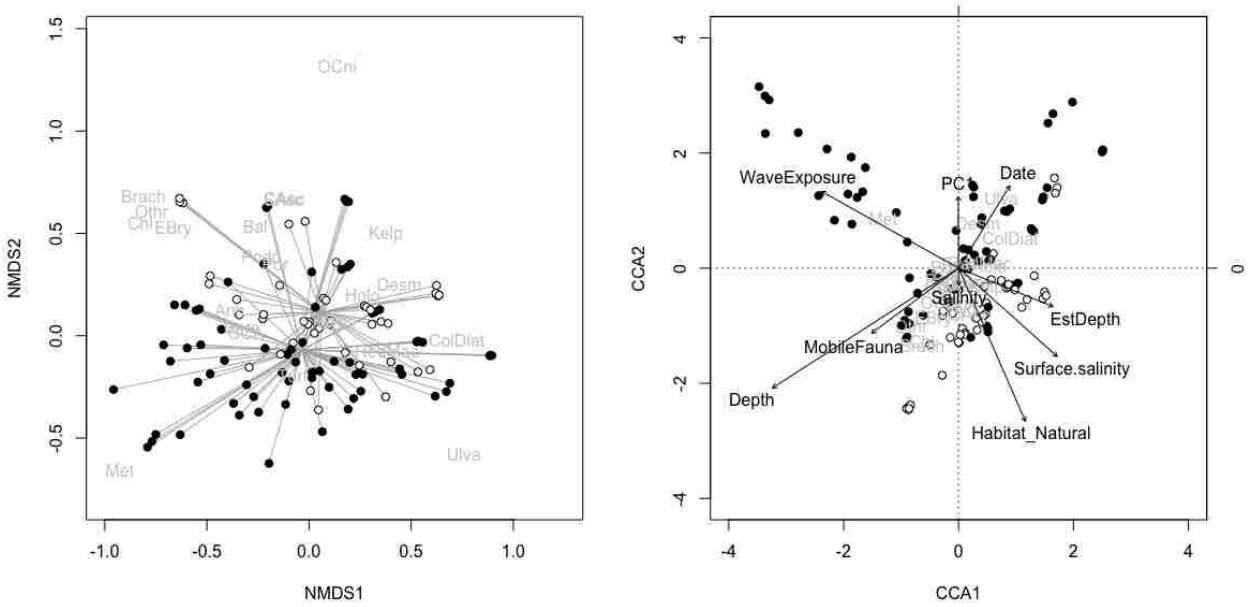

Figure 3. (*Left*) Non-metric multidimensional scaling (NMDS) ordination based on Bray-Curtis dissimilarity matrix of square-root transformed percent cover data from each of the 36 surveyed sites, with black points representing artificial rocky sites and white points representing natural rocky sites. Stress = 0.169 (k = 2). (Right) Biplot from the partical canonical correspondence analysis (CCA) of percent cover data against selected environmental variables. Urbanization metrics and the other predictor variables (Table 2) that are not shown were eliminated from consideration in the backward stepwise fitting process of partial CCA models. In both plots, species codes (shown in light gray) represent the following: Ann = Annelids, Bal = *Balanus spp*., Bare = Bare substrate, BBry = Branching bryozoans, Brach = Brachiopods, CAsc = Compound Ascidians, CCA = Crustose coralline algae, Chl = Scallops, ColDiat = Colonial diatoms, Desm = Desmarestiales, EBry = Encrusting bryozoans, Holo = Holothuroids, Hyd = Hydroids, Kelp = Laminariales, Met = *Metridium spp*., OCni = Other Cnidarians, Othr = Other species, Podo = *Pododesmus machrochisma*, Por = Porifera, RedMac = Red foliose macroalgae, SAsc = Social or solitary ascidian, Turf = Red filamentous algal turf, Ulva = Ulvoids.

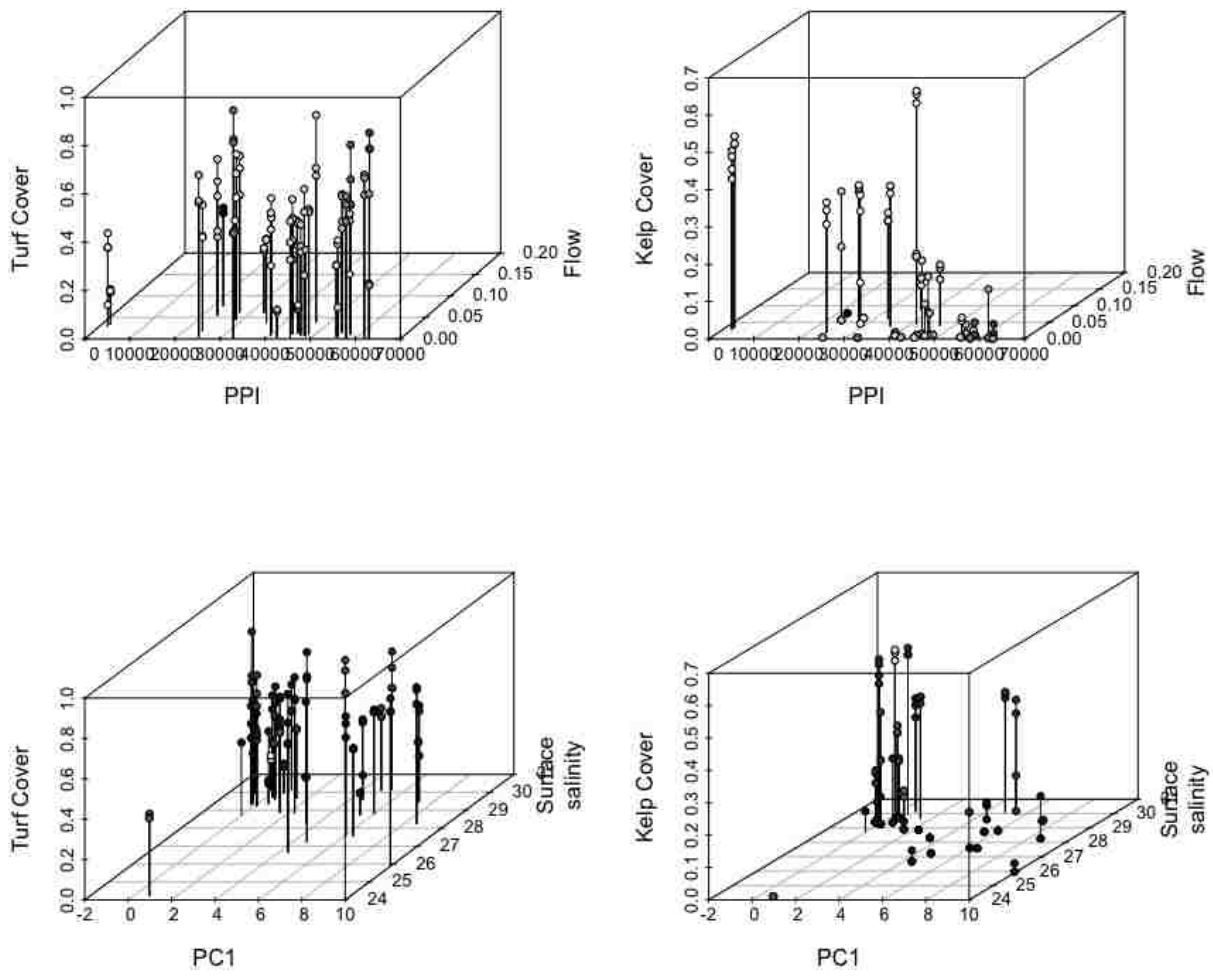

Figure 4. Relationships for red filamentous algal turf and kelp cover with covariates, (top row) Population Proximity Index (PPI) and flow, and (bottom row) PC1 and surface salinity. PC1 was the first principle component from PCA, and corresponded with population density, imperviousness, road density, and high intensity development. PPI was calculated within a 20 km radius of each site. PC1 and PPI were both negatively correlated with surface salinity and flow. Points in the top row plots are shaded by relative surface salinity, while plots on the bottom row are shaded by relative flow values. Red filamentous algal turf was positively related with urbanization and negatively related with surface salinity. Kelp was negatively related with PC1/PPI and positively related with surface salinity/flow (Table 5).

Supplementary material

APPENDIX 1: CoralNet

Table S1. Label set (species name and code) used in CoralNet to characterize benthic community composition and the aggregations for each code that were used in analyses. Aggregations were assigned broadly to account for any potential identification errors in photoquadrats with the lowest image clarity. Species are listed alphabetically within 3 groups: Invertebrates, Non-Biotic, and Macroalgae. All vertebrates were characterized as mobile fauna ("mob"). Line items in which the "Aggregation for Analysis" column is NA were excluded from our analyses.

Invertebrates	CoralNet Code	Aggregation for Analysis
Aplidium californicum	APCA	Compound Ascidians
Aplidium solidum	APSO	Compound Ascidians
Aphrocallistes vastus	APVA	Porifera
Balanus crenatus	BACR	*Balanus spp.*
Balanophyllia elegans	BAEL	Other Cnidarians
Balanus nubilis	BANB	*Balanus spp.*
Bryozoa: hard: branching	BHB	Branching Bryozoans
Bryozoa: hard: encrusting	BHE	Encrusting Bryozoans
Boltenia villosa	BOVI	Social or Solitary Ascidians
Botrylloides violaceus	BOVO	Compound Ascidians
Bugula californica	BUCA	Branching Bryozoans
Chlamys hastata	Cha	Scallops
Chelyosoma productum	CHEL	Social or Solitary Ascidians
Cliona californiana	CLCA	Porifera
Cnemidocarpa finmarkiensis	CNFI	Social or Solitary Ascidians
Corella spp.	COSP	Social or Solitary Ascidians
Crassadoma gigantea	CRDO	Scallops
Crisia spp.	CRIS	Branching Bryozoans
Cystodytes lobatus	CYDL	Compound Ascidians
Dendrobeania lichenoides	DELI	Encrusting Bryozoans
Didemnum carnulentum	DICA	Compound Ascidians
Diaperoecia californica	DICL	Branching Bryozoans
Didemnum tridemnum	DITR	Compound Ascidians
Dodecaceria concharum	DOCO	Annelids
Eurystomella bilabiata	EUBI	Encrusting Bryozoans
Eudistoma purpuropunctatum	EUPU	Compound Ascidians
Halocynthia igaboja	HAIG	Porifera
Halichondria panicea	HAPA	Porifera
Hydroids	HYDD	Hydroids

Leucilla nuttingi	LENU	Porifera
Leucosolenia spp.	LEUC	Porifera
Metridium farcimen	MEFA	*Metridium spp.*
Membranipora serrilamella	MESE	Encrusting Bryozoans
Metridium senile	MESN	*Metridium spp.*
Metandrocarpa taylori	META	Social or Solitary Ascidians
Mobile invertebrates	mob	Mobile fauna
Myxicola infundibulum	MYIN	Annelids
Nudibranch sp. - Egg Case Ribbon	NsEgg	Other
Pododesmus macrochisma	PDMC	*Pododesmus macrochisma*
Perophora annectens	PEAN	Social or Solitary Ascidians
Phyllochaetopterus prolifica	PHPR	Annelids
Psolidium bidiscum	PSBI	Holothuroids
Psolus chitonodes & Cucumaria spp.	PSCH	Holothuroids
Pyura haustor	PYRH	Social or Solitary Ascidians
Pycnoclavella stanleyi	PYST	Compound Ascidians
Strongylocentrotus droebachiensis	Sdr	Mobile fauna
Serpulidae worm	Serpulworm	Annelids
Spirorbid worms	Spirorworm	Annelids
Sponges	Sponge	Porifera
Stylantheca spp.	STLN	Hydroids
Styela sp.	STYE	Social or Solitary Ascidians
Sycon sp.	SYSP	Porifera
Terebratalia transversa	TETR	Brachiopods
Terebratalia unguicula	TEUG	Brachiopods
Thelepus crispus	THCR	Annelids
Tonicella spp.	Tli	Mobile fauna
Tunicate, social unidentified	TSOU	Social or Solitary Ascidians
Tunicate solitary unidentified	TSUN	Social or Solitary Ascidians
Tunicate, compound unidentified	TUCM	Compound Ascidians
Urticina columbiana	URCO	Other Cnidarians
Urticina crassicornis	URCR	Other Cnidarians
Worms: Polychaetes: Tube worms	WPTW	Annelids

Macroalgae

Benthic mat (diatoms)	BM	Colonial Diatoms
Agarum fimbriatum	AGFI	Kelp
Callophyllis spp.	CALL	Red Foliose Macroalgae
Crustose coralline algae	CCA	CCA
Chondracanthus exasperatus	CHEX	Red Foliose Macroalgae

Costaria costata	COST	Kelp
Cryptopleura ruprechtiana	CRRU	Red Foliose Macroalgae
Desmarestia munda	DEMU	*Desmarestia spp.*
Desmarestia sp.	DESM	*Desmarestia spp.*
Desmarestia viridis	DESV	*Desmarestia spp.*
Fucus distichus	FUCU	*Fucus spp.*
Gloiocladia laciniata	GLOI	Red Foliose Macroalgae
Laminaria complanata	LAMC	Kelp
Macroalgae: Encrusting	MAEN	Bare substrate
Macroalgae: Filamentous / filiform : red	MAFR	Red Filamentous Algal Turf
Macroalgae: Large canopy-forming : brown	MALCB	Kelp
Opuntiella californica	OPCA	Red Filamentous Algal Turf
Plocamium cartilagineum	PLCA	Red Foliose Macroalgae
Polyneura latissima	POLA	Red Foliose Macroalgae
Red Turf	RedTurf	Red Filamentous Algal Turf
Saccharina bongardiana	SACB	Kelp
Sarcodiotheca gaudichaudii	SAGA	Red Foliose Macroalgae
Saccharina latissima	SALA	Kelp
Sargassum muticum	SAMU	Sargassum muticum
Stenogramme interrupta	STNI	Red Foliose Macroalgae
Ulva sp.	ULVA	Ulvoids
Unspecified red algae: Branching: Fine/Thin	URB1	Red Filamentous Algal Turf
Unspecified red algae: Branching: Thick	URB2	Red Foliose Macroalgae
Unspecified red algae: Sheet: Thin/Membranous	URS1	Red Foliose Macroalgae
Unspecified red algae: Sheet: Thick/Leathery	URS2	Red Foliose Macroalgae
Non-Biotic		
Bare Substrate	Bare-Subst	Bare substrate
Rock Rubble	RockRub	NA
Shell/ Shell Hash	Shell	NA
Fuzz	Fuzz	Bare substrate
Shadow	SHAD	NA

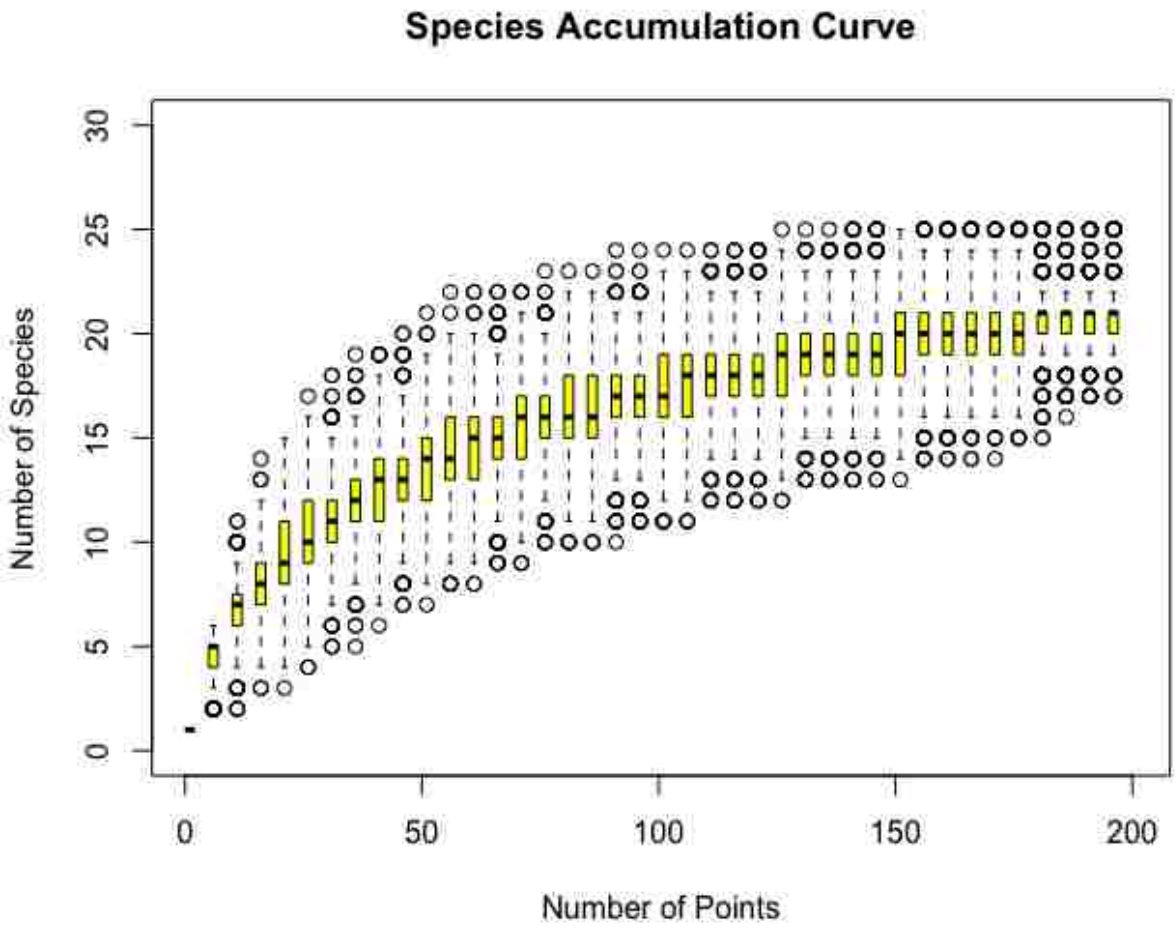

Figure S1. Species Accumulation Curve based on resampled annotation points. The curve shows the number of species identified versus the number of resampled annotation points across photoquadrats. Yellow boxes represent the quartile range across photoquadrats and resampling iterations (I = 100 per photoquadrat). We used 200 random annotation points were used to analyze percent cover in CoralNet.

APPENDIX 2: Representativeness of single transects

Due to low accuracy of automated annotations for photoquadrats in the turbid, temperate, estuarine environment in which the study was conducted, we relied exclusively upon human annotated photographs. All photos from one transect at each site was analyzed in full and averaged across photos to generate a community matrix with transect (1 per site) as replicates (T_Q). Four additional community matrices ($T_{q=1}$, $T_{q=2}$, $T_{q=3}$, and $T_{q=4}$) were then generated by randomly selecting 1, 2, 3, and 4 of the quadrats from within fully analyzed transects and averaging percent cover for each species group at the transect-level.

To assess the number of quadrats required to adequately represent benthic cover of transects, we performed a series of multivariate and univariate comparisons. Congruence of TQ and each Tq data were examined visually using NMDS ordination (Fig. S2) and evaluated quantitatively via Procrustes analysis. We used the *protest()* function in the vegan package in R with 999 permutations to test the significance of the Procrustes statistic, m2, for each comparison (Table S2). The "representativeness" of percent cover for specific species was assessed using basic scatter plots (Fig. S3) and regression statistics (Table S3).

Multivariate comparisons indicated significant congruence regardless of the number of quadrats used to estimate transect-level community composition (Table S2). This was also reflected in the NMDS ordination (Fig. S2), though the ordination points for q = 1 quadrat per transect were more dispersed than those for other community matrices. In univariate regressions (Table S3), significant correlations were observed for all species with 3 subsampled quadrats or greater. Based on these results, we annotated three quadrats from each of the remaining transects in our survey and generated transect-level percent cover data by averaging across these quadrats only.

Table S2. Results from Procrustes analysis using protest permutation tests on non-metric multidimensional scaling (NMDS) ordinations. The permutational technique was used to compare ordinations from transect-level community data generated from all quadrats in the transect (TQ) and a subset of 1, 2, 3, or 4 randomly selected quadrats in each transect ($T_{q=1}$, $T_{q=2}$, $T_{q=3}$, $T_{q=4}$). The table presents the Procrustes statistic, m^2, the correlation statistic, *r*, which is computed from the Procrustes sum of squares (SS) as *r = sqrt(1-SS)*, and a permutation-based significance estimate for m^2, *P*.

Comparison	m^2	r	P
T_Q vs $T_{q=1}$	0.4387	0.7492	0.0010
T_Q vs $T_{q=2}$	0.2820	0.8473	0.0010
T_Q vs $T_{q=3}$	0.0951	0.9513	0.0010
T_Q vs $T_{q=4}$	0.0608	0.9691	0.0010

Table S3. Regression coefficients and p-values for regressions comparing percent cover data generated from all quadrats vs a subset of quadrats within fully-annotated transects. Four comparisons were made for each benthic cover type, each using random subsamples of either 1, 2, 3, or 4 quadrats from each transect.

	Number of randomly selected quadrats (q)							
	$q = 1$		$q = 2$		$q = 3$		$q = 4$	
Benthic cover type	***Adj R^2***	***p-value***	***Adj R^2***	***p-value***	***Adj R^2***	***p-value***	***Adj R^2***	***p-value***
Annelids	0.4350	<0.0001	0.5373	<0.0001	0.7389	<0.0001	0.8372	<0.0001
Balanus spp.	0.5575	<0.0001	0.7988	<0.0001	0.9027	<0.0001	0.8737	<0.0001
Bare substrate	0.6665	<0.0001	0.8023	<0.0001	0.8859	<0.0001	0.9142	<0.0001
Brachiopods	*	*	0.5024	<0.0001	0.4762	<0.0001	0.7803	<0.0001
Branching bryozoans	*	*	*	*	0.4597	<0.0001	0.2062	0.0003
Colonial diatoms	0.5049	<0.0001	0.8426	<0.0001	0.8627	<0.0001	0.9528	<0.0001
Compound Ascidians	0.3011	<0.0001	0.6384	<0.0001	0.8065	<0.0001	0.6928	<0.0001
Crustose coralline algae	0.6061	<0.0001	0.8376	<0.0001	0.8875	<0.0001	0.9089	<0.0001
Desmarestia spp.	0.4414	<0.0001	0.6110	<0.0001	0.6316	<0.0001	0.5019	<0.0001
Encrusting bryozoans	0.7405	<0.0001	0.7294	<0.0001	0.7407	<0.0001	0.5525	<0.0001
Holothuroids	0.0824	0.0182	0.3818	<0.0001	0.4494	<0.0001	0.6605	<0.0001
Hydroids	0.5512	<0.0001	0.6927	<0.0001	0.8735	<0.0001	0.7881	<0.0001
Kelp	0.6299	<0.0001	0.7281	<0.0001	0.8291	<0.0001	0.8558	<0.0001
Metridium spp.	0.5974	<0.0001	0.7245	<0.0001	0.9623	<0.0001	0.9189	<0.0001
Other cnidarians	*	*	*	*	0.8248	<0.0001	0.4921	<0.0001
Pododesmus machrochisma	0.0953	0.0118	0.5472	<0.0001	0.7228	<0.0001	0.8053	<0.0001
Porifera	0.5178	<0.0001	0.5332	<0.0001	0.6901	<0.0001	0.6765	<0.0001
Red filamentous algal turf	0.4293	<0.0001	0.6593	<0.0001	0.8047	<0.0001	0.8611	<0.0001
Red foliose macroalgae	0.7197	<0.0001	0.8344	<0.0001	0.9235	<0.0001	0.9599	<0.0001
Scallops	0.6122	<0.0001	0.6652	<0.0001	0.8665	<0.0001	0.8560	<0.0001
Social or Solitary Ascidians	0.3588	<0.0001	0.4663	<0.0001	0.5257	<0.0001	0.5774	<0.0001
Ulva spp.	0.4759	<0.0001	0.7536	<0.0001	0.7010	<0.0001	0.9584	<0.0001

** Insufficient observations (variance = 0)*

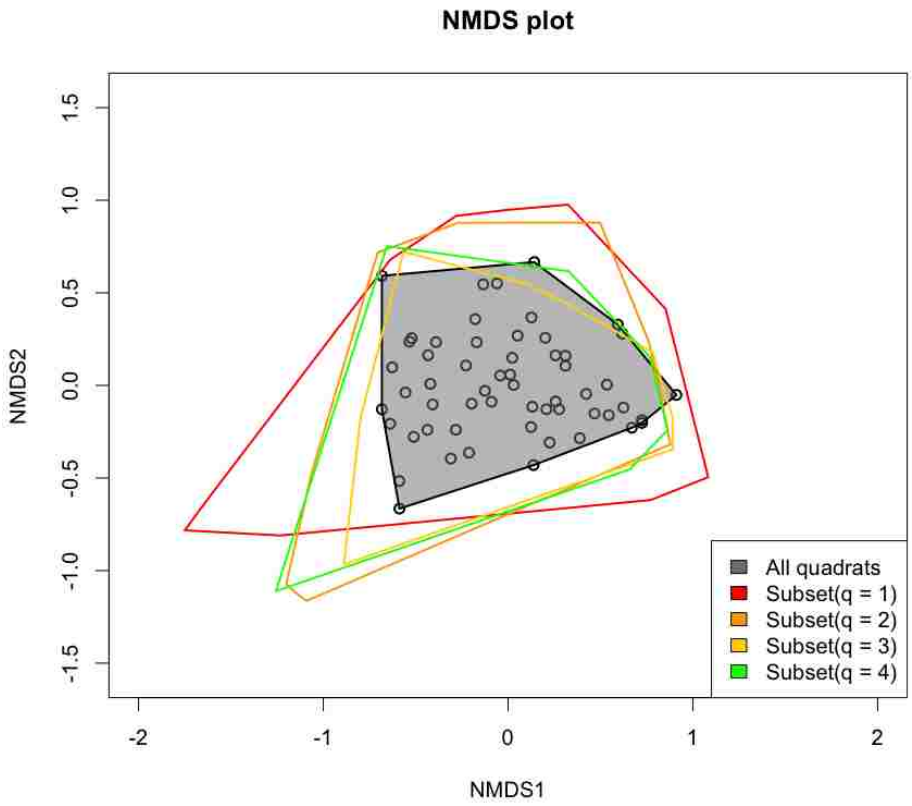

Figure S2. NMDS plot showing ordinations transect-level estimates of community composition generated from all quadrats (T_Q shown in gray), and from a subset of 1, 2, 3, or 4 randomly selected quadrats from each transect ($T_{q=1}$ (red), $T_{q=2}$ (orange), $T_{q=3}$ (yellow), and $T_{q=4}$ (green), respectively).

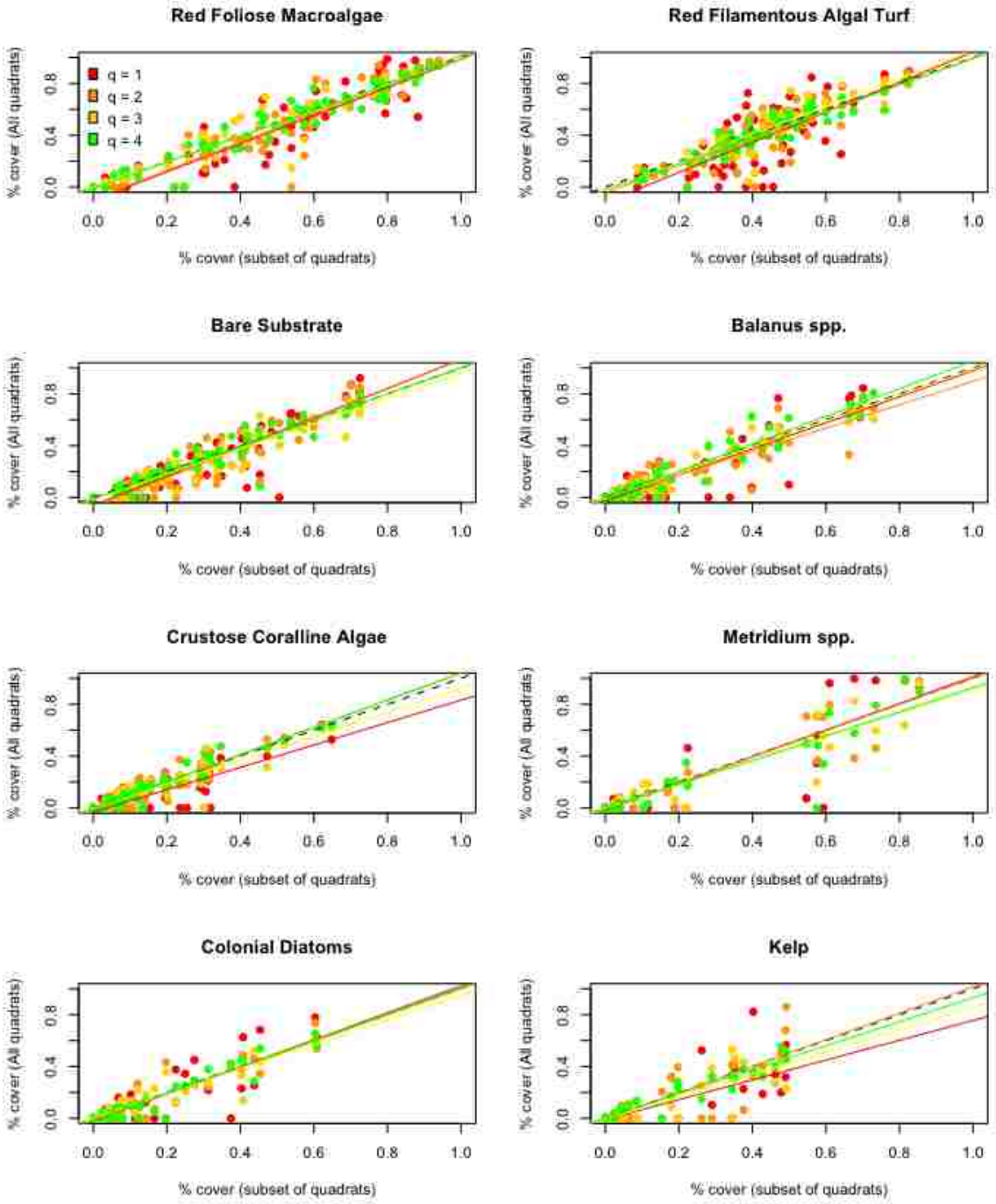

Figure S3. Scatterplots and regression lines for percent cover estimated from all quadrats versus a subset of quadrats for the eight most common benthic cover types in fully-annotated transects. Regressions are color coded, with data generated from a subset of q = 1, 2, 3, and 4 randomly selected quadrats shown in red, orange, yellow, and green, respectively.

APPENDIX 3: Predictor Variables

Table S4. Principal Component (PC) loadings for five urbanization-related metrics and the cumulative proportion of the variance explained by each PC (bottom row). Principal Component Analysis (PCA) was performed to reduce the dimensionality of urbanization metrics.

Variable	PC1	PC2	PC3	PC4	PC5
Population Density	0.49	-0.05	0.17	0.77	0.37
Imperviousness	0.53	-0.14	0.01	0.06	-0.84
Armoring	0.35	0.72	-0.58	-0.09	0.09
Road Density	0.44	0.22	0.67	-0.52	0.22
High Intensity Development	0.4	-0.64	-0.44	-0.36	0.33
Cumulative Proportion	61%	77%	89%	96%	100%

LITERATURE CITED

Aguilera, M.A., Broitman, B.R., Thiel, M., 2014. Spatial variability in community composition on a granite breakwater versus natural rocky shores: Lack of microhabitats suppresses intertidal biodiversity. Mar. Pollut. Bull. 87, 257–268.

Airoldi, L., 2003. The effects of sedimentation on rocky coast assemblages. Oceanogr. Mar. Biol. 41, 161–236.

Airoldi, L., Balata, D., Beck, M.W., 2008. The Gray Zone: Relationships between habitat loss and marine diversity and their applications in conservation. J. Exp. Mar. Bio. Ecol. 366, 8–15.

Airoldi, L., Beck, M.W., 2007. Loss , Status and Trends for Coastal Marine Habitats of Europe. Oceanogr. Mar. Biol. 45, 345–405.

Airoldi, L., Bulleri, F., 2011. Anthropogenic disturbance can determine the magnitude of opportunistic species responses on marine urban infrastructures. PLoS One 6, e22985.

Airoldi, L., Fontana, G., Ferrario, F., Franzitta, G., Perkol-Finkel, S., Magnani, A., Bianchelli, S., Pusceddu, A., Colangelo, M., Thrush, S., 2010. Detrital enrichment from marine urban structures and its far-field effects on soft- bottom assemblages, in: Rapp. Comm. Int. Mer Medit. p. 712.

Airoldi, L., Turon, X., Perkol-Finkel, S., Rius, M., 2015. Corridors for aliens but not for natives: Effects of marine urban sprawl at a regional scale. Divers. Distrib. 21, 755–768.

Alberti, M., 2008. Advances in urban ecology : integrating humans and ecological processes in urban ecosystems. Springer, Boston.

Alberti, M., Booth, D., Hill, K., Coburn, B., Avolio, C., Coe, S., Spirandelli, D., 2007. The impact of urban patterns on aquatic ecosystems: An empirical analysis in Puget lowland

sub-basins. Landsc. Urban Plan. 80, 345–361.

Alberti, M., Marzluff, J., Hunt, V.M., 2017. Urban driven phenotypic changes: empirical observations and theoretical implications for eco-evolutionary feedback. Philos. Trans. R. Soc. B Biol. Sci. 372, 20160029.

Alongi, D.M., Tenore, K.R., 1985. Effect of detritus supply on trophic relationships within experimental benthic food webs. I. Meiofauna-polychaete (*Capitella capitata* (Type I) Fabricius) interactions. J. Exp. Mar. Bio. Ecol. 88, 153–166.

Ambrose, R.F., 1983. Midden formation by octopuses: The role of biotic and abiotic factors. Mar. Behav. Physiol. 10, 137–144.

Ambrose, R.F., Anderson, T.W., 1990. Influence of an artificial reef on the surrounding infaunal community. Mar. Biol. 107, 41–52.

Anderson, M.J., 2006. Distance-based tests for homogeneity of multivariate dispersions. Biometrics 62, 245–253.

Anderson, M.J., 2001. A new method for non-parametric multivariate analysis of variance. Austral Ecol. 26, 32–46.

Anderson, M.J., Walsh, D.C.I., 2013. PERMANOVA, ANOSIM, and the Mantel test in the face of heterogeneous dispersions: What null hypothesis are you testing? Ecol. Monogr. 83, 557–574.

Anderson, R.C., 2003. A preliminary report on bioaccumulation in octopuses (*Enteroctopus dofleini*), in: Georgia Basin - Puget Sound Research Conference. pp. 1–5.

Anderson, R.C., Mather, J.A., 2010. It's all in the cues: octopuses (*Enteroctopus dofleini*) learn to open jars. Ferrantia 59, 8–13.

André, M., Solé, M., Lenoir, M., Durfort, M., Quero, C., Mas, A., Lombarte, A., Van Der

Schaar, M., López-Bejar, M., Morell, M., Zaugg, S., Houégnigan, L., 2011. Low-frequency sounds induce acoustic trauma in cephalopods. Front. Ecol. Environ. 9, 489–493.

Arguez, A., Durre, I., Applequist, S., Squires, M., Vose, R., Yin, X., Bilotta, R., 2010. NOAA's U.S. Hourly Climate Normals (1981-2010). Wind Speed and Direction. NOAA National Climatic Data Center.

Aronson, M.F.J., Handel, S.N., La Puma, I.P., Clemants, S.E., 2015. Urbanization promotes non-native woody species and diverse plant assemblages in the New York metropolitan region. Urban Ecosyst. 18, 31–45.

Aronson, M.F.J., La Sorte, F.A., Nilon, C.H., Katti, M., Goddard, M.A., Lepczyk, C.A., Warren, P.S., Williams, N.S.G., Cilliers, S., Clarkson, B., Dobbs, C., Dolan, R., Hedblom, M., Klotz, S., Kooijmans, J.L., Kühn, I., Macgregor-Fors, I., McDonnell, M., Mörtberg, U., Pysek, P., Siebert, S., Sushinsky, J., Werner, P., Winter, M., 2014. A global analysis of the impacts of urbanization on bird and plant diversity reveals key anthropogenic drivers. Proc. Biol. Sci. 281, 20133330.

Aronson, R.B., 1986. Life-History and Den Ecology of Octopus-Briareus Robson in a Marine Lake. J. Exp. Mar. Bio. Ecol. 95, 37–56.

Barros, F., Underwood, A.J., Lindegarth, M., 2001a. The Influence of Rocky Reefs on Structure of Benthic Macrofauna in Nearby Soft-sediments. Estuar. Coast. Shelf Sci. 52, 191–199.

Barros, F., Underwood, a J., Lindegarth, M., 2001b. The influence of rocky reefs on structure of benthic macrofauna in nearby soft-sediments. Estuar. Coast. Shelf Sci. 52, 191–199.

Bateman, P.W., Fleming, P.A., 2012. Big city life: Carnivores in urban environments. J. Zool. 287, 1–23.

Bates, A.J., Sadler, J.P., Fairbrass, A.J., Falk, S.J., Hale, J.D., Matthews, T.J., 2011. Changing

bee and hoverfly pollinator assemblages along an urban-rural gradient. PLoS One 6, e23459.

Beger, M., Grantham, H.S., Pressey, R.L., Wilson, K.A., Peterson, E.L., Dorfman, D., Mumby, P.J., Lourival, R., Brumbaugh, D.R., Possingham, H.P., 2010. Conservation planning for connectivity across marine, freshwater, and terrestrial realms. Biol. Conserv. 143, 565–575.

Beijbom, O., Edmunds, P.J., Roelfsema, C., Smith, J., Kline, D.I., Neal, B.P., Dunlap, M.J., Moriarty, V., Fan, T.Y., Tan, C.J., Chan, S., Treibitz, T., Gamst, A., Mitchell, B.G., Kriegman, D., 2015. Towards automated annotation of benthic survey images: Variability of human experts and operational modes of automation. PLoS One 10, e0130312.

Bertasi, F., Colangelo, M.A., Abbiati, M., Ceccherelli, V.U., 2007. Effects of an artificial protection structure on the sandy shore macrofaunal community: The special case of Lido di Dante (Northern Adriatic Sea). Hydrobiologia 586, 277–290.

Bianchi, T.S., Dawson, R., Sawangwong, P., 1988. The effects of macrobenthic deposit-feeding on the degradation of chloropigments in sandy sediments. J. Exp. Mar. Bio. Ecol. 122, 243–255.

Bianchi, T.S., Johansson, B., Elmgren, R., 2000. Breakdown of phytoplankton pigments in Baltic sediments: Effects of anoxia and loss of deposit-feeding macrofauna. J. Exp. Mar. Bio. Ecol. 251, 161–183.

Bishop, M.J., Coleman, M.A., Kelaher, B.P., 2010. Cross-habitat impacts of species decline: Response of estuarine sediment communities to changing detrital resources. Oecologia 163, 517–525.

Bishop, M.J., Kelaher, B.P., 2007. Impacts of detrital enrichment on estuarine assemblages: Disentangling effects of frequency and intensity of disturbance. Mar. Ecol. Prog. Ser. 341,

25–36.

Bolam, S.G., Fernandes, T.F., Read, P., Raffaelli, D., 2000. Effects of macroalgal mats on intertidal sandflats: An experimental study. J. Exp. Mar. Bio. Ecol. 249, 123–137.

Bolnick, D.I., Yang, L.H., Fordyce, J.A., Davis, J.M., Svanback, R., 2002. Measuring Individual-Level Resource Specialization. Ecology 83, 2936–2941.

Bolton, D., Mayer-Pinto, M., Clark, G.F., Dafforn, K.A., Brassil, W.A., Becker, A., Johnston, E.L., 2017. Coastal urban lighting has ecological consequences for multiple trophic levels under the sea. Sci. Total Environ. 576, 1–9.

Botto, F., Iribarne, O., Gutierrez, J., Bava, J., Gagliardini, A., Valiela, I., 2006. Ecological importance of passive deposition of organic matter into burrows of the SW Atlantic crab Chasmagnathus granulatus. Mar. Ecol. Prog. Ser. 312, 201–210.

Britton-Simmons, K.H., Foley, G., Okamoto, D., 2009. Spatial subsidy in the subtidal zone: Utilization of drift algae by a deep subtidal sea urchin. Aquat. Biol. 5, 233–243.

Buckley, R.M., Hueckel, G.J., 1989. Analysis of visual transects for fish assesment on artificial reefs. Bull. Mar. Sci. 44, 893–898.

Bulleri, F., 2006. Is it time for urban ecology to include the marine realm? Trends Ecol. Evol. 21, 658–659.

Bulleri, F., Airoldi, L., Branca, G.M., Abbiati, M., 2006. Positive effects of the introduced green alga, *Codium fragile* ssp. *tomentosoides*, on recruitment and survival of mussels. Mar. Biol. 148, 1213–1220.

Bulleri, F., Chapman, M., 2010. The introduction of coastal infrastructure as a driver of change in marine environments. J. Appl. Ecol. 47, 26–35.

Bulleri, F., Chapman, M.G., 2010. The introduction of coastal infrastructure as a driver of

change in marine environments. J. Appl. Ecol. 47, 26–35.

Bulleri, F., Chapman, M.G., Underwood, A.J., 2005. Intertidal assemblages on seawalls and vertical rocky shores in Sydney Harbour, Australia. Austral Ecol. 30, 655–667.

Bureau, U.S.C., 2010. 2010 Census Block, 2010 TIGER/Line Shapefile [WWW Document]. U.S. Dep. Commer. U.S. Census Bur. Geogr. Div. Geogr. Prod. Branch. URL http://www.census.gov/geo/maps-data/data/tiger-line.html (accessed 3.14.12).

Burns, R., 1985. The Shape and Form of Puget Sound. University of Washington, Seattle, Washington.

Burt, J., Bartholomew, A., Sale, P.F., 2011. Benthic development on large-scale engineered reefs: A comparison of communities among breakwaters of different age and natural reefs. Ecol. Eng. 37, 191–198.

Burt, J., Bartholomew, A., Usseglio, P., Bauman, A., Sale, P.F., 2009. Are artificial reefs surrogates of natural habitats for corals and fish in Dubai, United Arab Emirates? Coral Reefs 28, 663–675.

Cardoso, P.G., Pardal, M.A., Raffaelli, D., Baeta, A., Marques, J.C., 2004. Macroinvertebrate response to different species of macroalgal mats and the role of disturbance history. J. Exp. Mar. Bio. Ecol. 308, 207–220.

Chapman, M.G., 2003. Paucity of mobile species on constructed seawalls: Effects of urbanization on biodiversity. Mar. Ecol. Prog. Ser. 264, 21–29.

Cohen, J., 1960. A Coefficient of Agreement for Nominal Scales. Educ. Psychol. Meas. 20, 37–46.

Connell, S., Glasby, T., 1999. Do urban structures influence local abundance and diversity of subtidal epibiota? A case study from Sydney Harbour, Australia. Mar. Environ. Res. 47,

373–387.

Connell, S.D., 2007. Water quality and the loss of coral reefs and kelp forests: alternative states and the influence of fishing, in: Marine Ecology. Oxford University Press, Melbourne, pp. 556–568.

Connell, S.D., Foster, M.S., Airoldi, L., 2014. What are algal turfs? Towards a better description of turfs. Mar. Ecol. Prog. Ser. 495, 299–307.

Cooper, W., 2014. Relative index of abundance from visual order-of-magnitude REEF surveys applied to hogfish (*Lachnolaimus maximus*) in the Southeast US. St. Petersburg, FL.

Crooks, K., Soulé, M., 1999. Mesopredator release and avifaunal extinctions in a fragmented system. Nature 400, 563–566.

Crossland, C.J., Kremer, H.H., Lindeboom, H., Marshall Crossland, J.I., Le Tissier, M.D.A. (Eds.), 2005. Coastal fluxes in the anthropocene. Springer, Berlin.

Dafforn, K.A., Glasby, T.M., Airoldi, L., Rivero, N.K., Mayer-Pinto, M., Johnston, E.L., 2015. Marine urbanization: An ecological framework for designing multifunctional artificial structures. Front. Ecol. Environ. 13, 82–90.

Dafforn, K.A., Kelaher, B.P., Simpson, S.L., Coleman, M.A., Hutchings, P.A., Clark, G.F., Knott, N.A., Doblin, M.A., Johnston, E.L., 2013. Polychaete Richness and Abundance Enhanced in Anthropogenically Modified Estuaries Despite High Concentrations of Toxic Contaminants. PLoS One 8, e77018.

Danovaro, R., Gambi, C., Danovaro, R., Gambi, C., Mazzola, A., Mirto, S., 2002. Influence of artificial reefs on the surrounding infauna: analysis of meiofauna. ICES J. Mar. Sci. 59, S356–S362.

Davis, N., VanBlaricom, G.R., Dayton, P.K., 1982. Man-made structures on marine sediments:

Effects on adjacent benthic communities. Mar. Biol. 70, 295–303.

Dayton, P.K., 1985. Ecology of Kelp Communities. Annu. Rev. Ecol. Syst. 16, 215–245.

Deng, J.S., Wang, K., Hong, Y., Qi, J.G., 2009. Spatio-temporal dynamics and evolution of land use change and landscape pattern in response to rapid urbanization. Landsc. Urban Plan. 92, 187–198.

Dethier, M.N., Graham, E.S., Cohen, S., Tear, L.M., 1993. Visual versus random-point percent cover estimations: "objective' is not always better. Mar. Ecol. Prog. Ser. 96, 93–100.

Dethier, M.N., Raymond, W.W., McBride, A.N., Toft, J.D., Cordell, J.R., Ogston, A.S., Heerhartz, S.M., Berry, H.D., 2016. Multiscale impacts of armoring on Salish Sea shorelines: Evidence for cumulative and threshold effects. Estuar. Coast. Shelf Sci. 175, 106–117.

Dodge, R., Scheel, D., 1999. Remains of the prey-Recognizing the midden piles of *Octopus dofleini* (Wulker). The Veliger 42, 260–266.

Duarte, C., Pitt, K., Lucas, C., Purcell, J., Uye, S., Robinson, K., Brotz, L., Decker, M.B., Sutherland, K.R., Malej, A., Madin, L., Mianzan, H., Gili, J.-M., Fuentes, V., Atienza, D., Pages, F., Breitburg, D., Malek, J., Graham, W.M., Condon, R.H., 2012. Is global ocean sprawl a cause of jellyfish blooms? Front. Ecol. 11, 91–97.

Duduś, L., Zalewski, A., Kozioł, O., Jakubiec, Z., Król, N., 2014. Habitat selection by two predators in an urban area: The stone marten and red fox in Wrocław (SW Poland). Mamm. Biol. 79, 71–76.

Dugan, J., Airoldi, L., Chapman, M., 2011. Estuarine and coastal structures: environmental effects, a focus on shore and nearshore structures. Treatise Estuar. Coast. Sci. 8, 17–41.

Dugan, J.E., Hubbard, D.M., Rodil, I.F., Revell, D.L., Schroeter, S., 2008. Ecological effects of

coastal armoring on sandy beaches. Mar. Ecol. 29, 160–170.

Elahi, R., Dwyer, T.R., Sebens, K.P., 2014. Mesoscale variability in oceanographic retention sets the abiotic stage for subtidal benthic diversity. Mar. Ecol. Prog. Ser. 498, 117–132.

Elahi, R., O'Connor, M.I., Byrnes, J.E.K., Dunic, J., Eriksson, B.K., Hensel, M.J.S., Kearns, P.J., 2015. Recent Trends in Local-Scale Marine Biodiversity Reflect Community Structure and Human Impacts. Curr. Biol. 25, 1938–1943.

Elahi, R., Sebens, K.P., 2012. Consumers mediate natural variation between prey richness and resource use in a benthic marine community. Mar. Ecol. Prog. Ser. 452, 131–143.

Emmerson, M., 2000. Remedial habitat creation: does Nereis diversicolor play a confounding role in the colonisation and establishment of the pioneering saltmarsh plant, *Spartina anglica*? Helgol. Mar. Res. 54, 110–116.

EPA, 2009. Second Five-Year Review Report for the Pacific Sound Resources Superfund Site, US Environmental Protection Agency, Region 10. Seattle, Washington.

Epstein, H.E., Templeman, M.A., Kingsford, M.J., 2016. Fine-scale detection of pollutants by a benthic marine jellyfish. Mar. Pollut. Bull. 107, 340–346.

Evans, B.S., Ryder, T.B., Reitsma, R., Hurlbert, A.H., Marra, P.P., 2015. Characterizing avian survival along a rural-to-urban land use gradient. Ecology 96, 1631–1640. d

Faeth, S.H., Bang, C., Saari, S., 2011. Urban biodiversity: Patterns and mechanisms. Ann. N. Y. Acad. Sci. 1223, 69–81.

Fauchald, K., Jumars, P., 1979. The Diet of Worms: A studie of Polychaete Feeding Gilds. Oceanogr. Mar. Biol. An Annu. Rev. 17, 193–284.

Feely, R.A., Alin, S.R., Newton, J., Sabine, C.L., Warner, M., Devol, A., Krembs, C., Maloy, C., 2010. The combined effects of ocean acidification, mixing, and respiration on pH and

carbonate saturation in an urbanized estuary. Estuar. Coast. Shelf Sci. 88, 442–449.

Feist, B.E., Levin, P.S., 2016. Novel Indicators of Anthropogenic Influence on Marine and Coastal Ecosystems. Front. Mar. Sci. 3, 1–13.

Fenical, W., 1975. Halogenation in the Rhodophyta a review. J. Phycol. 11, 245–259.

Ferrario, F., Iveša, L., Jaklin, A., Perkol-Finkel, S., Airoldi, L., 2016. The overlooked role of biotic factors in controlling the ecological performance of artificial marine habitats. J. Appl. Ecol. 53, 16–24.

Firth, L.B., Knights, A.M., Bridger, D., Evans, A.J., Mieszkowska, N., Moore, P.J., O 'connor, N.E., Sheehan, E. V, Thompson, R.C., Hawkins, S.J., 2016. Ocean Sprawl: Challenges and opportunities for biodiversity management in a changing world. Oceanogr. Mar. Biol. An Annu. Rev. 54, 189–262.

Fortin, M.-J., Dale, M.R.T., 2005. Spatial analysis : a guide for ecologists. Cambridge University Press, Cambridge, UK.

Franz, D.R., Friedman, I., 2002. Effects of a macroalgal mat (*Ulva lactuca*) on estuarine sand flat copepods: An experimental study. J. Exp. Mar. Bio. Ecol. 271, 209–226.

Furlong, E.T., Carpenter, R., 1988. Pigment preservation and remineralization in oxic coastal marine sediments. Geochim. Cosmochim. Acta 52, 87–99.

Galgani, F., Hanke, G., Maes, T., 2015. Global Distribution, Composition, and Abundance of Marine Litter, in: Bergmann, M., Gutow, L., Klages, M. (Eds.), Marine Anthropogenic Litter. Springer, New York, pp. 29–56.

Galgani, F., Leaute, J.P., Moguedet, P., Souplet, A., Verin, Y., Carpentier, A., Goraguer, H., Latrouite, D., Andral, B., Cadiou, Y., Mahe, J.C., Poulard, J.C., Nerisson, P., 2000. Litter on the sea floor along European coasts. Mar. Pollut. Bull. 40, 516–527.

Gaston, K.J., Davies, T.W., Bennie, J., Hopkins, J., 2012. Reducing the ecological consequences of night-time light pollution: Options and developments. J. Appl. Ecol. 49, 1256–1266.

Gehrt, S.D., Riley, S.P.D., Cypher, B.L., 2010. Urban carnivores: ecology, conflict, and conservation. Johns Hopkins University Press, Baltimore.

George, S.L., Crooks, K.R., 2006. Recreation and large mammal activity in an urban nature reserve. Biol. Conserv. 133, 107–117.

Gittman, R.K., Peterson, C.H., Currin, C.A., Joel Fodrie, F., Piehler, M.F., Bruno, J.F., 2016a. Living shorelines can enhance the nursery role of threatened estuarine habitats. Ecol. Appl. 26, 249–263.

Gittman, R.K., Scyphers, S.B., Smith, C.S., Neylan, I.P., Grabowski, J.H., 2016b. Ecological Consequences of Shoreline Hardening: A Meta-Analysis. Bioscience 66, 763–773.

Gladstone-Gallagher, R. V., Lundquist, C.J., Pilditch, C.A., 2014. Response of temperate intertidal benthic assemblages to mangrove detrital inputs. J. Exp. Mar. Bio. Ecol. 460, 80–88.

Glasby, T., 2000. Surface composition and orientation interact to affect subtidal epibiota. J. Exp. Mar. Bio. Ecol. 248(2), 177-190

Glud, R., 2008. Oxygen dynamics of marine sediments. Mar. Biol. Res. 4, 243–289.

Gorgula, S.K., Connell, S.D., 2004. Expansive covers of turf-forming algae on human-dominated coast: The relative effects of increasing nutrient and sediment loads. Mar. Biol. 145, 613–619.

Gorman, D., Connell, S.D., 2009. Recovering subtidal forests in human-dominated landscapes. J. Appl. Ecol. 46, 1258–1265.

Gorman, D., Russell, B.D., Connell, S.D., 2009. Land-to-Sea Connectivity : Linking Human-

Derived Terrestrial Subsidies to Subtidal Habitat Change on Open Rocky Coasts. Ecol. Appl. 19, 1114–1126.

Granneman, J.E., Steele, M.A., 2015. Between Artificial and Natural Reefs 72, 2385–2397.

Hartwick, E.B., Ambrose, R.F., Robinson, S.M.C., 1984. Dynamics of shallow-water populations of *Octopus dofleini*. Mar. Biol. 82, 65–72.

Hawkins, S.J., Evans, A.J., Mieszkowska, N., Adams, L.C., Bray, S., Burrows, M.T., Firth, L.B., Genner, M.J., Leung, K.M.Y., Moore, P.J., Pack, K., Schuster, H., Sims, D.W., Whittington, M., Southward, E.C., In press. Distinguishing globally-driven changes from regional- and local-scale impacts: The case for long-term and broad-scale studies of recovery from pollution. Mar. Pollut. Bull.

Heery, E.C., Bishop, M.J., Critchley, L.P., Bugnot, A.B., Airoldi, L., Mayer-Pinto, M., Sheehan, E. V., Coleman, R.A., Loke, L.H.L., Johnston, E.L., Komyakova, V., Morris, R.L., Strain, E.M.A., Naylor, L.A., Dafforn, K.A., 2017. Identifying the consequences of ocean sprawl for sedimentary habitats. J. Exp. Mar. Bio. Ecol. 492, 31–48.

HSIP, 2013. Homeland Security Infrastructure Program Gold 2013, ed. National Geospatial - Intelligence Agency. Boulder, CO.

Hughes, R.G., Lloyd, D., Ball, L., Emson, D., 2000. The effects of the polychaete Nereis diversicolor on the distribution and transplanting success of *Zostera noltii*. Helgol. Mar. Res. 54, 129–136.

Hugo, G., 2011. Future demographic change and its interactions with migration and climate change. Glob. Environ. Chang. 21, S21-S33.

Ingalls, A.E., Aller, R.C., Lee, C., Sun, M., 2000. The influence of deposit-feeding on chlorophyll-a degradation in coastal marine sediments. J. Mar. Res. 58, 631–651.

Inglis, G.J., Kross, J.E., 2000. Evidence for systemic changes in the benthic fauna of tropical estuaries as a result of urbanization. Mar. Pollut. Bull. 41, 367–376.

Ioakeimidis, C., Zeri, C., Kaberi, H., Galatchi, M., Antoniadis, K., Streftaris, N., Galgani, F., Papathanassiou, E., Papatheodorou, G., 2014. A comparative study of marine litter on the seafloor of coastal areas in the Eastern Mediterranean and Black Seas. Mar. Pollut. Bull. 89, 296–304.

Jiang, Z.D., Gerwick, W.H., 1997. Novel oxylipins from the temperate red alga Polyneura latissima: Evidence for an arachidonate 9(S)-lipoxygenase. Lipids 32, 231–235.

Katsanevakis, S., Verriopoulos, G., 2004. Den ecology of *Octopus vulgaris* Cuvier, 1797, on soft sediment : availability and types of shelter. Sci. Mar. 68, 147–157.

Kelaher, B.P., Levinton, J.S., 2003. Variation in detrital enrichment causes spatio-temporal variation in soft-sediment assemblages. Mar. Ecol. Prog. Ser. 261, 85–97.

Kelly, R.P., O'Donnell, J.L., Lowell, N.C., Shelton, A.O., Samhouri, J.F., Hennessey, S.M., Feist, B.E., Williams, G.D., 2016. Genetic signatures of ecological diversity along an urbanization gradient. PeerJ 4, e2444.

Krause-Jensen, D., McGlathery, K., Rysgaard, S., Christensen, P.B., 1996. Production within dense mats of the filamentous macroalga *Chaetomorpha linum* in relation to light and nutrient availability. Mar. Ecol. Prog. Ser. 134, 207–216.

Krause-Jensen, D., Sagert, S., Schubert, H., Boström, C., 2008. Empirical relationships linking distribution and abundance of marine vegetation to eutrophication. Ecol. Indic. 8, 515–529.

Krishnakumar, P. k, Casillas, E., Varanasi, U., 1994. Effect of environmental contaminants on the health of Mytilus edulis from Puget Sound, Washington, USA. I. Cytochemical measures of lysosomal responses in the digestive cells using automatic image analysis. Mar.

Ecol. Prog. Ser. 106, 249–261.

Kristensen, E., Mikkelsen, O.L., 2003. Impact of the burrow-dwelling polychaete *Nereis diversicolor* on the degradation of fresh and aged macroalgal detritus in a coastal marine sediment. Mar. Ecol. Prog. Ser. 265, 141–153.

Lam, N.W.Y., Huang, R., Chan, B.K.K., 2009. Variations in intertidal assemblages and zonation patterns between vertical artificial seawalls and natural rocky shores: A case study from Victoria Harbour, Hong Kong. Zool. Stud. 48, 184–195.

Lastra, M., Page, H.M., Dugan, J.E., Hubbard, D.M., Rodil, I.F., 2008. Processing of allochthonous macrophyte subsidies by sandy beach consumers: Estimates of feeding rates and impacts on food resources. Mar. Biol. 154, 163–174.

Legendre, P., Anderson, M.J., 1999. Distance-Based Redundancy Analysis: Testing Multispecies Responses in Multifactorial Ecological Experiments. Ecol. Monogr. 69, 1–24.

Leite, A.S., Santos, L.L., Costa, Y., Hatje, V., 2014. Influence of proximity to an urban center in the pattern of contamination by marine debris. Mar. Pollut. Bull. 81, 242–247.

Light, S.F., Carlton, J.T., Light, S.F., 2007. The Light and Smith manual: intertidal invertebrates from central California to Oregon. University of California Press, Berkeley, California.

Long, E.R., Chapman, P.M., 1985. A Sediment Quality Triad: Measures of sediment contamination, toxicity and infaunal community composition in Puget Sound. Mar. Pollut. Bull. 16, 405–415. d

Long, E.R., Dutch, M., Weakland, S., Chandramouli, B., Benskin, J.P., 2013. Quantification of pharmaceuticals, personal care products, and perfluoroalkyl substances in the marine sediments of Puget Sound, Washington, USA. Environ. Toxicol. Chem. 32, 1701–1710.

Lorenzen, C.J., 1967. Determination of Chlorophyll and Pheo-Pigments: Spectrophotometric

Equations. Limnol. Oceanogr. 12, 343–346.

Luck, M., Wu, J., 2002. A gradient analysis of urban landscape pattern: A case study from the Phoenix metropolitan region, Arizona, USA. Landsc. Ecol. 17, 327–339.

Machado, P.M., de Sá, F.S., de Rezende, C.E., Zalmon, I.R., 2013. Artificial reef impact on macrobenthic community on south-eastern Brazil coast. Mar. Biodivers. Rec. 6, e40.

Magle, S.B., Lehrer, E.W., Fidino, M., 2016. Urban mesopredator distribution: Examining the relative effects of landscape and socioeconomic factors. Anim. Conserv. 19, 163–175.

Magle, S.B., Simoni, L.S., Lehrer, E.W., Brown, J.S., 2014. Urban predator-prey association: coyote and deer distributions in the Chicago metropolitan area. Urban Ecosyst. 875–891.

Mann, T., Martin, A.W., French, M., 1988. Entry of pollutants from seawater into the spermatophore and spermatozoa of the giant octopus of the North Pacific. Mar. Pollut. Bull. 19, 669–671.

Marczak, L.B., Thompson, R.M., Richardson, J.S., 2007. Meta-analysis: Trophic level, habitat, and productivity shape the food web effects of resource subsidies. Ecology 88, 140–148.

Marsden, I.D., Bressington, M.J., 2009. Effects of macroalgal mats and hypoxia on burrowing depth of the New Zealand cockle (*Austrovenus stutchburyi*). Estuar. Coast. Shelf Sci. 81, 438–444.

Martin, D., Bertasi, F., Colangelo, M.A., de Vries, M., Frost, M., Hawkins, S.J., Macpherson, E., Moschella, P.S., Satta, M.P., Thompson, R.C., Ceccherelli, V.U., 2005. Ecological impact of coastal defence structures on sediment and mobile fauna: Evaluating and forecasting consequences of unavoidable modifications of native habitats. Coast. Eng. 52, 1027–1051.

Martins, G.M., Neto, A.I., Cacabelos, E., 2016. Ecology of a key ecosystem engineer on hard coastal infrastructure and natural rocky shores. Mar. Environ. Res. 113, 88–94.

Marzinelli, E.M., Underwood, A.J., Coleman, R.A., 2011. Modified habitats influence kelp epibiota via direct and indirect effects. PLoS One 6, e21936.

McClain, C.R., Balk, M. a., Benfield, M.C., Branch, T. a., Chen, C., Cosgrove, J., Dove, A.D.M., Gaskins, L.C., Helm, R.R., Hochberg, F.G., Lee, F.B., Marshall, A., McMurray, S.E., Schanche, C., Stone, S.N., Thaler, A.D., 2015. Sizing ocean giants: patterns of intraspecific size variation in marine megafauna. PeerJ 3, e715.

McCook, L., 2001. Competition between corals and algal turfs along a gradient of terrestrial influence in the nearshore central Great Barrier Reef. Coral Reefs 19, 419–425.

McDonald, P.S., Essington, T.E., Davis, J.P., Galloway, A.W.E., Stevick, B.C., Jensen, G.C., Vanblaricom, G.R., Armstrong, D.A., 2015. Distribution, Abundance, and Habitat Associations of a Large Bivalve (*Panopea generosa*) in a Eutrophic Fjord Estuary. J. Shellfish Res. 34, 137–145.

McKinney, M.L., 2006. Urbanization as a major cause of biotic homogenization. Biol. Conserv. 127, 247–260.

McKinney, M.L., 2002. Urbanization, Biodiversity, and Conservation. Bioscience 52, 883–890.

Miller, M.A., Byrne, B.A., Jang, S.S., Dodd, E.M., Dorfmeier, E., Harris, M.D., Ames, J., Paradies, D., Worcester, K., Jessup, D.A., Miller, W.A., 2010. Enteric bacterial pathogen detection in southern sea otters (*Enhydra lutris nereis*) is associated with coastal urbanization and freshwater runoff. Vet. Res. 41, 1-13.

Ming-Yi, S., Lee, C., Aller, R.C., 1993. Laboratory studies of oxic and anoxic degradation of chlorophyll-a in Long Island Sound sediments. Geochim. Cosmochim. Acta 57, 147–157.

Moschella, P.S., Abbiati, M., Åberg, P., Airoldi, L., Anderson, J.M., Bacchiocchi, F., Bulleri, F., Dinesen, G.E., Frost, M., Gacia, E., Granhag, L., Jonsson, P.R., Satta, M.P., Sundelöf, A.,

Thompson, R.C., Hawkins, S.J., 2005. Low-crested coastal defence structures as artificial habitats for marine life: Using ecological criteria in design. Coast. Eng. 52, 1053–1071.

Musetta-Lambert, J.L., Scrosati, R.A., Keppel, E.A., Barbeau, M.A., Skinner, M.A., Courtenay, S.C., 2015. Intertidal communities differ between breakwaters and natural rocky areas on ice-scoured Northwest Atlantic coasts. Mar. Ecol. Prog. Ser. 539, 19–31.

Neira, C., Levin, L.A., Mendoza, G., Zirino, A., 2014. Alteration of benthic communities associated with copper contamination linked to boat moorings. Mar. Ecol. 35, 46–66.

Neumann, B., Vafeidis, A.T., Zimmermann, J., Nicholls, R.J., 2015. Future coastal population growth and exposure to sea-level rise and coastal flooding - A global assessment. PLoS One 10, e0118571.

NOAA, 2016a. NOAA's Earth System Research Laboratory, Physical Science Division: NOAA_OI_SST_V2 data [WWW Document]. URL http://www.esrl.noaa.gov/psd/ (accessed 11.18.16).

NOAA, 2016b. NOAA's National Centers for Environmental Information. NCEI PDO index. [WWW Document]. URL https://www.ncdc.noaa.gov/teleconnections/pdo/ (accessed 11.18.16).

NOAA, 2013. NOAA's Coastal Change Analysis Program (C-CAP) 1992 to 2010 Regional Land Cover Change Data - Coastal United States. Charleston, SC.

Nordstrom, K.F., 2014. Living with shore protection structures: A review. Estuar. Coast. Shelf Sci. 150, 11–23.

Nordström, M., Bonsdorff, E., Salovius, S., 2006. The impact of infauna (*Nereis diversicolor* and *Saduria entomon*) on the redistribution and biomass of macroalgae on marine soft bottoms. J. Exp. Mar. Bio. Ecol. 333, 58–70.

Norkko, A., Bonsdorff, E., 1996. Rapid zoobenthic community responses to accumulations of drifting algae. Mar. Ecol. Prog. Ser. 131, 143–157.

Norkko, A., Thrush, S.F., Cummings, V.J., Funnell, G.A., Schwarz, A.-M.M., Andrew, N.L., Hawes, I., 2004. Ecological role of *Phyllophora antarctica* drift accumulations in coastal soft-sediment communities of McMurdo Sound, Antarctica. Polar Biol. 27, 482–494.

Nylund, G.M., Weinberger, F., Rempt, M., Pohnert, G., 2011. Metabolomic assessment of induced and activated chemical defence in the invasive red alga *Gracilaria vermiculophylla*. PLoS One 6, e29359.

Oksanen, J., 2015. Multivariate analysis of ecological communities in R: vegan tutorial. R Doc. 43.

Olabarria, C., Incera, M., Garrido, J., Rossi, F., 2010. The effect of wrack composition and diversity on macrofaunal assemblages in intertidal marine sediments. J. Exp. Mar. Bio. Ecol. 396, 18–26.

Papaspyrou, S., Thessalou-Legaki, M., Kristensen, E., 2004. Impact of *Pestarella tyrrhena* on benthic metabolism in sediment microcosms enriched with seagrass and macroalgal detritus. Mar. Ecol. Prog. Ser. 281, 165–179.

Pedersen, M., Saenger, P., Fries, L., 1974. Simple Brominated Phenols In Red Algae. Phytochemistry 13, 2273–2279.

Polis, G. a., Anderson, W.B., Holt, R.D., 1997. Toward an Integration of Landscape and Food Web Ecology: The Dynamics of Spatially Subsidized Food Webs. Annu. Rev. Ecol. Syst. 28, 289–316.

Prange, S., Gehrt, S.D., 2004. Changes in mesopredator-community structure in response to urbanization. Can. J. Zool. 82, 1804–1817.

Prange, S., Gehrt, S.D., Wiggers, E.P., 2003. Demographic Factors Contributing to High Raccoon Densities in Urban Landscapes. J. Wildl. Manage. 67, 324–333.

Prugh, L.R., Stoner, C.J., Epps, C.W., Bean, W.T., Ripple, W.J., Laliberte, A.S., Brashares, J.S., 2009. The rise of the mesopredator. Bioscience 59, 779–791.

PSNERP, 2010. Puget Sound Basin PSNERP Database [WWW Document]. Puget Sound Nearshore Partnership, Olympia, WA.

Puget Sound Partnership, 2015. Report on the Puget Sound Vital Signs. Olympia, WA.

Raffaelli, D., 2000. Interactions between macro-algal mats and invertebrates in the Ythan estuary, Aberdeenshire, Scotland. Helgol. Mar. Res. 54, 71–79.

Reise, K., 1985. Tidal flat ecology: an experimental approach to species interactions. Springer-Verlag, New York.

Rhodes, J.R., Wiegand, T., McAlpine, C.A., Callaghan, J., Lunney, D., Bowen, M., Possingham, H.P., 2006. Modeling species' distributions to improve conservation in semiurban landscapes: Koala case study. Conserv. Biol. 20, 449–459.

Riley, S.P.D., Pollinger, J.P., Sauvajot, R.M., York, E.C., Bromley, C., Fuller, T.K., Wayne, R.K., 2006. A southern California freeway is a physical and social barrier to gene flow in carnivores. Mol. Ecol. 15, 1733–1741.

Riley, S.P.D., Riley, S.P.D., Bromley, C., Bromley, C., Poppenga, R.H., Poppenga, R.H., Uzal, F. a., Uzal, F. a., Whited, L., Whited, L., Sauvajot, R.M., Sauvajot, R.M., Service, N.P., Monica, S., National, M., Area, R., Drive, W.H., Oaks, T., 2007. Anticoagulant exposure and notoedric mange in bobcats and mountain lions in urban Southern California. J. Wildl. Manage. 71, 1874–1884.

Rochman, C.M., Browne, M.A., Underwood, A.J., van Franeker, J.A., Thompson, R.C., Amaral-

Zettler, L.A., 2016. The ecological impacts of marine debris: unraveling the demonstrated evidence from what is perceived. Ecology 97, 302–312.

Rohweder, J., Rogala, J.T., Johnson, B.L., Anderson, D., Clark, S., Chamberlin, F., Runyon, K., 2008. Application of wind fetch and wave models for habitat rehabilitation and enhancement projects, U.S. Geological Survey Open-File Report 2008-1200.

Rossi, F., 2006. Small-scale burial of macroalgal detritus in marine sediments: Effects of *Ulva* spp. on the spatial distribution of macrofauna assemblages. J. Exp. Mar. Bio. Ecol. 332, 84–95.

Rossi, F., Underwood, A.J., 2002. Small-scale disturbance and increased nutrients as influences on intertidal macrobenthic assemblages: Experimental burial of wrack in different intertidal environments. Mar. Ecol. Prog. Ser. 241, 29–39.

Russell, B.D., Elsdon, T.S., Gillanders, B.M., Connell, S.D., 2005. Nutrients increase epiphyte loads: Broad-scale observations and an experimental assessment. Mar. Biol. 147, 551–558.

Savage, C., Leavitt, P.R., Elmgren, R., 2010. Effects of land use, urbanization, and climate variability on coastal eutrophication in the Baltic Sea. Limnol. Oceanogr. 55, 1033–1046.

Scheel, D., 2015. Sea-surface temperature used to predict the relative density of giant Pacific octopuses (*Enteroctopus dofleini*) in intertidal habitats of Prince William Sound, Alaska. Mar. Freshw. Res. 66, 866–876.

Scheel, D., Anderson, R., 2012. Variability in the diet specialization of *Enteroctopus dofleini* (Cephalopoda: Octopodidae) in the eastern Pacific examined from midden contents. Am. Malacol. Bull. 30, 267–279.

Scheel, D., Bisson, L., 2012. Movement patterns of giant Pacific octopuses, *Enteroctopus dofleini* (Wülker, 1910). J. Exp. Mar. Bio. Ecol. 416–417, 21–31.

Scheel, D., Lauster, A., Vincent, T.L.S., 2007. Habitat ecology of *Enteroctopus dofleini* from middens and live prey surveys in Prince William Sound, Alaska, in: Landman, N.H., Davis, R.A., Mapes, R.H. (Eds.), Cephalopods Present and Past: New Insights and Fresh Perspectives. Springer, Dordrecht, pp. 434–458.

Schultz, J.A., Cloutier, R.N., Côté, I.M., 2016. Evidence for a trophic cascade on rocky reefs following sea star mass mortality in British Columbia. PeerJ 4, e1980.

Sebens, K.P., 1986. Spatial Relationships among encrusting marine organisms in the New England subtidal zone. Ecol. Monogr. 56, 73–96.

Semmens, J.M., Pecl, G.T., Gillanders, B.M., Waluda, C.M., Shea, E.K., Jouffre, D., Ichii, T., Zumholz, K., Katugin, O.N., Leporati, S.C., Shaw, P.W., 2007. Approaches to resolving cephalopod movement and migration patterns. Rev. Fish Biol. Fish. 17, 401–423.

Seto, K.C., Fragkias, M., Guneralp, B., Reilly, M.K., 2011. A meta-analysis of global urban land expansion. PLoS One 6, e23777.

Shelton, A.O., Francis, T.B., Feist, B.E., Williams, G.D., Lindquist, A., Levin, P.S., 2017. Forty years of seagrass population stability and resilience in an urbanizing estuary. J. Ecol. 105, 458–470.

Shipman, H., 2008. A geomorphic classification of Puget Sound nearshore landforms. Olympia, WA.

Shochat, E., Warren, P.S., Faeth, S.H., McIntyre, N.E., Hope, D., 2006. From patterns to emerging processes in mechanistic urban ecology. Trends Ecol. Evol. 21, 186–191.

Sim, V.X.Y., Dafforn, K.A., Simpson, S.L., Kelaher, B.P., Johnston, E.L., 2015. Sediment contaminants and infauna associated with recreational boating structures in a multi-use marine park. PLoS One 10, 1–15.

Small, C., Nicholls, R., 2003. A Global Analysis of Human Settlement in Coastal Zones. J. Coast. Res. 19, 584–599.

Snelgrove, P., 1999. Getting to the bottom of marine biodiversity: Sedimentary habitats: Ocean bottoms are the most widespread habitat on earth and support high biodiversity and key. Bioscience.

Spalding, M.D., Ruffo, S., Lacambra, C., Meliane, I., Hale, L.Z., Shepard, C.C., Beck, M.W., 2014. The role of ecosystems in coastal protection: Adapting to climate change and coastal hazards. Ocean Coast. Manag. 90, 50–57.

Speiser, D.I., Lampe, R.I., Lovdahl, V.R., Carrillo-Zazueta, B., Rivera, A.S., Oakley, T.H., 2013. Evasion of predators contributes to the maintenance of male eyes in sexually dimorphic *Euphilomedes* ostracods (Crustacea). Integr. Comp. Biol. 53, 78–88.

Spirandelli, D.J., 2014. Examining the effects of wastewater infrastructure on Puget Sound near-shore water quality across a gradient of urbanization. University of Washington.

Strain, E.M.A., Thomson, R.J., Micheli, F., Mancuso, F.P., Airoldi, L., 2014. Identifying the interacting roles of stressors in driving the global loss of canopy-forming to mat-forming algae in marine ecosystems. Glob. Chang. Biol. 20, 3300–3312.

Strayer, D.L., Findlay, S.E.G., Miller, D., Malcom, H.M., Fischer, D.T., Coote, T., 2012. Biodiversity in Hudson River shore zones: Influence of shoreline type and physical structure. Aquat. Sci. 74, 597–610.

Sutherland, D. a, MacCready, P., Banas, N.S., Smedstad, L.F., 2011. A Model Study of the Salish Sea Estuarine Circulation. J. Phys. Oceanogr. 41, 1125–1143.

Szymczak-Zyla, M., Kowalewska, G., Louda, J.W., 2008. The influence of microoranisms on chlorophyll a degradation in the marine environment. Limnol. Oceanogr. 53, 851–862.

Taylor, S.L., Bishop, M.J., Kelaher, B.P., Glasby, T.M., 2010. Impacts of detritus from the invasive alga *Caulerpa taxifolia* on a soft sediment community. Mar. Ecol. Prog. Ser. 420, 73–81.

Teagle, H., Hawkins, S.J., Moore, P.J., Smale, D.A., 2017. The role of kelp species as biogenic habitat formers in coastal marine ecosystems. J. Exp. Mar. Bio. Ecol. 492, 81–98.

Thiel, M., Hinojosa, I.A., Miranda, L., Pantoja, J.F., Rivadeneira, M.M., Vásquez, N., 2013. Anthropogenic marine debris in the coastal environment: A multi-year comparison between coastal waters and local shores. Mar. Pollut. Bull. 71, 307–316.

Thornber, C.S., Jones, E., Stachowicz, J.J., 2008. Differences in herbivore feeding preferences across a vertical rocky intertidal gradient. Mar. Ecol. Prog. Ser. 363, 51–62.

Thrush, S.F., Lawrie, S.M., Hewitt, J.E., Cummings, V.J., 1999. The Problem of Scale: Uncertainties and Implications for Soft-Bottom Marine Communities and the Assessment of Human Impacts, in: Biogeochemical Cycling and Sediment Ecology. Springer Netherlands, Dordrecht, pp. 195–210.

Toft, J.D., Cordell, J.R., Simenstad, C.A., Lia A. Stamatiou, 2007. Fish Distribution, Abundance, and Behavior along City Shoreline Types in Puget Sound. North Am. J. Fish. Manag. 27, 465–480.

Uno, S., Cotton, J., Philpott, S.M., 2010. Diversity, abundance, and species composition of ants in urban green spaces. Urban Ecosyst. 13, 425–441.

USGS, 2014. NLCD 2011 Percent Developed Imperviousness (2011 Edition). Sioux Falls, SD.

Valiela, I., Foreman, K., LaMontagne, M., Hersh, D., Costa, J., Peckol, P., DeMeo-Andreson, B., D'Avanzo, C., Babione, M., Sham, H., Brawley, J., Lajtha, K., 1992. Couplings of Watersheds and Coastal Waters : Sources and Consequences of Nutrient Enrichment in

Waquoit Bay , Massachusetts. Estuaries 15, 443–457.

Vargas-Fonseca, E., Olds, A.D., Gilby, B.L., Connolly, R.M., Schoeman, D.S., Huijbers, C.M., Hyndes, G.A., Schlacher, T.A., VanDerWal, J., 2016. Combined effects of urbanization and connectivity on iconic coastal fishes. Divers. Distrib. 22, 1328–1341.

Von Glasow, R., Jickells, T.D., Baklanov, A., Carmichael, G.R., Church, T.M., Gallardo, L., Hughes, C., Kanakidou, M., Liss, P.S., Mee, L., Raine, R., Ramachandran, P., Ramesh, R., Sundseth, K., Tsunogai, U., Uematsu, M., Zhu, T., 2013. Megacities and large urban agglomerations in the coastal zone: Interactions between atmosphere, land, and marine ecosystems. Ambio 42, 13–28.

Vonk, J.A., Kneer, D., Stapel, J., Asmus, H., 2008. Shrimp burrow in tropical seagrass meadows: An important sink for litter. Estuar. Coast. Shelf Sci. 79, 79–85.

Wang, J., Chen, C., 2009. Biosorbents for heavy metals removal and their future. Biotechnol. Adv. 27, 195–226.

Wilding, T.A., 2006. The benthic impacts of the Loch Linnhe Artificial Reef. Hydrobiologia 555, 345–353.

Williams, R., Wright, A.J., Ashe, E., Blight, L.K., Bruintjes, R., Canessa, R., Clark, C.W., Cullis-Suzuki, S., Dakin, D.T., Erbe, C., Hammond, P.S., Merchant, N.D., O'Hara, P.D., Purser, J., Radford, A.N., Simpson, S.D., Thomas, L., Wale, M.A., 2015. Impacts of anthropogenic noise on marine life: Publication patterns, new discoveries, and future directions in research and management. Ocean Coast. Manag. 115, 17–24.

Winer, B.J., 1971. Statistical principles in experimental design. McGraw-Hill, New York.

Witman, J.D., Etter, R.J., Smith, F., 2004. The relationship between regional and local species diversity in marine benthic communities: a global perspective. Proc. Natl. Acad. Sci. U. S.

A. 101, 15664–15669.

Wolfe, J.R., Pattengill-Semmens, C.V., 2013. Estimating fish populations from REEF citizen science volunter diver order of magnitude surveys. CalCOFI Rep 54, 127–140.

Xian, G., Homer, C., Demitz, J., Fry, J., Hossain, N., Wickham, J., 2011. Change of impervious surface area between 2001 and 2006 in the conterminous United States. Photogramm. Eng. Remote Sensing 77, 758–762.

Yasuhara, M., Hunt, G., Breitburg, D., Tsujimoto, A., Katsuki, K., 2012. Human-induced marine ecological degradation: Micropaleontological perspectives. Ecol. Evol. 2, 3242–3268.

Zanuttigh, B., Martinelli, L., Lamberti, A., Moschella, P., Hawkins, S., Marzetti, S., Ceccherelli, V.U., 2005. Environmental design of coastal defence in Lido di Dante, Italy. Coast. Eng. 52, 1089–1125.

Zhou, P., Huang, C., Fang, H., Cai, W., Li, D., Li, X., Yu, H., 2011. The abundance, composition and sources of marine debris in coastal seawaters or beaches around the northern South China Sea (China). Mar. Pollut. Bull. 62, 1998–2007.

VITA

Eliza Heery was born on 8 January 1983 in Berkeley, California and grew up in San Francisco. She attended Marin Academy High School, where she graduated in 2000. Her path into science was strongly influenced by her participation in the Careers in Science (CiS) program at the California Academy of Sciences during high school and college. She completed a B.S. degree in biology from Emory University in 2004, participated in the Three Seas Program (Northeastern University) in 2001/2002, and earned a M.S. degree in fisheries stock assessment from Virginia Tech, working under Dr. James Berkson. Eliza worked as an analyst for the West Coast Groundfish Observer Program at the Northwest Fisheries Science Center (National Oceanic and Atmospheric Administration, NOAA) from 2008 to 2011. She conducted her Ph.D. research in the Biology Department at the University of Washington under the guidance of Dr. Kenneth P. Sebens from 2011 to 2017.